Published for SISSA by Springer

Received: *April 10, 2014*
Accepted: *May 13, 2014*
Published: *June 6, 2014*

Search for supersymmetry at $\sqrt{s} = 8$ TeV in final states with jets and two same-sign leptons or three leptons with the ATLAS detector

The ATLAS collaboration

E-mail: atlas.publications@cern.ch

Abstract: A search for strongly produced supersymmetric particles is conducted using signatures involving multiple energetic jets and either two isolated leptons (e or μ) with the same electric charge, or at least three isolated leptons. The search also utilises jets originating from b-quarks, missing transverse momentum and other observables to extend its sensitivity. The analysis uses a data sample corresponding to a total integrated luminosity of 20.3 fb^{-1} of $\sqrt{s} = 8$ TeV proton-proton collisions recorded with the ATLAS detector at the Large Hadron Collider in 2012. No deviation from the Standard Model expectation is observed. New or significantly improved exclusion limits are set on a wide variety of supersymmetric models in which the lightest squark can be of the first, second or third generations, and in which R-parity can be conserved or violated.

Keywords: Hadron-Hadron Scattering

ArXiv ePrint: 1404.2500

doi:10.1007/JHEP06(2014)035

JHEP06(2014)035

Contents

1 Introduction

Supersymmetry (SUSY) [1–9] is a generalisation of space-time symmetries that predicts new bosonic partners for the fermions and new fermionic partners for the bosons of the Standard Model (SM). If R-parity is conserved [10, 11], SUSY particles are produced in pairs and the lightest supersymmetric particle (LSP) is stable. In a large variety of models, the LSP is the lightest neutralino ($\tilde{\chi}_1^0$) and provides a possible candidate for dark matter.

JHEP06(2014)035

The coloured superpartners of quarks and gluons, the squarks ($\tilde{q}$) and gluinos ($\tilde{g}$), could be produced in strong interaction processes at the Large Hadron Collider (LHC) and decay via cascades ending with a stable $\tilde{\chi}_1^0$. The undetected $\tilde{\chi}_1^0$ would result in substantial missing transverse momentum ($\boldsymbol{p}_{\mathrm{T}}^{\mathrm{miss}}$ and its magnitude $E_{\mathrm{T}}^{\mathrm{miss}}$). The rest of the cascade would yield final states with multiple jets and possibly leptons arising from the decay of sleptons ($\tilde{\ell}$), the superpartners of leptons, or W, Z and Higgs (h) bosons. If R-parity is violated (RPV), the LSP is not stable, which would lead to similar signatures but with lower, or no, $E_{\mathrm{T}}^{\mathrm{miss}}$.

In the Minimal Supersymmetric Standard Model [12–14] (MSSM), the scalar partners of right-handed and left-handed quarks, $\tilde{q}_R$ and $\tilde{q}_L$, can mix to form two mass eigenstates, $\tilde{q}_1$ and $\tilde{q}_2$, where $\tilde{q}_1$ denotes the lighter particle. This mixing effect is proportional to the corresponding SM fermion masses and therefore is more important for the third generation. Furthermore, SUSY can solve the hierarchy problem of the SM (also referred to as the naturalness problem) [15–19] if the masses of the gluinos, higgsinos[1] (the superpartners of Higgs bosons) and top squarks ($\tilde{t}$) are not heavier than the $\mathcal{O}$(TeV) scale. A light left-handed top squark also implies that the left-handed bottom squark ($\tilde{b}_L$) may be relatively light because of the SM weak-isospin symmetry. As a consequence, the lightest bottom squark ($\tilde{b}_1$) and top squark ($\tilde{t}_1$) could be produced with relatively large cross sections at the LHC, either directly in pairs or through $\tilde{g}\tilde{g}$ production followed by $\tilde{g} \to \tilde{b}_1 b$ or $\tilde{g} \to \tilde{t}_1 t$ decays (gluino-mediated production).

In this paper, events containing multiple jets and either two leptons of the same electric charge (same-sign leptons, SS) or at least three leptons (3L) are used to search for strongly produced supersymmetric particles. Throughout this paper, the term leptons (ℓ) refers to electrons and/or muons only. Signatures with SS or 3L are predicted in many SUSY scenarios. Gluinos produced in pairs or in association with a squark can lead to SS signatures when decaying to any final state that includes leptons because gluinos are Majorana fermions. Squark production, directly in pairs or through $\tilde{g}\tilde{g}$ or $\tilde{g}\tilde{q}$ production with subsequent $\tilde{g} \to q\tilde{q}$ decay, can also lead to SS or 3L signatures when the squarks decay in cascades involving top quarks (t), charginos, neutralinos or sleptons, which subsequently decay as $t \to bW$, $\tilde{\chi}_i^{\pm} \to W^{\pm(*)}\tilde{\chi}_j^0$, $\tilde{\chi}_i^0 \to h/Z^{(*)}\tilde{\chi}_j^0$, or $\tilde{\ell} \to \ell\tilde{\chi}_1^0$, respectively. Similar signatures are also predicted by non-SUSY models such as minimal Universal Extra Dimensions (mUED) [20]. Since this search benefits from low SM backgrounds, it allows the use of relatively loose kinematic requirements on $E_{\mathrm{T}}^{\mathrm{miss}}$, increasing the sensitivity to scenarios with small mass differences between SUSY particles (compressed scenarios) or where R-parity is violated. This search is thus sensitive to a wide variety of models based on very different assumptions.

The analysis uses pp collision data from the full 2012 data-taking period, corresponding to an integrated luminosity of 20.3 fb^{-1} collected at $\sqrt{s}$=8 TeV, and significantly extends the reach of previous searches performed by the ATLAS [21] and CMS [22–25] Collaborations. Five statistically independent signal regions (SR) are designed to cover the SUSY processes illustrated in figure 1. Two signal regions requiring SS and jets identified to originate from b-quarks (b-jets) are optimised for gluino-mediated top squark and direct bottom

[1] The charginos $\tilde{\chi}_{1,2}^{\pm}$ and neutralinos $\tilde{\chi}_{1,2,3,4}^0$ are the mass eigenstates formed from the linear superposition of the SUSY partners of the Higgs and electroweak gauge bosons (higgsinos, winos and binos).

JHEP06(2014)035

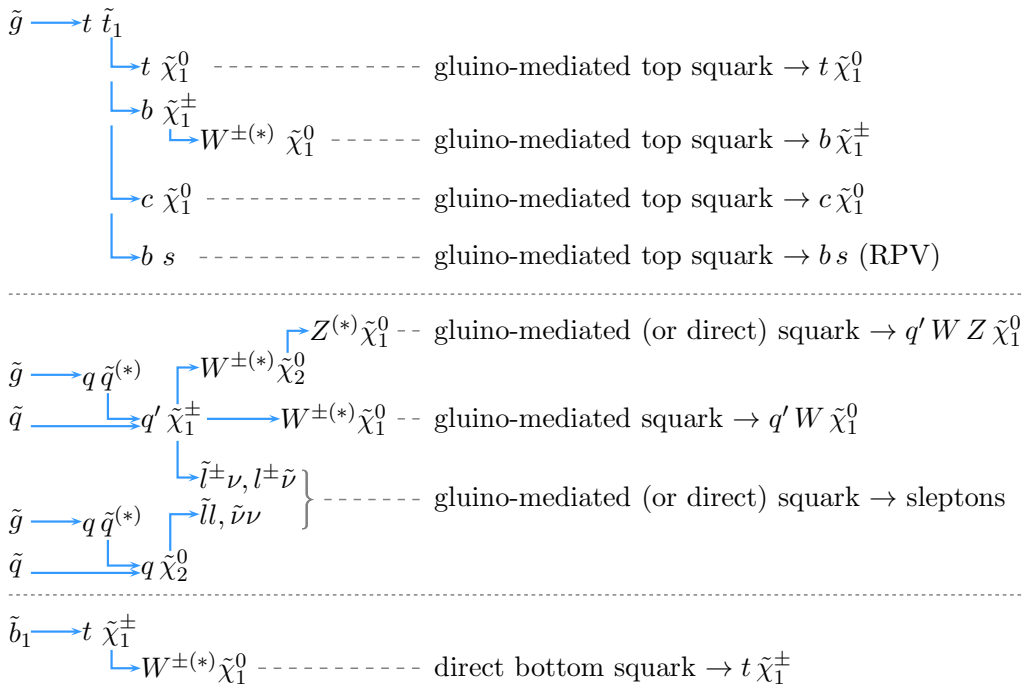

Figure 1. Overview of the SUSY processes considered in the analysis. The initial supersymmetric particles are always produced in pairs: $pp \to \tilde{g}\tilde{g}$, $\tilde{b}\bar{\tilde{b}}$ or $\tilde{q}\bar{\tilde{q}}$. The notation q ($\tilde{q}$) refers to quark (squark) of the first or second generation. The slepton and sneutrino decay as $\tilde{\ell} \to \ell\tilde{\chi}_1^0$ and $\tilde{\nu} \to \nu\tilde{\chi}_1^0$, respectively. Leptons in the final state can arise from the decay of any W or Z bosons or sleptons that are produced. The charge-conjugate processes are also considered.

squark production. These are complemented with a signal region requiring a b-jet veto, optimised for the gluino-mediated production of first- and second-generation squarks. Two signal regions requiring 3L are designed for scenarios characterised by multi-step decays.

Backgrounds with prompt SS or 3L events arising from rare SM processes, such as $t\bar{t}W$, $t\bar{t}Z$, $W^{\pm}W^{\pm}$ and WZ, are estimated with Monte Carlo simulations. Backgrounds from hadrons mis-identified as leptons, leptons originating from heavy-flavour decays, electrons from photon conversions, and electrons with mis-measured charge are estimated with data-driven methods. The background predictions are cross-checked with alternative methods and tested with data in validation regions chosen to be close in phase space to the signal regions. The probability (p-value) of the background-only hypothesis is then estimated independently in each signal region. To maximise the sensitivity of the analysis across the entire phase space, a simultaneous fit is performed in all signal regions to place model-dependent exclusion limits on several SUSY benchmark scenarios.

2 ATLAS detector and data sample

ATLAS is a multi-purpose detector [26] designed for the study of pp and heavy-ion collisions at the LHC. It provides nearly full solid angle[2] coverage around the interaction point.

[2]ATLAS uses a right-handed coordinate system with its origin at the nominal interaction point (IP) in the centre of the detector and the z-axis along the beam pipe. The x-axis points from the IP to the centre

JHEP06(2014)035

Charged particles are tracked by the inner detector, which covers the pseudorapidity region $|\eta| < 2.5$. In order to measure their momenta, the inner detector is embedded in the 2 T magnetic field of a thin superconducting solenoid. Sampling calorimeters span the pseudorapidity range up to $|\eta| = 4.9$. High-granularity liquid-argon (LAr) electromagnetic calorimeters are present up to $|\eta| = 3.2$. Hadronic calorimeters with scintillating tiles as active material cover $|\eta| < 1.7$ while LAr technology is used for hadronic calorimetry from $|\eta| = 1.5$ to $|\eta| = 4.9$. The calorimeters are surrounded by a muon spectrometer. The magnetic field is provided by air-core toroid magnets. Three layers of precision gas chambers track muons up to $|\eta| = 2.7$ and muon trigger chambers cover the range $|\eta|$ ¡ 2.4. A three-level trigger system is used to select interesting events for storage and subsequent analysis.

The data set, after the application of beam, detector and data quality requirements, has an integrated luminosity of 20.3 ± 0.6 fb^{-1}. The luminosity is measured using techniques similar to those described in ref. [27] with a preliminary calibration of the luminosity scale derived from beam-overlap scans performed in November 2012. The number of pp interactions occurring in the same bunch crossing varies between approximately 10 and 30 with an average of 20.7 for this data set.

3 Simulated event samples

Simulated events are used to model the SUSY signal, optimise the event selection requirements, compute systematic uncertainties and estimate some of the SM backgrounds with prompt same-sign lepton pairs or three leptons. These include top quark(s) plus bosons ($W/Z/H$), diboson ($W^{\pm}W^{\pm}$, WZ, ZZ, WH, ZH), triboson (WWW, WZZ, ZZZ) and $t\bar{t}t\bar{t}$ production. Other sources of background such as $t\bar{t}$, W/Z+jets, $W\gamma$, $W^{+}W^{-}$, $t\bar{t}\gamma$ and single-top production are estimated with data-driven methods described in section 6.

Samples of $t\bar{t}V$+jets ($V = W, Z$), $t\bar{t}WW$, single top quark plus a Z boson, VVV+jets and $t\bar{t}t\bar{t}$ are generated with MadGraph-5.1.4.8 [28] interfaced to Pythia-6.426 [29]. Alternative $t\bar{t}V$+jets samples generated with Alpgen-2.14 [30] interfaced with Herwig-6.520 [31] and Jimmy-4.31 [32] are employed to estimate the sensitivity of the analysis to Monte Carlo modelling. The Pythia-8.165 [33] generator is used to model $t\bar{t}H$ production, for which the Higgs boson mass is set to 125 GeV. The WZ and $W^{\pm}W^{\pm}$ processes are modelled using Sherpa-1.4.1 [34] with matrix elements producing up to three final-state partons. The ZZ process is generated with Powheg-1.0 [35] interfaced to Pythia-8.165. Monte Carlo modelling systematic uncertainties for the ZZ process are estimated using two sets of aMc@nlo [36] samples where next-to-leading-order (NLO) matrix elements are matched to either Pythia-6.426 or Herwig-6.520 with Jimmy-4.31 parton showers according to the Mc@nlo formalism [37]. Monte Carlo samples of $t\bar{t}$ events are used to provide corrections to the data-driven background estimates, described in section 6.1, for kinematic regions where the sample size is not sufficient to measure the $t\bar{t}$ contri-

of the LHC ring, and the y-axis points upward. Cylindrical coordinates (r,ϕ) are used in the transverse plane, ϕ being the azimuthal angle around the beam pipe. The pseudorapidity is defined in terms of the polar angle θ as $\eta = -\ln\tan(\theta/2)$.

JHEP06(2014)035

bution directly in data. Four different samples are used: POWHEG-1.0 interfaced with PYTHIA-6.426, POWHEG-1.0 interfaced with HERWIG-6.520 and JIMMY-4.31, MC@NLO-4.06 interfaced with HERWIG-6.520 and JIMMY-4.31 and ALPGEN-2.14 interfaced with HERWIG-6.520 and JIMMY-4.31.

The NLO CT10 [38] parton distribution function (PDF) set is used with SHERPA, POWHEG and MC@NLO while the CTEQ6L1 [39] PDF set is used with MADGRAPH, PYTHIA and ALPGEN. The predicted background yields are obtained by normalising the simulated samples to theoretical cross sections from the most precise available calculations [40–42].

The SUSY signal samples are generated with HERWIG++2.5.2 [43] or MADGRAPH-5.1.4.8 interfaced with PYTHIA-6.426, in both cases using the PDF set CTEQ6L1. Signal cross sections are calculated to next-to-leading order in the strong coupling constant, adding the resummation of soft gluon emission at next-to-leading-logarithmic accuracy (NLO+NLL) [44–48]. The cross section and its uncertainty are taken from an envelope of cross-section predictions using different PDF sets and factorisation and renormalisation scales, as described in ref. [49]. The mUED samples are generated with HERWIG++2.5.2 using the CTEQ6L1 PDF set and the leading-order cross section from HERWIG++.

The parton shower parameters of the simulated samples were tuned to match ATLAS data observables sensitive to initial- and final-state QCD radiation, colour reconnection, hadronisation, and multiple parton interactions. The tuned parameter set AUET2 [50] is used with PYTHIA 6, HERWIG 6 and PYTHIA 8 (except that the tune P2011C [51] is used for the POWHEG + PYTHIA $t\bar{t}$ sample), and the set UEEE3 [52] is used with HERWIG++. The effect of additional proton-proton collisions in the same or neighbouring bunch crossings, called "pile-up", is modelled by overlaying minimum-bias events, simulated with PYTHIA-8.160 using the AUET2 tune, onto the original hard-scattering event. Simulated events are weighted to reproduce the observed distribution of the average number of collisions per bunch crossing in data. Monte Carlo samples are passed through a detector simulation [53] based on GEANT4 [54] or on a fast simulation using a parametric response to the showers in the electromagnetic and hadronic calorimeters [55] and GEANT4-based simulation elsewhere.

Simulated events are reconstructed with the same algorithms as data. Corrections derived from data control samples are applied to account for differences between data and simulation for the lepton trigger and reconstruction efficiencies, momentum scale and resolution, and for the efficiency and mis-tag rate for tagging jets originating from b-quarks.

4 Physics object reconstruction

Jets are reconstructed from topological clusters [56, 57] formed from calorimeter cells by using the anti-k_t algorithm [58, 59] with a cone size parameter of 0.4 implemented in the FASTJET package [60]. Jet energies are corrected [57] for detector inhomogeneities and the non-compensating response of the calorimeter using factors derived from test beam, cosmic ray and pp collision data, as well as from the detailed GEANT4 detector simulation. The impact of multiple overlapping pp interactions is accounted for using a technique,

JHEP06(2014)035

based on jet areas, that provides an event-by-event and jet-by-jet pile-up correction [61]. Selected jets are required to have transverse momentum $p_{\mathrm{T}} > 40$ GeV and $|\eta| < 2.8$. The identification of b-jets is performed using a neural-network-based b-tagging algorithm [62] with an efficiency of 70% in simulated $t\bar{t}$ events. The probabilities for mistakenly b-tagging a jet originating from a c-quark or a light-flavour parton are approximately 20% and 1% [63, 64], respectively. The kinematic requirements on b-jets are $p_{\mathrm{T}} > 20$ GeV and $|\eta| < 2.5$. Signal jets and b-jets are selected independently, hence b-jets with $p_{\mathrm{T}} > 40$ GeV are included in both jet and b-jet multiplicities.

Electron candidates are reconstructed using a cluster in the electromagnetic calorimeter matched to a track in the inner detector. Preselected electrons must satisfy the "medium" selection criteria described in ref. [65], re-optimised for 2012 data, and fulfil $p_{\mathrm{T}} > 10$ GeV, $|\eta| < 2.47$ and requirements on the impact parameter of the track. Muon candidates are identified by matching an extrapolated inner detector track to one or more track segments in the muon spectrometer [66]. Preselected muons must fulfil $p_{\mathrm{T}} > 10$ GeV and $|\eta| < 2.5$.

Signal leptons are defined by requiring tighter quality criteria and increasing the p_{T} threshold to 15 GeV. Signal electrons must satisfy the "tight" selection criteria [65]. In addition, for both the signal electrons and muons, isolation requirements based on tracking and calorimeter information and impact parameter requirements are applied. The electron track isolation discriminant is computed as the summed scalar p_{T} of additional tracks inside a cone of radius $\Delta R = \sqrt{(\Delta\eta)^2 + (\Delta\phi)^2} = 0.2$ around the electron. The tracks considered must originate from the same vertex associated with the electron and have $p_{\mathrm{T}} > 0.4$ GeV. The electron calorimeter isolation discriminant is defined as the scalar sum of the transverse energy, E_{T}, of topological clusters within a cone of radius $\Delta R = 0.2$ around the electron cluster and is corrected for any contribution from the electron energy and pile-up. The muon track and calorimeter isolation discriminants are the same as the ones used for electrons, except for the isolation cone radius being $\Delta R = 0.3$ and calorimeter cells around the muon extrapolated track being used for the calorimeter isolation discriminant. For leptons with $p_{\mathrm{T}} < 60$ GeV, both track and calorimeter isolation are required to be smaller than 6% and 12% of the electron's and muon's p_{T}, respectively. For leptons with $p_{\mathrm{T}} > 60$ GeV, an upper limit of 3.6 GeV and 7.2 GeV is imposed on both the calorimeter and track isolation requirements for electrons and muons, respectively. The track associated with the electron or muon candidate must have a longitudinal impact parameter z_0 satisfying $|z_0 \sin\theta| < 0.4$ mm and fulfil the requirement for the significance of the transverse impact parameter, d_0, of $|d_0/\sigma(d_0)| < 3$. The track parameters z_0 and d_0 are defined with respect to the reconstructed primary vertex. For events with multiple vertices along the beam axis, the vertex with the largest $\sum p_{\mathrm{T}}^2$ of associated tracks is taken as the primary vertex. Furthermore, the primary vertex must be made of at least five tracks with $p_{\mathrm{T}} > 0.4$ GeV and its position must be consistent with the beam spot envelope.

Ambiguities between the reconstructed jets and leptons are resolved by applying the following criteria sequentially. Jets with a separation $\Delta R < 0.2$ from an electron candidate are rejected. Any lepton candidate with a distance $\Delta R < 0.4$ to the closest remaining jet is discarded. If an electron and a muon have a separation $\Delta R < 0.1$, the electron is discarded. For these requirements, jets with $p_{\mathrm{T}} > 20$ GeV and preselected leptons are considered.

JHEP06(2014)035

The missing transverse momentum vector, $\boldsymbol{p}_{\mathrm{T}}^{\mathrm{miss}}$ with magnitude $E_{\mathrm{T}}^{\mathrm{miss}}$, is constructed as the negative of the vector sum of the calibrated transverse momenta of all muons and electrons with $p_{\mathrm{T}} > 10$ GeV, jets with $p_{\mathrm{T}} > 20$ GeV and calorimeter energy clusters with $|\eta| < 4.9$ not assigned to these objects [67].

5 Event selection

Events are selected using a combination (logical OR) of $E_{\mathrm{T}}^{\mathrm{miss}}$ and non-isolated single-lepton and dilepton triggers. The thresholds applied to $E_{\mathrm{T}}^{\mathrm{miss}}$ and the leading and subleading lepton p_{T} are lower than those applied offline to ensure that trigger efficiencies are constant in the phase space of interest. The trigger threshold for $E_{\mathrm{T}}^{\mathrm{miss}}$ is 80 GeV. The p_{T} thresholds for single-lepton triggers are 60 GeV and 36 GeV for electrons and muons, respectively. The dilepton triggers feature lower thresholds in p_{T}, down to 12 GeV for electrons and 8 GeV for muons, allowing events with multiple soft leptons to be kept. The efficiencies of $E_{\mathrm{T}}^{\mathrm{miss}}$-only triggers in the phase space of interest are close to 100%. The electron triggers reach efficiencies above 95% and muon triggers have efficiencies between 75% and 100%, being lowest in the region $|\eta| < 1.05$.

Events from non-collision backgrounds are rejected using dedicated quality criteria [57]. Events of interest are selected if they contain at least two leptons passing the requirements described in section 4 and if the highest-p_{T} lepton satisfies $p_{\mathrm{T}} > 20$ GeV. Events with a leading pair of leptons having an invariant mass $m_{\ell\ell} < 12$ GeV are removed. This requirement rejects events with pairs of energetic leptons from decays of heavy hadrons and has negligible impact on the signal acceptance.

5.1 Signal regions

The signal regions are determined with an optimisation procedure using simulated events from the simplified models illustrated in figure 1. The data are divided into two mutually exclusive SS and 3L samples. In the SS sample, the two highest-p_{T} leptons must have the same electric charge and fulfil $p_{\mathrm{T}} >$ [20,15] GeV, and there must be no other signal lepton with $p_{\mathrm{T}} > 15$ GeV. In the 3L sample, the three highest-p_{T} leptons must fulfil $p_{\mathrm{T}} >$ [20,15,15] GeV, respectively. No requirements on the total electric charge are applied to this sample. Good sensitivity to the signatures in all signal models is obtained by defining five non-overlapping signal regions with selection requirements based on the following kinematic variables: $E_{\mathrm{T}}^{\mathrm{miss}}$; jet and b-jet multiplicities (N_{jets} and $N_{b-\mathrm{jets}}$); effective mass m_{eff} computed from all signal leptons and selected jets as $m_{\mathrm{eff}} = E_{\mathrm{T}}^{\mathrm{miss}} + \sum p_{\mathrm{T}}^{\ell} + \sum p_{\mathrm{T}}^{\mathrm{jet}}$; transverse mass computed from the highest-p_{T} lepton (ℓ_1) and $E_{\mathrm{T}}^{\mathrm{miss}}$ as $m_{\mathrm{T}} = \sqrt{2p_{\mathrm{T}}^{\ell_1} E_{\mathrm{T}}^{\mathrm{miss}}(1 - \cos[\Delta\phi(\ell_1, p_{\mathrm{T}}^{\mathrm{miss}})])}$; and invariant mass $m_{\ell\ell}$ computed with opposite-charge same-flavour leptons.

As detailed in table 1, the selection requirements of the five signal regions are:

- **SR3b**: SS or 3L events with at least five jets and at least three b-jets;
- **SR0b**: SS events with at least three jets, zero b-jets, large $E_{\mathrm{T}}^{\mathrm{miss}}$ and large m_{T};

JHEP06(2014)035

SR	Leptons	$N_{b-\text{jets}}$	Other variables	Additional requirement on m_{eff}
SR3b	SS or 3L	≥ 3	$N_{\text{jets}} \geq 5$	m_{eff}>350 GeV
SR0b	SS	$= 0$	$N_{\text{jets}} \geq 3$, $E_{\text{T}}^{\text{miss}}$> 150 GeV, m_{T}> 100 GeV	m_{eff}>400 GeV
SR1b	SS	≥ 1	$N_{\text{jets}} \geq 3$, $E_{\text{T}}^{\text{miss}}$> 150 GeV, m_{T}>100 GeV, SR3b veto	m_{eff}>700 GeV
SR3Llow	3L	—	$N_{\text{jets}} \geq 4$, $50 < E_{\text{T}}^{\text{miss}} < 150$ GeV, Z boson veto, SR3b veto	m_{eff}>400 GeV
SR3Lhigh	3L	—	$N_{\text{jets}} \geq 4$, $E_{\text{T}}^{\text{miss}}$> 150 GeV, SR3b veto	m_{eff}>400 GeV

Table 1. Definition of the signal regions (see text for details).

- **SR1b**: similar to SR0b, but with at least one b-jet;
- **SR3Llow**: 3L events with at least four jets, small $E_{\text{T}}^{\text{miss}}$ and Z boson veto;
- **SR3Lhigh**: 3L events with at least four jets and large $E_{\text{T}}^{\text{miss}}$.

The Z boson veto in SR3Llow rejects events with any opposite-charge same-flavour lepton combination of invariant mass $84 < m_{\ell\ell} < 98$ GeV. An additional m_{eff} requirement is applied to maximise the expected significance of selected SUSY models in each signal region. This requirement on m_{eff} is relaxed in the model-dependent limit-setting procedure described in section 7.2. The signal regions are all mutually exclusive. An SR3b veto, which rejects events satisfying the SR3b selection, is included in the definition of other signal regions that would otherwise have a small overlap with SR3b.

Each signal region is motivated by different SUSY scenarios and different SUSY parameter settings. The SR3b signal region targets gluino-mediated top squark scenarios resulting in signatures with four b-quarks. This signal region does not require large values of $E_{\text{T}}^{\text{miss}}$ or m_{T}, hence it is sensitive to compressed scenarios with small mass differences or to unstable LSPs. The SR0b signal region is sensitive to gluino-mediated and directly produced squarks of the first and second generations, which do not enhance the production of b-quarks. Third-generation squark models resulting in signatures with two b-quarks, such as direct bottom squark or gluino-mediated top squark $\rightarrow c\tilde{\chi}_1^0$ production, are targeted by SR1b. The 3L signal regions have no requirement on the number of b-jets. They target scenarios where squarks decay in multi-step cascades, such as gluino-mediated (or direct) squark $\rightarrow q'WZ\tilde{\chi}_1^0$ and gluino-mediated (or direct) squark $\rightarrow$ sleptons (see figure 1). The signal region with low $E_{\text{T}}^{\text{miss}}$ requirement, SR3Llow, targets compressed regions of the phase space where SUSY decay cascades would produce off-shell W and Z bosons. Backgrounds from Z boson production in association with jets are suppressed by a Z boson veto. Models with large $E_{\text{T}}^{\text{miss}}$ and on-shell vector bosons are targeted by SR3Lhigh. Hence no Z boson veto is applied in this signal region, but Z + jets backgrounds are suppressed by the larger $E_{\text{T}}^{\text{miss}}$ requirement.

JHEP06(2014)035

6 Background estimation

Searches in SS and 3L events are characterised by low SM backgrounds. Three main classes of backgrounds can be distinguished. They are, in decreasing order of importance for this search: (1) prompt multi-leptons, (2) "fake" leptons, which denotes hadrons mis-identified as leptons, leptons originating from heavy-flavour decays, and electrons from photon conversions, and (3) charge mis-measured leptons.

6.1 Background estimation methods

6.1.1 Prompt lepton background

The background with prompt leptons arises mainly from W or Z bosons, decaying leptonically, produced in association with a top-antitop quark pair where at least one of the top quarks decays leptonically, and from diboson processes (WZ, ZZ, $W^{\pm}W^{\pm}$) in association with jets. The $t\bar{t}V$ and diboson backgrounds are dominant for signal regions with and without b-jets, respectively. The prompt multi-lepton backgrounds are estimated from Monte Carlo samples normalised to NLO calculations as described in section 3. The rarer processes $t\bar{t}H$, single top quark plus a Z boson, $t\bar{t}t\bar{t}$ and VVV+jets, each of which constitutes at most 10% of the background in the signal regions, are also included. The production of $t\bar{t}WW$, WH and ZH (where the Higgs boson decay can produce isolated leptons from W, Z or τ) were verified to give a negligible contribution to the signal regions.

6.1.2 Fake-lepton background

The number of events with at least one fake lepton is estimated using a data-driven method. A fake-enriched class of "loose" leptons is introduced, composed of preselected leptons (defined in section 4) with $p_{\mathrm{T}} > 15$ GeV failing the signal lepton selection. If the ratio of the number of signal leptons to the number of loose leptons is known separately for prompt and fake leptons, the number of events with at least one fake lepton can be predicted. For illustration, when only pairs of leptons are considered, the equation that relates the number of events with signal (S) or loose (L) leptons to the number of events with prompt (P) or fake (F) leptons:

$$\begin{pmatrix} N_{SS} \\ N_{SL} \\ N_{LS} \\ N_{LL} \end{pmatrix} = \Lambda \cdot \begin{pmatrix} N_{PP} \\ N_{PF} \\ N_{FP} \\ N_{FF} \end{pmatrix}, \tag{6.1}$$

where the first and second indices refer to the leading and subleading lepton of the pairs, can be inverted to obtain the expected number of events with at least one fake lepton. The matrix Λ is given by

$$\Lambda = \begin{pmatrix} \varepsilon_1\varepsilon_2 & \varepsilon_1\zeta_2 & \zeta_1\varepsilon_2 & \zeta_1\zeta_2 \\ \varepsilon_1(1-\varepsilon_2) & \varepsilon_1(1-\zeta_2) & \zeta_1(1-\varepsilon_2) & \zeta_1(1-\zeta_2) \\ (1-\varepsilon_1)\varepsilon_2 & (1-\varepsilon_1)\zeta_2 & (1-\zeta_1)\varepsilon_2 & (1-\zeta_1)\zeta_2 \\ (1-\varepsilon_1)(1-\varepsilon_2) & (1-\varepsilon_1)(1-\zeta_2) & (1-\zeta_1)(1-\varepsilon_2) & (1-\zeta_1)(1-\zeta_2) \end{pmatrix}, \tag{6.2}$$

JHEP06(2014)035

where ε_1 and ε_2 (ζ_1 and ζ_2) are the ratios of the number of signal and loose leptons for the leading and subleading prompt (fake) leptons, respectively. This analysis employs a generalised matrix method where an arbitrary number of loose leptons can be present in the event. For example, an event containing three leptons that pass, in decreasing order of p_{T}, the signal-loose-signal selections is considered a SS signal event if the first and third lepton have the same charge. In addition, this event is included in the fake-lepton background calculation for 3L events since the second lepton passes only the loose selections. In general, eqs. (6.1)–(6.2) are adapted by dynamically adjusting the size of the matrix Λ according to the number of loose leptons in the event under study. No upper limit on the number of loose leptons is set. Each event is employed in all its possible incarnations (signal and/or as part of the background calculation) as illustrated in the example above, but is only included in one of the signal regions, which are exclusive by definition.

The efficiencies ε and ζ are measured in data as a function of the lepton p_{T} and η. The prompt lepton efficiencies are determined from a data sample enriched with prompt leptons from $Z \to \ell^+\ell^-$ decays, obtained by requiring $80 < m_{\ell\ell} < 100$ GeV. As the background is dominated by events with one real lepton and one fake lepton, the fake-lepton efficiencies are measured from a data set enriched with one prompt muon (by requiring it to pass the signal lepton selection and $p_{\mathrm{T}} > 40$ GeV) and an additional fake lepton (by requiring it to pass the loose selections). The fake electron background has contributions from heavy flavour decays, as well as from conversions and fake pions. The fake-electron efficiency is therefore determined from two samples of SS $e\mu$ events to be sensitive to the different types of fake electrons, one with a b-jet veto and another with at least one b-jet. The fake-muon efficiency is determined from a sample of same-sign dimuon events where at least two jets with $p_{\mathrm{T}} > 25\,\mathrm{GeV}$ are required. The event yields in these control regions are corrected for the contamination of prompt SS using Monte Carlo simulation. The $e\mu$ SS control regions are also corrected for the presence of charge mis-measured electrons using the likelihood fit method described in section 6.1.3, but applied to loose electrons. The contamination from signal events is verified to be negligible in the same-sign $e\mu$ and $\mu\mu$ control regions. The size of the data sample is not sufficient to allow the extraction of the fake-lepton efficiencies for muons with $p_{\mathrm{T}} > 40\,\mathrm{GeV}$ or for events with at least three b-jets. For these events the fake-lepton efficiencies obtained from data in similar kinematic regions, i.e. muons with $25 < p_{\mathrm{T}} < 40$ GeV or events with at least one b-jet, are employed and corrected with extrapolation factors obtained from the $t\bar{t}$ Monte Carlo samples.

6.1.3 Background from lepton charge mis-measurement

Background from charge mis-measurement, commonly referred to as "charge-flip", consists of events with two opposite-sign leptons for which the charge of a lepton is mis-identified. Such events constitute a background only for the SS signal regions. The dominant mechanism of charge mis-identification is due to the radiation of a hard photon from an electron followed by an asymmetric conversion, for which the electron with the opposite charge has the larger p_{T} ($e^{\pm} \to e^{\pm}\gamma \to e^{\mp}e^{\pm}e^{\pm}$). The probability of mis-identifying the charge of a muon is determined in simulation to be negligible in the kinematic range relevant to this analysis. The electron charge-flip background is estimated using a fully data-driven tech-

JHEP06(2014)035

nique. The charge-flip probability is extracted in two Z boson control samples, one with same-sign electron pairs and the other with opposite-sign electron pairs. The invariant mass of these same-sign and opposite-sign electron pairs is required[3] to be between 75 GeV and 100 GeV. Background events are subtracted using the invariant mass sidebands. A likelihood fit is employed which takes as input the numbers of same-sign and opposite-sign electron pairs observed in the sample. The charge-flip probability is a free parameter of the fit and is extracted as a function of the electron p_{T} and η. The probability of electron charge-flip varies from approximately 10^{-4} to 10^{-2} in the range $0 \leq |\eta| \leq 2.47$ and $15 < p_{\mathrm{T}} < 200$ GeV, increasing with electron $|\eta|$ and p_{T}. The event yield of this background in the signal regions is obtained by applying the measured charge-flip probability to data regions with the same kinematic requirements as the signal regions but with opposite-sign lepton pairs. The contamination from fake leptons and signal events is found to be negligible in these opposite-sign control regions.

6.2 Systematic uncertainties on the background estimation

The systematic uncertainties on the sources of prompt SS and 3L events arise from the Monte Carlo simulation and normalisation of these processes. The cross sections used to normalise the Monte Carlo samples are varied according to the uncertainty on the theory calculation, i.e. 22% for $t\bar{t}W$ [40] and $t\bar{t}Z$ [41] and 7% for diboson production (computed with MCFM [42], considering scales, parton distribution functions and α_s uncertainties). Normalisation uncertainties between 35% and 100% are applied to processes with smaller contributions. Uncertainties caused by the limited accuracy of the $t\bar{t}V$+jets and diboson+jets Monte Carlo generators are estimated by varying the renormalisation and factorisation scales and the QCD initial- and final-state radiation used to generate these samples. Additional Monte Carlo modelling uncertainties are included, such as the limited number of hard jets that can be produced from matrix element calculations in the MadGraph+Pythia and Sherpa samples, which is the largest modelling uncertainty for the diboson+jets process, and the difference between the predictions of various Monte Carlo generators such as MadGraph versus Alpgen, which is the largest modelling uncertainty for the $t\bar{t}V$+jets process.

Monte Carlo simulation-based estimates also suffer from detector simulation uncertainties. These are dominated by the uncertainties on the jet energy scale and the b-tagging efficiency. The jet energy scale uncertainty is derived using a combination of simulations, test beam data and *in situ* measurements [57, 68]. Additional contributions from the jet flavour composition, calorimeter response to different jet flavours, pile-up and b-jet calibration uncertainties are taken into account. The efficiency to tag real and fake b-jets is corrected in Monte Carlo events by applying b-tagging scale factors, extracted in $t\bar{t}$ and dijet samples, that compensate for the residual difference between data and simulation [62, 64, 69]. The associated systematic uncertainty is computed by varying the scale factors within their uncertainty. Uncertainties in the jet energy resolution are obtained

[3] An asymmetric window around the Z boson mass is chosen because charge-flip electrons lose more energy in the detector than electrons for which the charge is properly reconstructed.

JHEP06(2014)035

Background	Method	SR3b	SR0b	SR1b	SR3Llow	SR3Lhigh
Charge-flip	Nominal	0.2 ± 0.1	0.2 ± 0.1	0.5 ± 0.1	–	–
	Tag and probe	0.2 ± 0.1	0.2 ± 0.1	0.5 ± 0.2	–	–
Fake	Nominal	0.7 ± 0.6	$1.2^{+1.5}_{-1.2}$	$0.8^{+1.2}_{-0.8}$	1.6 ± 1.6	< 0.1
	Monte Carlo based	$2.0^{+1.4}_{-1.3}$	5 ± 5	$0.6^{+1.4}_{-0.6}$	$1.0^{+0.8}_{-0.7}$	< 0.1
Total 3 b-jets	Nominal	2.1 ± 0.7	–	–	–	–
	b-jets matrix method	2.9 ± 0.9	–	–	–	–

Table 2. Comparison of the predicted number of background events in the signal regions using the nominal and cross-check methods. Both the statistical and systematic uncertainties are included.

with an *in situ* measurement of the jet response asymmetry in dijet events [70]. Other uncertainties on the lepton reconstruction [65, 71], calibration of calorimeter energy clusters not associated with physics objects in the $E_{\mathrm{T}}^{\mathrm{miss}}$ calculation [67], luminosity [27] and simulation of pile-up events are included but have a negligible impact on the final results.

The fake-lepton background uncertainty includes the statistical uncertainty from the SS control regions, the dependence of the fake-lepton efficiency on the event selections and the contamination of the SS control regions by real leptons. Uncertainties on the extrapolation of the fake-lepton efficiency to poorly populated kinematic regions are estimated by comparing the prediction of different $t\bar{t}$ Monte Carlo samples. For the charge-flip background prediction, the main uncertainties originate from the statistical uncertainty of the charge-flip probability measurements and the background contamination of the sample used to extract the charge-flip probability.

6.3 Cross-checks of the data-driven background estimates

Three alternative methods were developed to cross-check the background estimates from data-driven methods. The results are summarised in table 2, showing the background predictions for the nominal methods, described in section 6.1, and the cross-check methods described below. In each case consistent predictions are obtained, but with generally larger uncertainties for the alternative methods.

For the electron charge-flip background, a simpler "tag and probe" method is employed which selects electron pairs with an invariant mass consistent with a Z boson decay. One electron is required to have $|\eta| < 1.37$. Its charge is assumed to be measured correctly. The charge-flip probability is extracted as a function of p_{T} and η of the other electron, which is required to be in the pseudorapidity region $1.52 < |\eta| < 2.47$, by computing the ratio of same-sign to opposite-sign pairs. The charge-flip probability for central electrons is extracted by requiring that both electrons are in the same p_{T} and η region. This charge-flip probability is applied in the same manner as the nominal charge-flip probability, as described in section 6.1, to obtain a prediction in the signal regions.

The fake-lepton background estimate were cross-checked with a simulation-based technique. This method relies on kinematic extrapolation from control regions, with low jet

JHEP06(2014)035

multiplicity and $E_{\mathrm{T}}^{\mathrm{miss}}$, to the signal regions that require high jet multiplicity and $E_{\mathrm{T}}^{\mathrm{miss}}$. The separate control regions are characterised by the presence or the absence of a b-jet, and by the flavours of the two leading leptons. Backgrounds with prompt leptons are obtained from Monte Carlo simulation as described in section 6.1.1. Backgrounds with fake leptons and charge-flip electrons are obtained from Monte Carlo simulations normalised to match data in the control regions. The normalisation is done using five multipliers. One multiplier is used to correct the rate of electron charge mis-identifications. The other four corrections are for processes producing either fake electrons or muons that originate from b-jets or light jets.

The background in the SR3b region is expected to be completely dominated by events with at least one light or charm jet mis-tagged as a b-jet, i.e. a fake b-tag. A cross-check of the background estimate in this signal region is performed by determining the number of events with at least one fake b-tag. A generalised matrix method applied to the estimation of fake b-tags is used, similar to that described in section 6.1.2, with the following differences. Loose leptons are replaced by jets, signal leptons by b-tagged jets, and the different tight/loose incarnations are combined in each event. The efficiency for fake b-tags is estimated in a $t\bar{t}$-enriched sample with at least one signal lepton, at least four jets with $p_{\mathrm{T}} > 20\,\mathrm{GeV}$, of which at least two must be b-tagged, and $100 < E_{\mathrm{T}}^{\mathrm{miss}} < 200$ GeV. The efficiency for fake b-tags is calculated using the additional b-jets found in each event after subtracting contamination from events with three or more real b-jets (such as $t\bar{t}b\bar{b}$). The efficiency to tag real b-jets is determined independently of the efficiency for fake b-tags, as described in refs. [62, 69]. The efficiencies for tagging real and fake b-jets are fed into the matrix method to predict the background in SR3b. Small contributions from processes with three real b-jets are estimated from simulation.

6.4 Validation of background estimates

The data-driven background estimates are based on control regions that employ less stringent requirements on the jet and b-jet multiplicities, total transverse energy and/or $E_{\mathrm{T}}^{\mathrm{miss}}$ than the signal regions. To ensure their validity in the signal regions, the background estimates are validated in events with kinematic properties closer to the signal regions. This is first performed by individually probing each of the kinematic variables used to define the signal regions in events containing a same-sign lepton pair. The event is not rejected if it contains more than two leptons. Several relevant kinematic distributions are studied for each lepton channel and for events with and without a b-jet. No significant discrepancies are observed. Some example distributions are shown in figure 2.

Each of the background types (fake electron, fake muon, charge-flip electron and prompt SS) is dominant, and thus validated directly, in particular regions of the kinematic phase space examined by these SS validation regions. However, the prompt SS contributions are typically dominated by inclusive WZ production, while the prompt SS or 3L background in the signal regions is expected to be dominated by $t\bar{t}V$ and WZ events produced in association with several hard jets. The Monte Carlo modelling of these rare processes is tested in a further set of dedicated validation regions. The event selections are presented in table 3. They are based on the object definitions described in section 4, and

JHEP06(2014)035

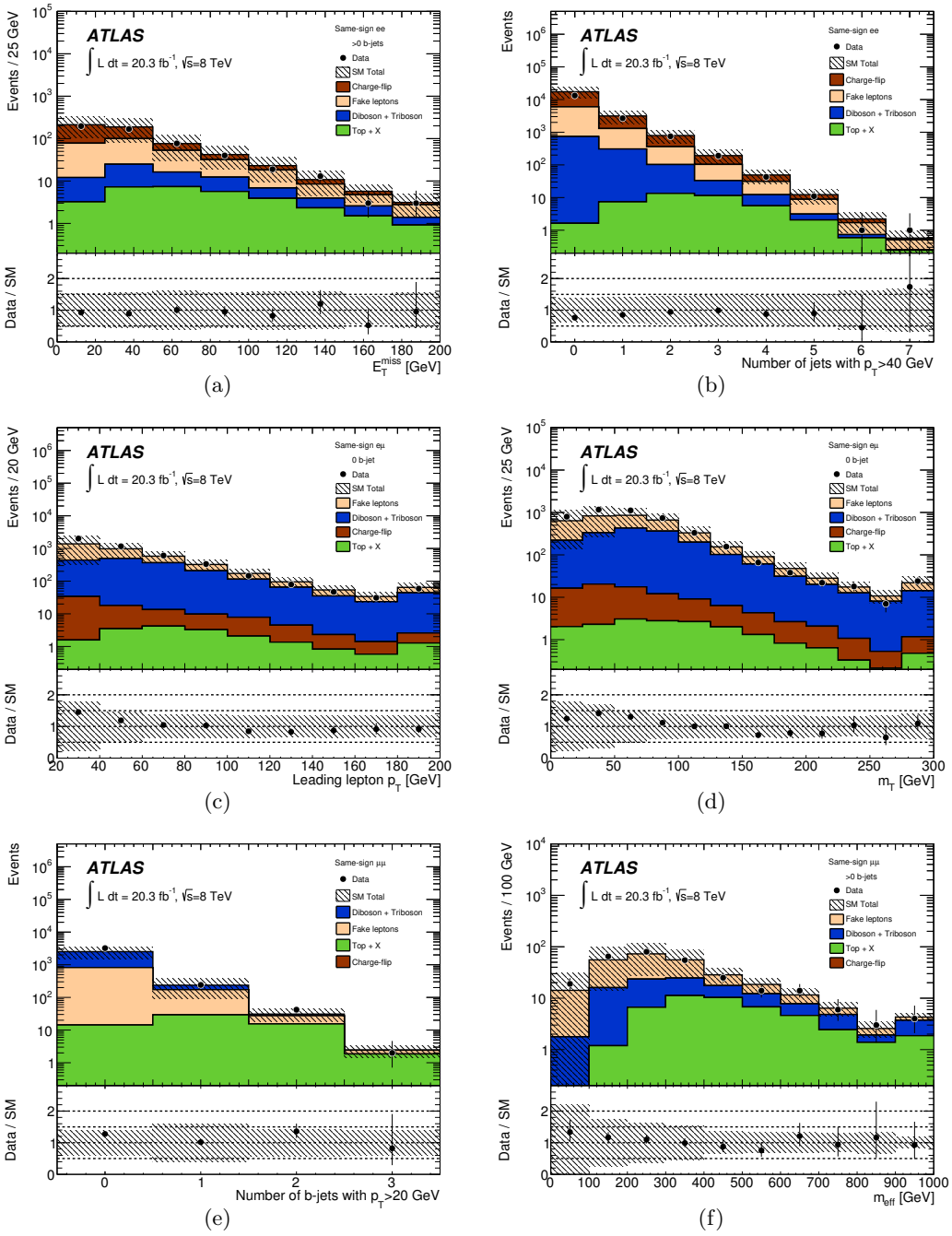

Figure 2. Distributions of kinematic variables in SS background validation regions: (a) $E_{\mathrm{T}}^{\mathrm{miss}}$ for events with at least one b-jet and (b) number of jets for the ee channel, (c) leading lepton p_{T} for events with no b-jet and (d) transverse mass, m_{T}, for events with no b-jet for the $e\mu$ channel, and (e) number of b-jets and (f) effective mass, m_{eff}, for events with at least one b-jet for the $\mu\mu$ channel. The statistical and systematic uncertainties on the background prediction are included in the uncertainty band. The last bin includes overflows. The lower part of the figure shows the ratio of data to the background prediction.

JHEP06(2014)035

Background Probed	Leptons ($p_{\mathrm{T}} > 20$ GeV)	N_{jets}	$N_{b-\mathrm{jets}}$	$E_{\mathrm{T}}^{\mathrm{miss}}$ (GeV)	m_{T} (GeV)	Additional cuts
$t\bar{t}W$	SS $\mu\mu$	≥ 1 (30 GeV)	$= 2$	20 to 120	> 80	–
$t\bar{t}Z$	3L	≥ 2 (40 GeV)	1 or 2	20 to 120	–	$m_{\mathrm{eff}} > 300$ GeV, Z boson mass
WZ+jets	SS $\mu\mu$	≥ 2 (20 GeV)	Veto	20 to 120	> 100	–

Table 3. Definition of the validation regions for rare SM backgrounds. The required jet p_{T} threshold is indicated in parentheses under the column N_{jets}. The Z boson mass cut demands at least one opposite-charge same-flavour lepton pair satisfying $84 < m_{\ell\ell} < 98$ GeV.

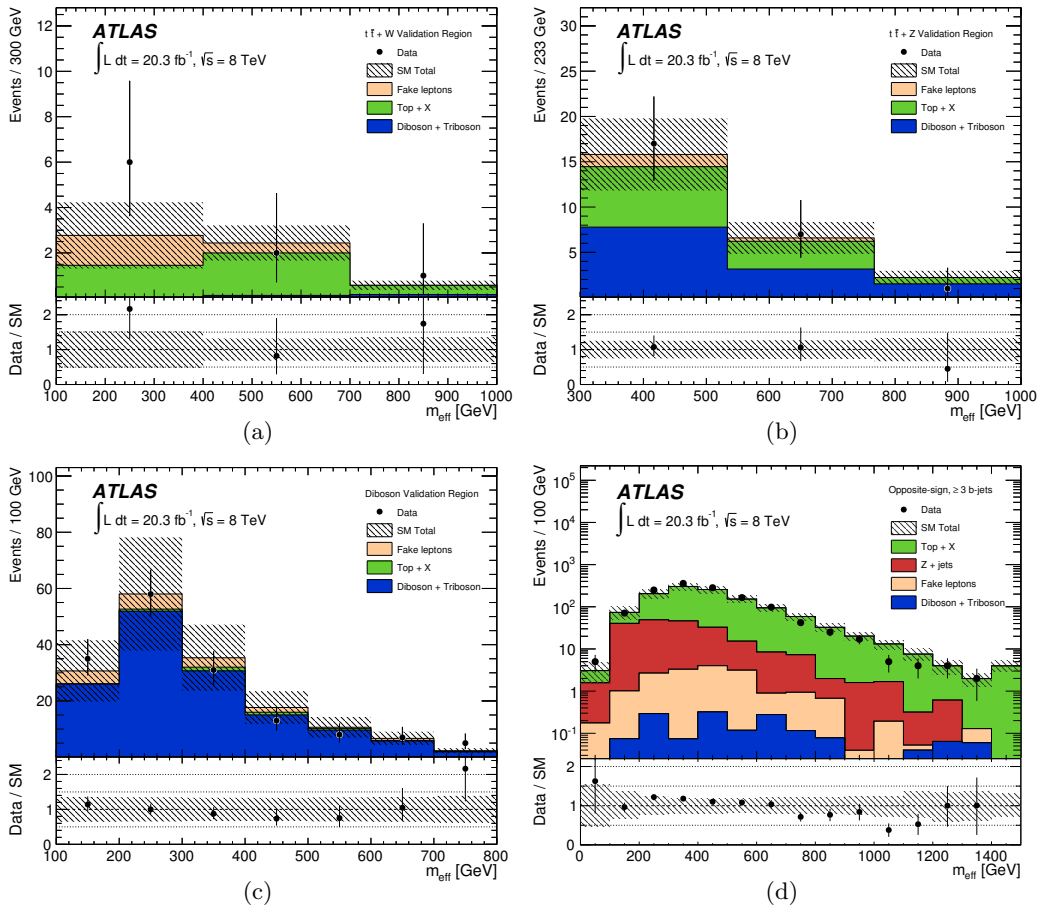

Figure 3. Effective mass (m_{eff}) distributions for the (a) $t\bar{t}W$, (b) $t\bar{t}Z$, (c) WZ+jets and (d) OS plus three b-jets validation regions. The statistical and systematic uncertainties on the background prediction are included in the uncertainty band. The last bin includes overflows. The lower part of the figure shows the ratio of data to the background prediction.

impose different jet p_{T} thresholds and require $p_{\mathrm{T}} > 20$ GeV for the leptons to increase the rejection of fake-lepton events. The $t\bar{t}W$ and WZ+jets validation regions employ only SS $\mu\mu$ events to avoid fake-electron events. The signal contamination is verified to be negligible for the $t\bar{t}Z$ and WZ+jets validation regions and at most 25% for the $t\bar{t}W$ validation

JHEP06(2014)035

region for non-excluded SUSY models. The m_{eff} distributions of these validation regions are shown in figures 3(a)–3(c). The prediction is observed to agree with the data, therefore validating the Monte Carlo modelling of these rare SM processes.

The SR3b signal region receives a large contribution of $t\bar{t}V$ events where at least one light or charm jet is mis-tagged as a b-jet. The Monte Carlo modelling of this mis-tag rate is validated in a large opposite-sign dilepton sample where at least three b-tags are required. This sample is dominated by dilepton $t\bar{t}$ events where the third b-jet is mis-tagged. Figure 3(d) shows the m_{eff} distribution in this sample, for which the Monte Carlo simulation prediction is shown to describe the data.

7 Results and interpretation

Figure 4 shows the effective mass distribution of the observed data events and SM predictions for the five signal regions, after all selections except the one on m_{eff}. SUSY models of particular sensitivity to each signal region are also shown for illustration purposes. These models, illustrated in figure 1 and described in section 7.2, are: gluino-mediated top squark $\rightarrow bs$ (RPV) with gluino mass of 945 GeV and top squark mass of 417 GeV for SR3b; gluino-mediated squark $\rightarrow q'W\tilde{\chi}_1^0$ with gluino mass of 705 GeV, $\tilde{\chi}_1^\pm$ mass of 450 GeV and $\tilde{\chi}_1^0$ mass of 225 GeV for SR0b; gluino-mediated top squark $\rightarrow c\tilde{\chi}_1^0$ with gluino mass of 700 GeV, top squark mass of 400 GeV and $\tilde{\chi}_1^0$ mass of 380 GeV for SR1b; gluino-mediated squark $\rightarrow$ sleptons with gluino mass of 905 GeV, $\tilde{\chi}_2^0$ and $\tilde{\chi}_1^\pm$ masses of 705 GeV, slepton and sneutrino masses of 605 GeV and $\tilde{\chi}_1^0$ mass of 505 GeV for SR3Llow; and direct bottom squark $\rightarrow t\tilde{\chi}_1^\pm$ with bottom squark mass of 450 GeV, $\tilde{\chi}_1^\pm$ mass of 200 GeV and $\tilde{\chi}_1^0$ mass of 60 GeV for SR3Lhigh.

The numbers of observed data events and expected background events in the five signal regions, after the application of the additional requirements on m_{eff}, are presented in table 4. Expected signal yields from the SUSY models appearing in figure 4 are also shown. Diboson production in association with jets is a large source of background for signal regions that do not require the presence of b-jets, namely SR0b, SR3Llow and SR3Lhigh. In SR1b and SR3b, which require one or more b-jets, the largest background contribution arises from $t\bar{t}V$ events. The background from fake leptons is particularly significant in signal regions with no or low requirements on $E_{\text{T}}^{\text{miss}}$, such as SR3b and SR3Llow. Background from electron charge mis-identification is small in all SS signal regions, and not applicable in the 3L signal regions.

The level of agreement between the background prediction and data is quantified by computing the p-value for the number of observed events to be consistent with the background-only hypothesis, denoted by $p(s = 0)$ in table 4. To do so, the number of events in each signal region is described using a Poisson probability density function (pdf). The statistical and systematic uncertainties on the expected background values are modelled with nuisance parameters constrained by a Gaussian function with a width corresponding to the size of the uncertainty considered. The data and predicted background agree well for SR3b, SR3Llow and SR3Lhigh. No events with total electric charge of ± 3 are observed in the 3L signal regions. For SR0b and SR1b, small excesses are observed corresponding

JHEP06(2014)035

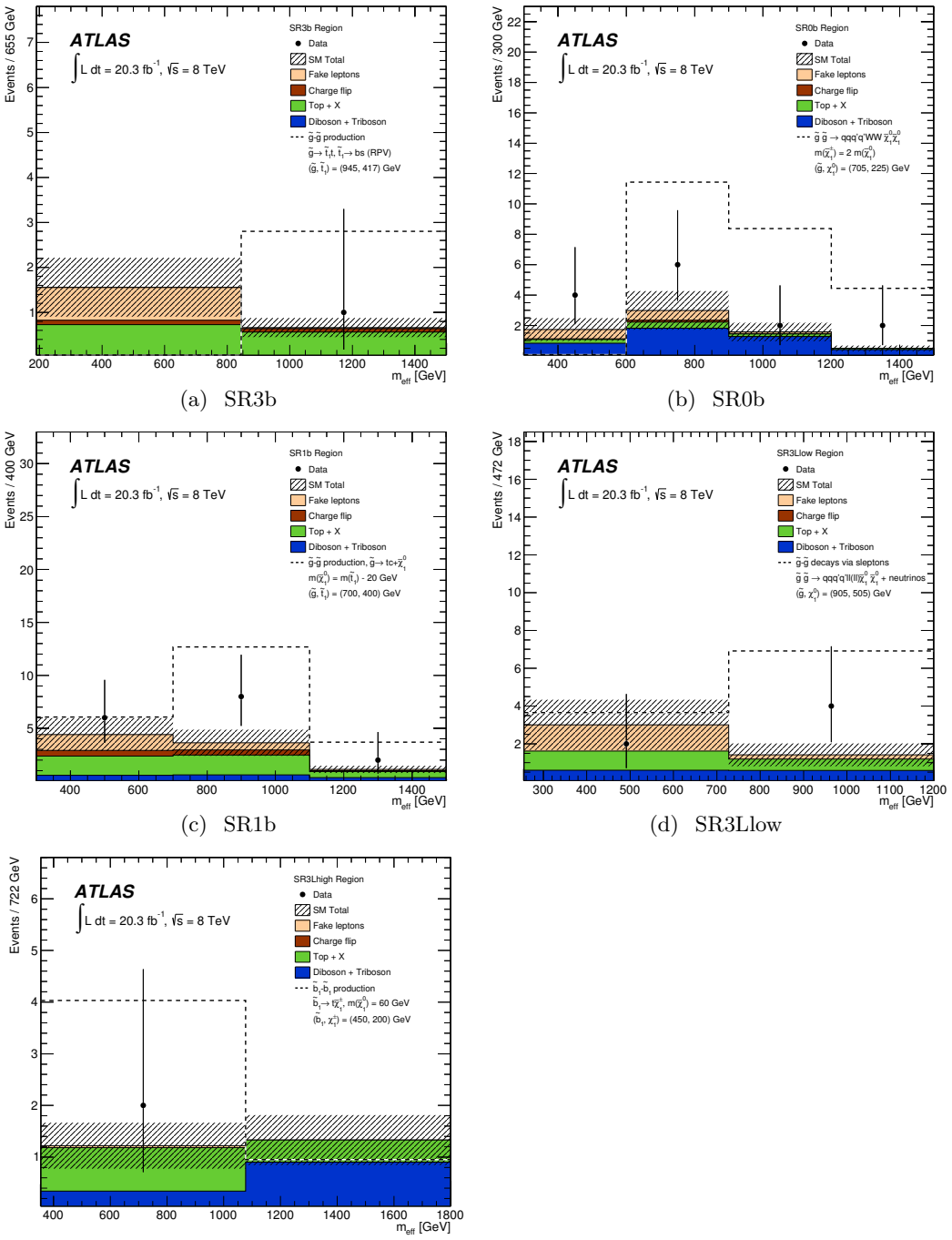

(a) SR3b (b) SR0b

(c) SR1b (d) SR3Llow

(e) SR3Lhigh

Figure 4. Effective mass (m_{eff}) distributions in the signal regions SR3b, SR0b, SR1b, SR3Llow and SR3Lhigh, used as input for the exclusion fits. The statistical and systematic uncertainties on the background prediction are included in the uncertainty band. The last bin includes overflows. Signal expectations from SUSY models of particular sensitivity in each signal region are shown for illustration (see text).

JHEP06(2014)035

	SR3b	SR0b	SR1b	SR3Llow	SR3Lhigh
Observed events	1	14	10	6	2
Total expected background events	2.2 ± 0.8	6.5 ± 2.3	4.7 ± 2.1	4.3 ± 2.1	2.5 ± 0.9
$p(s = 0)$	0.50	0.03	0.07	0.29	0.50
Expected signal events for chosen benchmark models	3.4 ± 0.7	24.3 ± 3.5	16.4 ± 3.0	10.6 ± 1.0	5.0 ± 0.8
Components of the background					
$t\bar{t}V$, $t\bar{t}H$, tZ and $t\bar{t}t\bar{t}$	1.3 ± 0.5	0.9 ± 0.4	2.5 ± 1.7	1.6 ± 1.0	1.3 ± 0.7
Dibosons and tribosons	< 0.1	4.2 ± 1.7	0.9 ± 0.4	1.2 ± 0.6	1.2 ± 0.6
Fake leptons	0.7 ± 0.6	$1.2^{+1.5}_{-1.2}$	$0.8^{+1.2}_{-0.8}$	1.6 ± 1.6	< 0.1
Charge-flip electrons	0.2 ± 0.1	0.2 ± 0.1	0.5 ± 0.1	—	—
Systematic uncertainties on expected background					
Fake-lepton background	± 0.6	$^{+1.5}_{-1.2}$	$^{+1.2}_{-0.8}$	± 1.6	< 0.1
Theory unc. on dibosons	< 0.1	± 1.5	± 0.3	± 0.4	± 0.4
Jet and $E_{\mathrm{T}}^{\mathrm{miss}}$ scale and resolution	± 0.1	± 0.7	± 0.4	± 0.4	± 0.3
Monte Carlo statistics	± 0.1	± 0.5	± 0.2	± 0.4	± 0.4
b-jet tagging	± 0.2	± 0.5	± 0.1	< 0.1	± 0.1
Theory unc. on $t\bar{t}V$, $t\bar{t}H$, tZ and $t\bar{t}t\bar{t}$	± 0.4	± 0.3	± 1.7	± 1.0	± 0.6
Trigger, luminosity and pile-up	< 0.1	± 0.1	± 0.1	± 0.1	± 0.1
Charge-flip background	± 0.1	± 0.1	± 0.1	—	—
Lepton identification	< 0.1	± 0.1	< 0.1	± 0.1	± 0.1

Table 4. Number of observed data events and expected backgrounds and summary of the systematic uncertainties on the background predictions for SR3b, SR0b, SR1b, SR3Llow and SR3Lhigh. The p-value of the observed events for the background-only hypothesis is denoted by $p(s = 0)$. By convention, the $p(s = 0)$ value is truncated at 0.50 when the number of observed data events is smaller than the expected backgrounds. The expected signal events correspond to the SUSY models considered for each signal region in figure 4 with their experimental uncertainties. The breakdown of the systematic uncertainties on the expected backgrounds, expressed in units of events, is also shown. The individual uncertainties are correlated and therefore do not necessarily add up in quadrature to the total systematic uncertainty.

to 1.8 and 1.5 standard deviations, respectively. The significance is calculated using the uncertainty on the total expected background yields quoted in table 4 and the Poissonian uncertainty of the total expected background value. If SR0b and SR1b are combined, the significance of the excess becomes 2.1 standard deviations.

Table 4 also presents the breakdown of uncertainties on the background predictions described in section 6.2. For all signal regions the background uncertainty is dominated by the statistical uncertainty on the expected number of background events. The largest systematic uncertainties arise from the estimation of the fake-lepton probability and from the theoretical predictions for diboson+jets and $t\bar{t}V$+jets processes. Uncertainties on the predicted background event yields are quoted as symmetric, except where the negative error reaches zero predicted events, in which case the negative error was truncated.

JHEP06(2014)035

Signal channel	$\langle\sigma_{\text{vis}}\rangle^{95}_{\text{obs}}$[fb]	S^{95}_{obs}	S^{95}_{exp}
SR3b	0.19	3.9	$4.4^{+1.7}_{-0.6}$
SR0b	0.80	16.3	$8.9^{+3.6}_{-2.0}$
SR1b	0.65	13.3	$8.0^{+3.3}_{-2.0}$
SR3Llow	0.42	8.6	$7.2^{+2.9}_{-1.3}$
SR3Lhigh	0.23	4.6	$5.0^{+1.6}_{-1.1}$

Table 5. The 95% CL upper limits on the visible cross section ($\langle\sigma_{\text{vis}}\rangle^{95}_{\text{obs}}$), defined as the product of acceptance, reconstruction efficiency and production cross section, and the observed and expected 95% CL upper limits on the number of BSM events (S^{95}_{obs} and S^{95}_{exp}). Results are obtained with pseudo-experiments.

7.1 Model-independent upper limits

No significant excess of events over the SM expectations is observed in any signal region. Upper limits at 95% CL on the number of beyond the SM (BSM) events for each signal region are derived using the CL_s prescription [72]. Normalising these by the integrated luminosity of the data sample, they can be interpreted as upper limits on the visible BSM cross section (σ_{vis}), where σ_{vis} is defined as the product of acceptance, reconstruction efficiency and production cross section. The results are given in table 5, where $\langle\sigma_{\text{vis}}\rangle^{95}_{\text{obs}}$ is the 95% CL upper limit on the visible cross section, and S^{95}_{obs} and S^{95}_{exp} are the observed and expected 95% CL upper limits on the number of BSM events, respectively. The limits presented in table 5 are calculated from pseudo-experiments. For comparison, corresponding limits calculated with asymptotic formulae [73] on the observed (expected) number of BSM events in SR3b, SR0b, SR1b, SR3Llow and SR3Lhigh are 3.8 (4.4), 15.9 (8.9), 12.6 (7.9), 8.4 (7.2), and 4.3 (5.0), respectively.

7.2 Model-dependent limits

The measurement is used to place exclusion limits on 14 SUSY models and one mUED model. For each model, the limits are calculated from asymptotic formulae with a simultaneous fit to all signal regions based on the profile likelihood method. When doing so, the final m_{eff} requirements are relaxed in each signal region (i.e. the requirements in the rightmost column in table 1 are not applied) and the fit inputs are the binned m_{eff} distributions shown in figure 4. Most of the nuisance parameters are correlated between all bins, except for uncertainties of statistical nature, which are modelled with uncorrelated parameters. The signal pdf is correlated in all bins and multiplied by an overall normalisation scale treated as a free parameter in the fit. This procedure increases the statistical power of the analysis for model-dependent exclusion.

The observed and expected limits resulting from the exclusion fits are displayed as solid red lines and dashed grey lines, respectively, in figures 5–8. The $\pm 1\sigma^{\text{SUSY}}_{\text{theory}}$ lines around the observed limits are obtained by changing the SUSY cross section by one standard deviation ($\pm 1\sigma$), as described in section 3. All mass limits on supersymmetric particles quoted later

JHEP06(2014)035

in this section are derived from the $-1\sigma^{\text{SUSY}}_{\text{theory}}$ theory line. The yellow band around the expected limit shows the $\pm 1\sigma$ uncertainty, including all statistical and systematic uncertainties except the theoretical uncertainties on the SUSY cross section. The uncertainties on the SUSY signal include the detector simulation uncertainties described in section 6.2. For simplified models, 95% CL upper limits on cross sections obtained using the signal efficiency and acceptance specific to each model are available in the HepData database [74]. When available, exclusion limits set by previous ATLAS searches [75–79] are also shown for comparison.

Three categories of simplified models are used to design the signal regions and interpret the results: gluino-mediated top squark, gluino-mediated (or direct) first- and second-generation squark, and direct bottom squark production, as illustrated in figure 1. In addition, three complete SUSY models and one mUED model are used for interpretation only.

7.2.1 Gluino-mediated top squarks

Results for four simplified models of gluino-mediated top squark production are presented in figure 5. In each case, gluinos are produced in pairs, the top squark $\tilde{t}_1$ is assumed to be the lightest squark, and the $\tilde{g} \to t\tilde{t}_1^{(*)}$ branching fraction is set to 100%. The top squark, however, decays to a different channel in each model: $\tilde{t}_1 \to t\tilde{\chi}_1^0$, $\tilde{t}_1 \to b\tilde{\chi}_1^{\pm}$, $\tilde{t}_1 \to c\tilde{\chi}_1^0$ or $\tilde{t}_1 \to bs$, with a 100% branching fraction.

In the gluino-mediated top squark $\to t\tilde{\chi}_1^0$ model, the mass of the top squark is set to $m_{\tilde{t}_1} = 2.5\,\text{TeV}$ and the masses of all other squarks are much higher (they are assumed to be decoupled). Gluinos decay through mediation by an off-shell top squark to a pair of top quarks and a stable neutralino, $\tilde{g} \to t\tilde{t}_1^* \to t\bar{t}\,\tilde{\chi}_1^0$. The final state is therefore $\tilde{g}\tilde{g} \to bbbb\,WWWW\,\tilde{\chi}_1^0\tilde{\chi}_1^0$, with the constraint that $m_{\tilde{g}} > 2m_t + m_{\tilde{\chi}_1^0}$. Results are interpreted in the parameter space of the gluino and $\tilde{\chi}_1^0$ masses (see figure 5(a)). Gluino masses below 950 GeV are excluded at 95% CL, for any $\tilde{\chi}_1^0$ mass. The sensitivity is dominated by SR3b.

In the gluino-mediated top squark $\to b\tilde{\chi}_1^{\pm}$ model, the top squark is on-shell, the $\tilde{\chi}_1^{\pm}$ mass is set to 118 GeV, the $\tilde{\chi}_1^0$ mass set to 60 GeV and the $\tilde{\chi}_1^0$ is stable. Hence the chargino decays through an off-shell W boson, and the final state is $\tilde{g}\tilde{g} \to bbbb\,WWW^*W^*\,\tilde{\chi}_1^0\tilde{\chi}_1^0$, with the constraint that $m_{\tilde{g}} > m_t + m_{\tilde{t}_1}$. Results are interpreted in the parameter space of the gluino and top squark masses (see figure 5(b)). Gluino masses below 1 TeV are excluded at 95% CL for top squark masses above 200 GeV. The sensitivity is dominated by SR3b.

In the gluino-mediated top squark $\to c\tilde{\chi}_1^0$ model, the on-shell top squark and stable neutralino have close-by masses, $\Delta m(\tilde{t}, \tilde{\chi}_1^0) = 20$ GeV, which forbids the top squark decay to a top quark but allows the decay to a charm quark. The final state is therefore $\tilde{g}\tilde{g} \to bb\,cc\,WW\,\tilde{\chi}_1^0\tilde{\chi}_1^0$, with the constraint that $m_{\tilde{g}} > m_t + m_c + m_{\tilde{\chi}_1^0}$. Results are interpreted in the parameter space of the gluino and top squark masses (see figure 5(c)). Gluino masses below 640 GeV are excluded at 95% CL, for any $\tilde{t}_1$ and $\tilde{\chi}_1^0$ masses. The sensitivity is dominated by SR1b.

In the gluino-mediated top squark $\to bs$ (RPV) model, top squarks are assumed to decay with an R-parity-violating and baryon-number-violating coupling $\lambda''_{323} = 1$, as pro-

JHEP06(2014)035

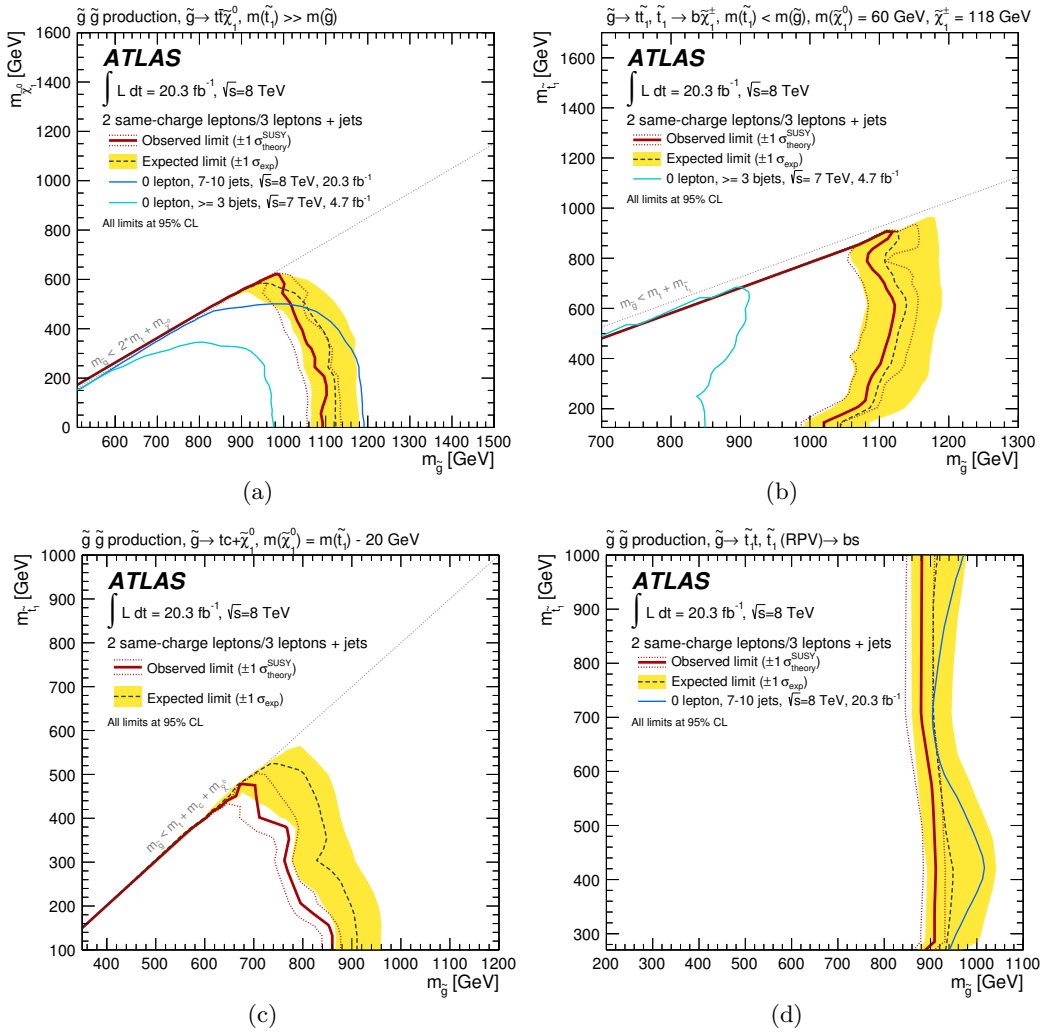

Figure 5. Observed and expected exclusion limits on gluino-mediated top squark production, obtained with 20.3 fb^{-1} of pp collisions at $\sqrt{s}$=8 TeV, for four different top squark decay modes (see text). When available, results are compared with the limits obtained by previous ATLAS searches [78, 79].

posed in ref. [80]. The final state is therefore $\tilde{g}\tilde{g} \to bbbb\ ss\ WW$, characterised by the presence of four b-quarks but only moderate missing transverse momentum. Results are interpreted in the parameter space of the gluino and top squark masses (see figure 5(d)). Gluino masses below 850 GeV are excluded at 95% CL, almost independently of the top squark mass. The sensitivity is dominated by SR3b.

Stringent limits are hence placed on gluino-mediated top squark scenarios favoured by naturalness arguments. The SR3b signal region is sensitive to almost any scenario with SS or $\geq$3 leptons and $\geq$3 b-quarks. This is demonstrated in the gluino-mediated top squark $\to bs$ (RPV) model, where $m_{\tilde{g}} < 850$ GeV is excluded by SR3b alone in the absence of a large $E_{\mathrm{T}}^{\mathrm{miss}}$ signature. In R-parity-conserving scenarios, the sensitivity is further increased by including the SR3Lhigh and SR1b signal regions. Results on gluino-mediated $\tilde{t}_1 \to t\tilde{\chi}_1^0$

JHEP06(2014)035

and $\tilde{t}_1 \to b\tilde{\chi}_1^{\pm}$ show that $m_{\tilde{g}} \lesssim 950$ GeV is excluded for on-shell or off-shell top squarks, largely independently of the top squark mass, as long as the top squark decay involves b-quarks. As shown for the gluino-mediated top squark $\to t\tilde{\chi}_1^0$ model, this conclusion holds for $\Delta m(\tilde{g}, \tilde{\chi}_1^0) \simeq 2m_t$ as well. In the especially difficult gluino-mediated top squark $\to c\tilde{\chi}_1^0$ case, where only two b-quarks and two W bosons are produced, gluino masses can still be excluded up to 840 GeV.

7.2.2 Gluino-mediated (or direct) first- and second-generation squarks

Results for five simplified models of direct and gluino-mediated first- and second-generation squark production are presented in figure 6. In all models, the four squarks of first and second generations, collectively referred to as "squarks" ($\tilde{q}$), are assumed to be left-handed and degenerate in mass. These squarks are pair-produced, either directly ($\tilde{q}\tilde{q}$) or via gluinos ($\tilde{g}\tilde{g} \to qq\tilde{q}\tilde{q}$), and the $\tilde{\chi}_1^0$ is assumed to be stable. Different assumptions on the decay of the squarks are considered: $\tilde{q} \to q'W\tilde{\chi}_1^0$, $\tilde{q} \to q'WZ\tilde{\chi}_1^0$ and $\tilde{q} \to$ sleptons. The masses of the resulting supersymmetric particles are set according to commonly used conventions in order to cover a variety of scenarios.

In the gluino-mediated or direct squark $\to q'W\tilde{\chi}_1^0$ model, the $\tilde{\chi}_1^{\pm}$ and $\tilde{\chi}_1^0$ masses are related by $m_{\tilde{\chi}_1^{\pm}} = 2m_{\tilde{\chi}_1^0}$. For gluino-mediated and direct squark production, the final states are therefore

$$\tilde{g}\tilde{g} \to qqq'q'\ W^{(*)}W^{(*)}\ \tilde{\chi}_1^0\tilde{\chi}_1^0,$$
$$\tilde{q}\tilde{q} \to q'q'\ W^{\pm(*)}W^{\mp(*)}\ \tilde{\chi}_1^0\tilde{\chi}_1^0.$$

The $\tilde{g}\tilde{g}$ model is the simplest strong-production scenario from which prompt same-sign leptons can arise, due to the Majorana nature of gluinos. However, the $\tilde{q}\tilde{q}$ model can only produce opposite-sign leptons, for which this search has no sensitivity. Results are interpreted in the parameter space of the gluino and $\tilde{\chi}_1^0$ masses (see figure 6(a)). This scenario is excluded at 95% CL for gluino masses up to 860 GeV and $\tilde{\chi}_1^0$ masses up to 400 GeV. The sensitivity is dominated by SR0b.

In the gluino-mediated or direct squark $\to q'WZ\tilde{\chi}_1^0$ model, squarks decay as

$$\tilde{q} \to q'\ \tilde{\chi}_1^{\pm} \to q'W\tilde{\chi}_2^0 \to q'WZ\tilde{\chi}_1^0.$$

The intermediate particle masses are set to

$$m_{\tilde{\chi}_1^{\pm}} = (m_{\tilde{g}} + m_{\tilde{\chi}_1^0})/2,$$
$$m_{\tilde{\chi}_2^0} = (m_{\tilde{\chi}_1^{\pm}} + m_{\tilde{\chi}_1^0})/2.$$

The final states are therefore

$$\tilde{g}\tilde{g} \to qqq'q'\ W^{(*)}W^{(*)}Z^{(*)}Z^{(*)}\ \tilde{\chi}_1^0\tilde{\chi}_1^0,$$
$$\tilde{q}\tilde{q} \to q'q'\ W^{\pm(*)}W^{\mp(*)}Z^{(*)}Z^{(*)}\ \tilde{\chi}_1^0\tilde{\chi}_1^0.$$

The W and Z bosons are on-shell (off-shell) at large (small) mass differences $\Delta m(\tilde{g}, \tilde{\chi}_1^0)$ and $\Delta m(\tilde{q}, \tilde{\chi}_1^0)$. Results are interpreted in the parameter space of the gluino (squark) and

JHEP06(2014)035

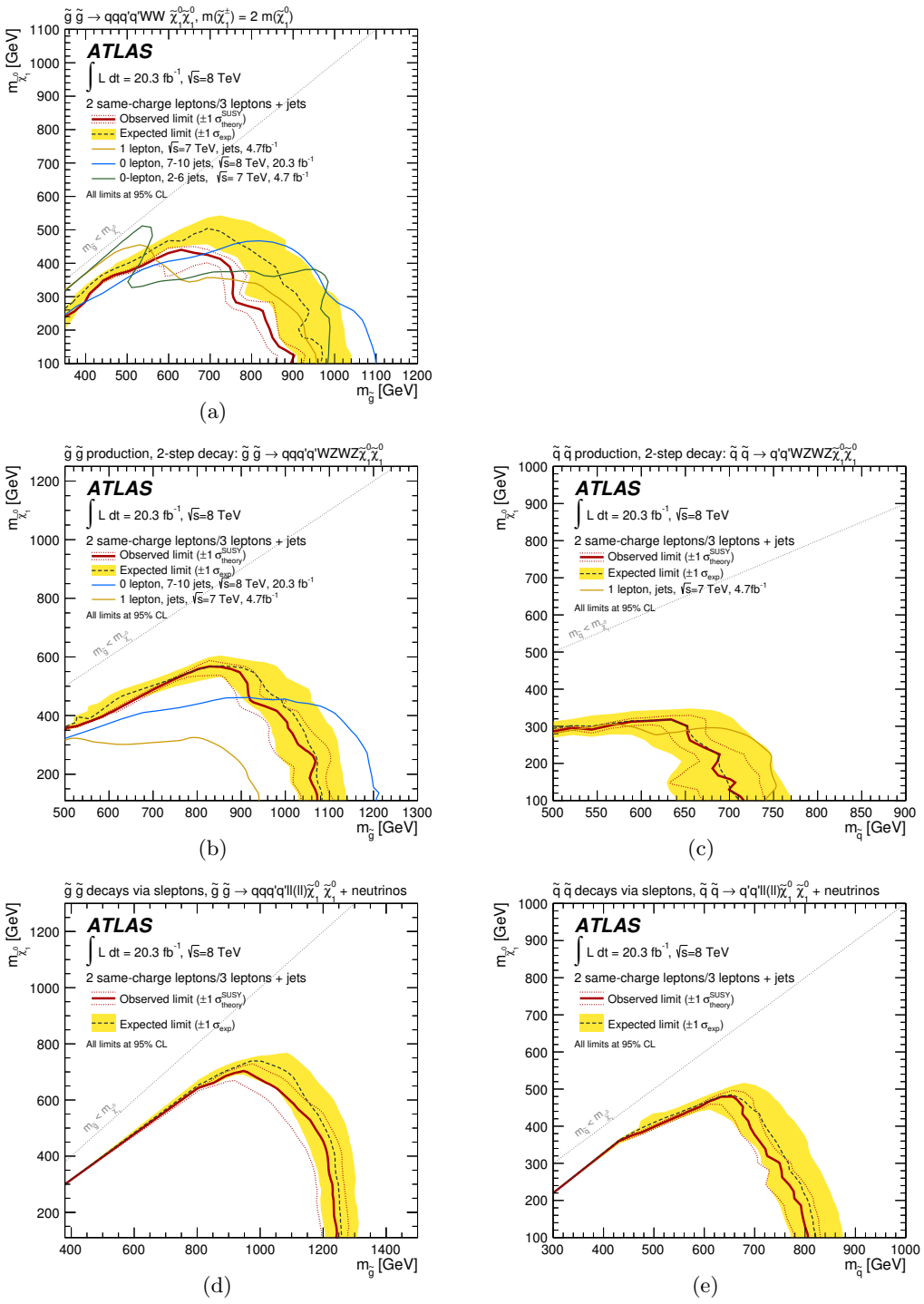

Figure 6. Observed and expected exclusion limits on gluino-mediated production of first- and second-generation squarks (left) and direct production of first- and second-generation squarks (right), obtained with 20.3 fb^{-1} of pp collisions at $\sqrt{s}$=8 TeV, for three different squark decay cascades (see text). When available, results are compared with the limits obtained by previous ATLAS searches [75, 76, 79].

JHEP06(2014)035

$\tilde{\chi}_1^0$ masses (see figures 6(b) and 6(c)). These scenarios are excluded at 95% CL for gluino (squark) masses up to 1040 (670) GeV and $\tilde{\chi}_1^0$ masses up to 520 (300) GeV. The sensitivity is dominated by SR3Lhigh at large $\Delta m(\tilde{g}, \tilde{\chi}_1^0)$ and $\Delta m(\tilde{q}, \tilde{\chi}_1^0)$ and by SR3Llow at small $\Delta m(\tilde{g}, \tilde{\chi}_1^0)$ and $\Delta m(\tilde{q}, \tilde{\chi}_1^0)$.

In the gluino-mediated or direct squark $\rightarrow$ sleptons model, squarks are assumed to decay as $\tilde{q} \rightarrow q' \tilde{\chi}_1^\pm$ or $\tilde{q} \rightarrow q \tilde{\chi}_2^0$ with equal probability. The $\tilde{\chi}_1^\pm$ decays with equal probability as $\tilde{\chi}_1^\pm \rightarrow \tilde{\ell}\nu$ or $\tilde{\chi}_1^\pm \rightarrow \ell\tilde{\nu}$. The $\tilde{\chi}_2^0$ decays with equal probability as $\tilde{\chi}_2^0 \rightarrow \ell\tilde{\ell}$ or $\tilde{\chi}_2^0 \rightarrow \nu\tilde{\nu}$. Finally the slepton decays as $\tilde{\ell} \rightarrow \ell\tilde{\chi}_1^0$, and the sneutrino decays as $\tilde{\nu} \rightarrow \nu\tilde{\chi}_1^0$. All three flavours of sleptons are considered and are degenerate in mass. The masses of the $\tilde{\chi}_1^\pm$ and $\tilde{\chi}_2^0$ are assumed to be equal and set to $m_{\tilde{\chi}_1^\pm} = m_{\tilde{\chi}_2^0} = (m_{\tilde{g}/\tilde{q}} + m_{\tilde{\chi}_1^0})/2$. The masses of the slepton and sneutrino are assumed to be equal and set to $m_{\tilde{\ell}} = m_{\tilde{\nu}} = (m_{\tilde{\chi}_2^0} + m_{\tilde{\chi}_1^0})/2$. The resulting decay chains are

$$\begin{aligned}
\tilde{q} &\rightarrow q' \tilde{\chi}_1^\pm \rightarrow q'\tilde{\ell}\nu \rightarrow q'\ell\nu\tilde{\chi}_1^0, \\
\tilde{q} &\rightarrow q' \tilde{\chi}_1^\pm \rightarrow q'\ell\tilde{\nu} \rightarrow q'\ell\nu\tilde{\chi}_1^0, \\
\tilde{q} &\rightarrow q \tilde{\chi}_2^0 \rightarrow q\ell\tilde{\ell} \rightarrow q\ell\ell\tilde{\chi}_1^0, \\
\tilde{q} &\rightarrow q \tilde{\chi}_2^0 \rightarrow q\nu\tilde{\nu} \rightarrow q\nu\nu\tilde{\chi}_1^0.
\end{aligned}$$

Pair production of squarks or gluinos therefore leads to final states with missing transverse momentum, two or four light jets, and up to four charged leptons. Results are interpreted in the parameter space of the gluino (squark) and $\tilde{\chi}_1^0$ masses (see figures 6(d) and 6(e)). These scenarios are excluded at 95% CL for gluino (squark) masses up to 1200 (780) GeV and $\tilde{\chi}_1^0$ masses up to 660 (460) GeV. The sensitivity is dominated by SR3Lhigh.

The signal regions SR0b, SR3Lhigh and SR3Llow are thus sensitive to first- and second-generation squark production in R-parity-conserving scenarios. The reach in gluino and $\tilde{\chi}_1^0$ masses varies by more than 300 GeV between the most difficult case (gluino-mediated squark $\rightarrow q'W\tilde{\chi}_1^0$, with lowest leptonic branching fraction) and the most favourable case (gluino-mediated squark decaying via sleptons, with largest leptonic branching fraction). In an intermediate case, the gluino-mediated squark $\rightarrow q'WZ\tilde{\chi}_1^0$ model demonstrates the sensitivity of the SR3Lhigh signal region to signals involving on-shell Z bosons, which is an improvement compared to ref. [21]. Similarly, the limits on direct squark production are most stringent for long decay cascades involving sleptons, and less stringent for decays involving W and Z bosons because of the smaller leptonic branching fractions. However, none of the signal regions are sensitive to compressed first- and second-generation squark scenarios with $\Delta m(\tilde{g}, \tilde{\chi}_1^0)$ or $\Delta m(\tilde{q}, \tilde{\chi}_1^0)$ smaller than ~100 GeV.

7.2.3 Direct bottom squarks

Results for direct bottom squark production are shown in figure 7 for two simplified models. Both models assume bottom squark pair production, decaying as $\tilde{b}_1 \rightarrow t\tilde{\chi}_1^\pm$, followed by the chargino decay $\tilde{\chi}_1^\pm \rightarrow W^{(*)\pm}\tilde{\chi}_1^0$, with branching fractions of 100%. In one model, the neutralino mass is fixed to $m_{\tilde{\chi}_1^0} = 60$ GeV. In the other model, the $\tilde{\chi}_1^\pm$ and $\tilde{\chi}_1^0$ masses are related by $m_{\tilde{\chi}_1^\pm} = 2m_{\tilde{\chi}_1^0}$. The $\tilde{\chi}_1^0$ is stable in both models. The final state is therefore $\tilde{b}_1\tilde{b}_1 \rightarrow bb\, WWW^{(*)}W^{(*)}\, \tilde{\chi}_1^0\tilde{\chi}_1^0$, with the constraint that $m_{\tilde{b}_1} > m_t + m_{\tilde{\chi}_1^\pm}$. In the fixed $m_{\tilde{\chi}_1^0}$

JHEP06(2014)035

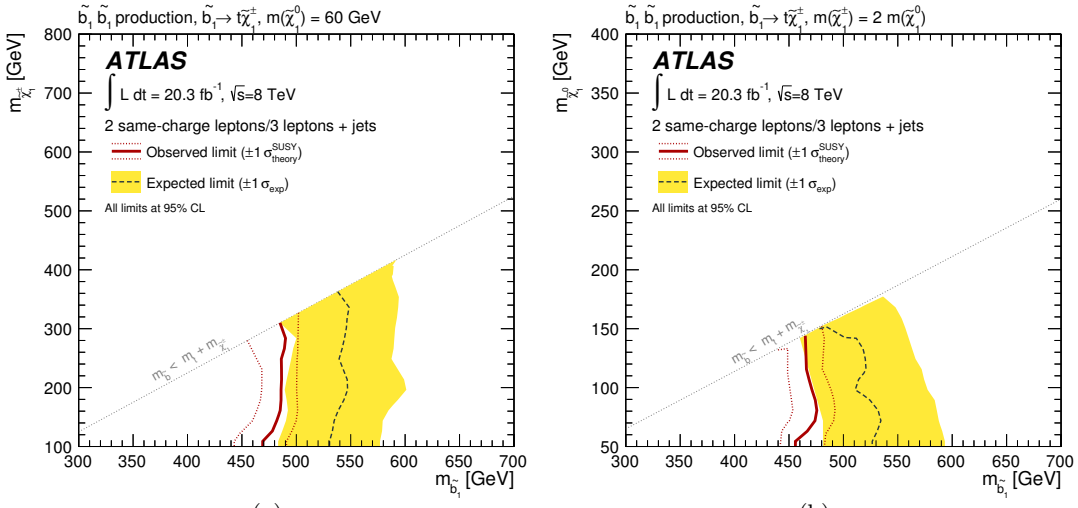

(a) (b)

Figure 7. Observed and expected exclusion limits on direct bottom squark production, obtained with 20.3 fb^{-1} of pp collisions at $\sqrt{s}$=8 TeV, for $\tilde{b} \to t\tilde{\chi}_1^{\pm}$ decays with $m_{\tilde{\chi}_1^0} = 60$ GeV (left) and $m_{\tilde{\chi}_1^0} = m_{\tilde{\chi}_1^{\pm}}/2$ (right).

model, results are interpreted in the parameter space of the bottom squark and $\tilde{\chi}_1^{\pm}$ masses (see figure 7(a)). In the varied $m_{\tilde{\chi}_1^0}$ model, results are interpreted in the parameter space of the bottom squark and $\tilde{\chi}_1^0$ masses (see figure 7(b)). Bottom squark masses are excluded below 440 GeV at 95% CL, for any chargino (neutralino) mass in the fixed (varied) $m_{\tilde{\chi}_1^0}$ model. The sensitivity is dominated by SR3Lhigh, SR3Llow and SR1b in both models. These limits on $\tilde{b}_1 \to t\tilde{\chi}_1^{\pm}$ complement the study of $\tilde{b}_1 \to b\tilde{\chi}_1^0$ processes performed in ref. [81].

7.2.4 MSUGRA/CMSSM, bRPV, GMSB and mUED

This analysis is designed and optimised to cover the SUSY processes included in the simplified models presented above. To demonstrate the versatility of the search, results are also interpreted in the context of complete models that include a mixture of different processes. Results are presented in figure 8 for four standard benchmark models: MSUGRA/CMSSM [82–87], bilinear R-parity violation (bRPV) [88], minimal Gauge-Mediated Supersymmetry Breaking (GMSB) [89–94] and mUED.

The MSUGRA/CMSSM model is characterised by five parameters: the universal scalar and gaugino mass parameters m_0 and $m_{1/2}$, the universal trilinear coupling parameter A_0, the ratio of the vacuum expectation values of the two Higgs doublets $\tan(\beta)$, and the sign of the Higgsino mass parameter μ. Three of the parameters are fixed: $\tan(\beta) = 30$, $A_0 = -2m_0$ and $\mu > 0$, which accommodates a lightest Higgs boson mass between 122 and 128 GeV for $m_{1/2} > 400$ GeV and $m_0 > 1400$ GeV. Results are expressed as a function of m_0 and $m_{1/2}$ (see figure 8(a)). Values of $m_{1/2}$ are excluded below 360 GeV at 95% CL, for m_0 values below 6 TeV. The sensitivity is dominated by SR3b, SR3Lhigh and SR1b.

The bRPV model allows for bilinear R-parity-violating terms in the superpotential, resulting in an unstable LSP. The R-parity-violating couplings are embedded in an

JHEP06(2014)035

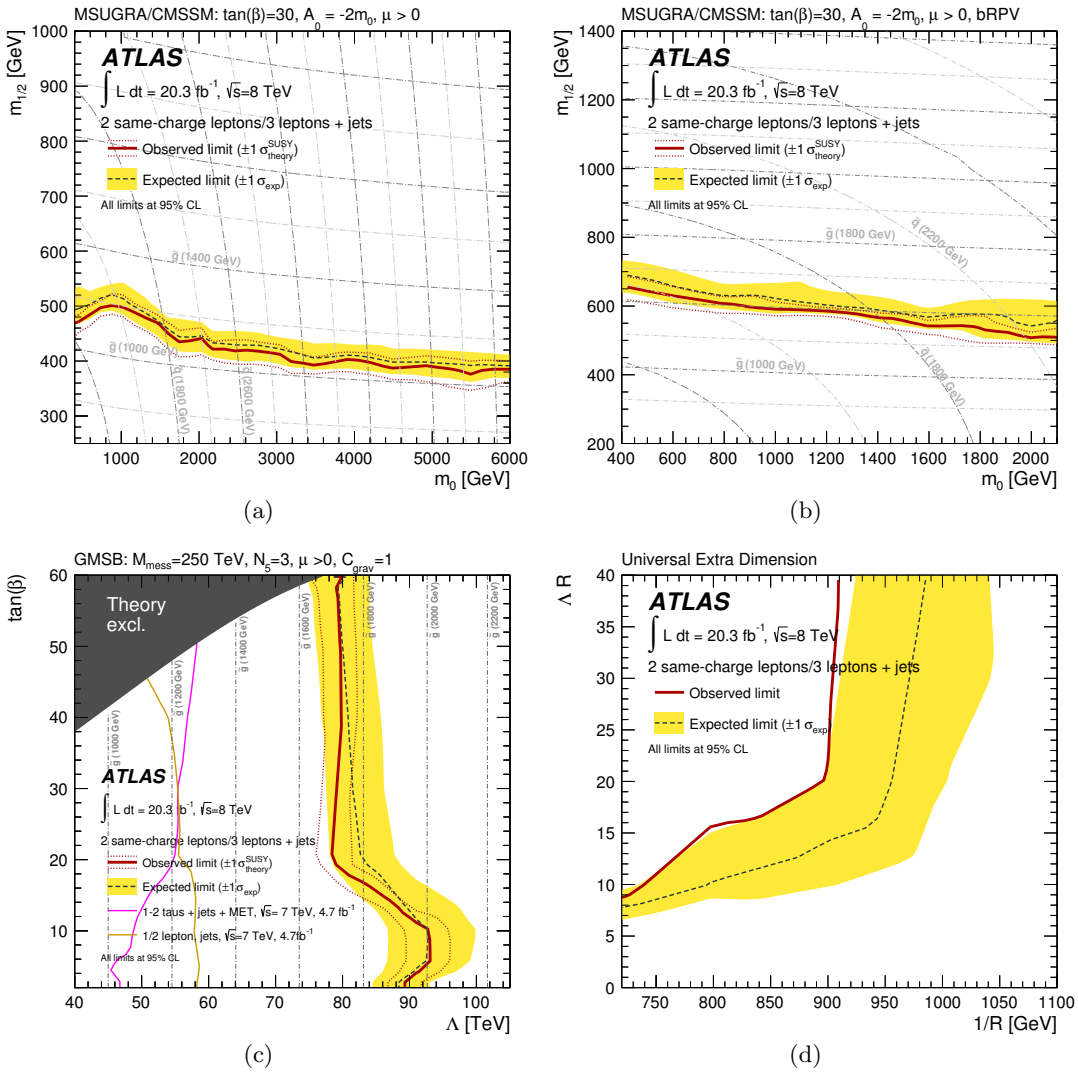

Figure 8. Observed and expected exclusion limits for the MSUGRA/CMSSM, bRPV, GMSB and mUED models, obtained with 20.3 fb^{-1} of pp collisions at $\sqrt{s}$=8 TeV. When available, results are compared with the limits obtained by previous ATLAS searches [75, 77, 79].

MSUGRA/CMSSM SUSY production model as described above. For a chosen set of MSUGRA/CMSSM parameters, the bilinear R-parity violating parameters are determined under the tree-level-dominance scenario [95] by fitting them to the neutrino oscillation data as described in ref. [96]. The neutralino LSP decays within the detector through decay modes that include neutrinos [97]. Results are expressed as a function of m_0 and $m_{1/2}$ (see figure 8(b)). Values of $m_{1/2}$ are excluded between 200 GeV and 490 GeV at 95% CL for m_0 values below 2.1 TeV. Signal models with $m_{1/2} < 200$ GeV are not considered in this analysis because the lepton acceptance is significantly reduced due to the increased LSP lifetime in that region. The sensitivity is dominated by SR3b in the entire plane.

The GMSB model is described by six parameters: the SUSY-breaking mass scale felt by the low-energy sector (Λ), the messenger mass (M_{mess}), the number of SU(5) messenger

JHEP06(2014)035

fields (N_5), the ratio of the vacuum expectation values of the two Higgs doublets ($\tan(\beta)$), the sign of Higgs sector mixing parameter μ and the scale factor for the gravitino mass (C_{grav}). Four parameters are fixed to the values previously used in refs. [75, 98, 99]: $M_{\text{mess}} = 250\,\text{TeV}$, $N_5 = 3$, $\mu > 0$ and $C_{\text{grav}} = 1$. Results are expressed as a function of Λ and $\tan(\beta)$ (see figure 8(c)). The region of small Λ and large $\tan(\beta)$ shown as a grey area in figure 8(c) is excluded theoretically since it leads to tachyonic states. Values of Λ below 75 TeV are excluded at 95% CL, for $\tan(\beta)$ below 60. The sensitivity is dominated by SR3Lhigh.

The mUED model is the minimal extension of the SM with one additional universal spatial dimension. In this non-SUSY model, the Kaluza-Klein (KK) quark decay chain to the lightest KK particle, the KK photon, gives a signature very similar to the supersymmetric decay chain of a squark to the lightest neutralino. The properties of the model depend on two parameters: the compactification radius R and the cut-off scale Λ. The Higgs boson mass is fixed to 125 GeV. Results are expressed as a function of $1/R$ and ΛR (see figure 8(d)). Uncertainties on the signal cross section are not considered for this model. Values of $1/R$ below 850 GeV are excluded at 95% CL, for ΛR above 18. The sensitivity drops with decreasing ΛR because of the reduced mass splitting between the KK states. The sensitivity is dominated by SR3Lhigh and SR0b.

8 Conclusion

A search for supersymmetry in multi-jets events with exactly two same-sign leptons or at least three leptons is presented. Proton-proton collision data from the full 2012 data-taking period were analysed, corresponding to an integrated luminosity of 20.3 fb^{-1} collected at $\sqrt{s}$=8 TeV by the ATLAS detector at the LHC. The search also utilises b-jets, missing transverse momentum and other observables to extend its sensitivity. Five signal regions were determined with a quantitative optimisation procedure using a large number of simplified models. Standard Model backgrounds were estimated using Monte Carlo simulations and data-driven techniques, and were tested in validation regions. Observations are in agreement with SM expectations in each signal region and constraints are set on the visible cross section for new physics processes. Exclusion limits are placed on 14 SUSY models and one mUED model, using a binned fit performed simultaneously in the five signal regions. Gluino-mediated top squark scenarios, favoured by naturalness arguments, are excluded for $m_{\tilde{g}} <$ [600–1000] GeV, largely independently of the top squark mass and decay mode. Similar limits are placed on gluino-mediated production of first- and second-generation quarks for $m_{\tilde{\chi}_1^0} <$ [300–600] GeV. Limits are also placed on pair-production of bottom squarks and squarks of the first and second generations decaying in long cascades. These results put new or significantly improved limits in SUSY parameter regions where the lightest squark can be of the first, second or third generation, where the mass differences between the supersymmetric particles can be large or compressed, and where R-parity can be conserved or violated.

JHEP06(2014)035

Acknowledgments

We thank CERN for the very successful operation of the LHC, as well as the support staff from our institutions without whom ATLAS could not be operated efficiently.

We acknowledge the support of ANPCyT, Argentina; YerPhI, Armenia; ARC, Australia; BMWF and FWF, Austria; ANAS, Azerbaijan; SSTC, Belarus; CNPq and FAPESP, Brazil; NSERC, NRC and CFI, Canada; CERN; CONICYT, Chile; CAS, MOST and NSFC, China; COLCIENCIAS, Colombia; MSMT CR, MPO CR and VSC CR, Czech Republic; DNRF, DNSRC and Lundbeck Foundation, Denmark; EPLANET, ERC and NSRF, European Union; IN2P3-CNRS, CEA-DSM/IRFU, France; GNSF, Georgia; BMBF, DFG, HGF, MPG and AvH Foundation, Germany; GSRT and NSRF, Greece; ISF, MINERVA, GIF, I-CORE and Benoziyo Center, Israel; INFN, Italy; MEXT and JSPS, Japan; CNRST, Morocco; FOM and NWO, Netherlands; BRF and RCN, Norway; MNiSW and NCN, Poland; GRICES and FCT, Portugal; MNE/IFA, Romania; MES of Russia and ROSATOM, Russian Federation; JINR; MSTD, Serbia; MSSR, Slovakia; ARRS and MIZŠ, Slovenia; DST/NRF, South Africa; MINECO, Spain; SRC and Wallenberg Foundation, Sweden; SER, SNSF and Cantons of Bern and Geneva, Switzerland; NSC, Taiwan; TAEK, Turkey; STFC, the Royal Society and Leverhulme Trust, United Kingdom; DOE and NSF, United States of America.

The crucial computing support from all WLCG partners is acknowledged gratefully, in particular from CERN and the ATLAS Tier-1 facilities at TRIUMF (Canada), NDGF (Denmark, Norway, Sweden), CC-IN2P3 (France), KIT/GridKA (Germany), INFN-CNAF (Italy), NL-T1 (Netherlands), PIC (Spain), ASGC (Taiwan), RAL (U.K.) and BNL (U.S.A.) and in the Tier-2 facilities worldwide.

References

[1] H. Miyazawa, *Baryon number changing currents*, *Prog. Theor. Phys.* **36** (1966) 1266.

[2] P. Ramond, *Dual theory for free fermions*, *Phys. Rev.* **D 3** (1971) 2415 [INSPIRE].

[3] Y. Golfand and E.P. Likhtman, *Extension of the algebra of Poincaré group generators and violation of p invariance*, *JETP Lett.* **13** (1971) 323 [INSPIRE].

[4] A. Neveu and J.H. Schwarz, *Factorizable dual model of pions*, *Nucl. Phys.* **B 31** (1971) 86 [INSPIRE].

[5] A. Neveu and J.H. Schwarz, *Quark model of dual pions*, *Phys. Rev.* **D 4** (1971) 1109 [INSPIRE].

[6] J.-L. Gervais and B. Sakita, *Field theory interpretation of supergauges in dual models*, *Nucl. Phys.* **B 34** (1971) 632 [INSPIRE].

[7] D.V. Volkov and V.P. Akulov, *Is the neutrino a Goldstone particle?*, *Phys. Lett.* **B 46** (1973) 109 [INSPIRE].

JHEP06(2014)035

[8] J. Wess and B. Zumino, *A lagrangian model invariant under supergauge transformations*, *Phys. Lett.* **B 49** (1974) 52 [INSPIRE].

[9] J. Wess and B. Zumino, *Supergauge transformations in four-dimensions*, *Nucl. Phys.* **B 70** (1974) 39 [INSPIRE].

[10] P. Fayet, *Spontaneously broken supersymmetric theories of weak, electromagnetic and strong interactions*, *Phys. Lett.* **B 69** (1977) 489 [INSPIRE].

[11] G.R. Farrar and P. Fayet, *Phenomenology of the production, decay and detection of new hadronic states associated with supersymmetry*, *Phys. Lett.* **B 76** (1978) 575 [INSPIRE].

[12] P. Fayet, *Supersymmetry and weak, electromagnetic and strong interactions*, *Phys. Lett.* **B 64** (1976) 159 [INSPIRE].

[13] P. Fayet, *Relations between the masses of the superpartners of leptons and quarks, the goldstino couplings and the neutral currents*, *Phys. Lett.* **B 84** (1979) 416 [INSPIRE].

[14] S. Dimopoulos and H. Georgi, *Softly broken supersymmetry and* SU(5), *Nucl. Phys.* **B 193** (1981) 150 [INSPIRE].

[15] E. Witten, *Dynamical breaking of supersymmetry*, *Nucl. Phys.* **B 188** (1981) 513 [INSPIRE].

[16] M. Dine, W. Fischler and M. Srednicki, *Supersymmetric technicolor*, *Nucl. Phys.* **B 189** (1981) 575 [INSPIRE].

[17] S. Dimopoulos and S. Raby, *Supercolor*, *Nucl. Phys.* **B 192** (1981) 353 [INSPIRE].

[18] N. Sakai, *Naturalness in supersymmetric guts*, *Z. Phys.* **C 11** (1981) 153 [INSPIRE].

[19] R.K. Kaul and P. Majumdar, *Cancellation of quadratically divergent mass corrections in globally supersymmetric spontaneously broken gauge theories*, *Nucl. Phys.* **B 199** (1982) 36 [INSPIRE].

[20] H.-C. Cheng, K.T. Matchev and M. Schmaltz, *Bosonic supersymmetry? Getting fooled at the CERN LHC*, *Phys. Rev.* **D 66** (2002) 056006 [hep-ph/0205314] [INSPIRE].

[21] ATLAS collaboration, *Search for gluinos in events with two same-sign leptons, jets and missing transverse momentum with the ATLAS detector in pp collisions at* $\sqrt{s} = 7$ *TeV*, *Phys. Rev. Lett.* **108** (2012) 241802 [arXiv:1203.5763] [INSPIRE].

[22] CMS collaboration, *Search for new physics in events with same-sign dileptons and b jets in pp collisions at* $\sqrt{s} = 8$ *TeV*, *JHEP* **03** (2013) 037 [*Erratum ibid.* **1307** (2013) 041] [arXiv:1212.6194] [INSPIRE].

[23] CMS collaboration, *Search for new physics with same-sign isolated dilepton events with jets and missing transverse energy*, *Phys. Rev. Lett.* **109** (2012) 071803 [arXiv:1205.6615] [INSPIRE].

[24] CMS collaboration, *Search for new physics in events with same-sign dileptons and b-tagged jets in pp collisions at* $\sqrt{s} = 7$ *TeV*, *JHEP* **08** (2012) 110 [arXiv:1205.3933] [INSPIRE].

[25] CMS collaboration, *Search for new physics in events with same-sign dileptons and jets in pp collisions at* $\sqrt{s} = 8$ *TeV*, *JHEP* **01** (2014) 163 [arXiv:1311.6736] [INSPIRE].

[26] ATLAS collaboration, *The ATLAS experiment at the CERN Large Hadron Collider*, 2008 *JINST* **3** S08003 [INSPIRE].

[27] ATLAS collaboration, *Improved luminosity determination in pp collisions at* $\sqrt{s} = 7$ *TeV using the ATLAS detector at the LHC*, *Eur. Phys. J.* **C 73** (2013) 2518 [arXiv:1302.4393] [INSPIRE].

[28] J. Alwall et al., *MadGraph/MadEvent v4: the new web generation*, *JHEP* **09** (2007) 028 [arXiv:0706.2334] [INSPIRE].

JHEP06(2014)035

[29] T. Sjöstrand, S. Mrenna and P.Z. Skands, *PYTHIA 6.4 physics and manual*, *JHEP* **05** (2006) 026 [hep-ph/0603175] [INSPIRE].

[30] M.L. Mangano, M. Moretti, F. Piccinini, R. Pittau and A.D. Polosa, *ALPGEN, a generator for hard multiparton processes in hadronic collisions*, *JHEP* **07** (2003) 001 [hep-ph/0206293] [INSPIRE].

[31] G. Corcella et al., *HERWIG 6: an event generator for hadron emission reactions with interfering gluons (including supersymmetric processes)*, *JHEP* **01** (2001) 010 [hep-ph/0011363] [INSPIRE].

[32] J.M. Butterworth, J.R. Forshaw and M.H. Seymour, *Multiparton interactions in photoproduction at HERA*, *Z. Phys.* **C 72** (1996) 637 [hep-ph/9601371] [INSPIRE].

[33] T. Sjöstrand, S. Mrenna and P.Z. Skands, *A brief introduction to PYTHIA 8.1*, *Comput. Phys. Commun.* **178** (2008) 852 [arXiv:0710.3820] [INSPIRE].

[34] T. Gleisberg et al., *Event generation with SHERPA 1.1*, *JHEP* **02** (2009) 007 [arXiv:0811.4622] [INSPIRE].

[35] S. Frixione, P. Nason and C. Oleari, *Matching NLO QCD computations with parton shower simulations: the POWHEG method*, *JHEP* **11** (2007) 070 [arXiv:0709.2092] [INSPIRE].

[36] R. Frederix et al., *Four-lepton production at hadron colliders: aMC@NLO predictions with theoretical uncertainties*, *JHEP* **02** (2012) 099 [arXiv:1110.4738] [INSPIRE].

[37] S. Frixione and B.R. Webber, *Matching NLO QCD computations and parton shower simulations*, *JHEP* **06** (2002) 029 [hep-ph/0204244] [INSPIRE].

[38] H.-L. Lai et al., *New parton distributions for collider physics*, *Phys. Rev.* **D 82** (2010) 074024 [arXiv:1007.2241] [INSPIRE].

[39] J. Pumplin et al., *New generation of parton distributions with uncertainties from global QCD analysis*, *JHEP* **07** (2002) 012 [hep-ph/0201195] [INSPIRE].

[40] J.M. Campbell and R.K. Ellis, $t\bar{t}W^{+-}$ *production and decay at NLO*, *JHEP* **07** (2012) 052 [arXiv:1204.5678] [INSPIRE].

[41] M.V. Garzelli, A. Kardos, C.G. Papadopoulos and Z. Trócsányi, $t\bar{t}$ $W^{\pm}$ *and* $t\bar{t}Z$ *hadroproduction at NLO accuracy in QCD with parton shower and hadronization effects*, *JHEP* **11** (2012) 056 [arXiv:1208.2665] [INSPIRE].

[42] J.M. Campbell, R.K. Ellis and C. Williams, *Vector boson pair production at the LHC*, *JHEP* **07** (2011) 018 [arXiv:1105.0020] [INSPIRE].

[43] M. Bahr et al., *HERWIG++ physics and manual*, *Eur. Phys. J.* **C 58** (2008) 639 [arXiv:0803.0883] [INSPIRE].

[44] W. Beenakker, R. Hopker, M. Spira and P.M. Zerwas, *Squark and gluino production at hadron colliders*, *Nucl. Phys.* **B 492** (1997) 51 [hep-ph/9610490] [INSPIRE].

[45] A. Kulesza and L. Motyka, *Threshold resummation for squark-antisquark and gluino-pair production at the LHC*, *Phys. Rev. Lett.* **102** (2009) 111802 [arXiv:0807.2405] [INSPIRE].

[46] A. Kulesza and L. Motyka, *Soft gluon resummation for the production of gluino-gluino and squark-antisquark pairs at the LHC*, *Phys. Rev.* **D 80** (2009) 095004 [arXiv:0905.4749] [INSPIRE].

[47] W. Beenakker et al., *Soft-gluon resummation for squark and gluino hadroproduction*, *JHEP* **12** (2009) 041 [arXiv:0909.4418] [INSPIRE].

[48] W. Beenakker et al., *Squark and gluino hadroproduction*, *Int. J. Mod. Phys.* **A 26** (2011) 2637 [arXiv:1105.1110] [INSPIRE].

JHEP06(2014)035

[49] M. Krämer et al., *Supersymmetry production cross sections in pp collisions at* $\sqrt{s} = 7$ *TeV*, arXiv:1206.2892 [INSPIRE].

[50] ATLAS collaboration, *ATLAS tunes of PYTHIA 6 and PYTHIA 8 for MC11*, ATL-PHYS-PUB-2011-009 (2011).

[51] P.Z. Skands, *Tuning Monte Carlo generators: the Perugia tunes*, *Phys. Rev.* **D 82** (2010) 074018 [arXiv:1005.3457] [INSPIRE].

[52] S. Gieseke, C. Rohr and A. Siodmok, *Colour reconnections in HERWIG++*, *Eur. Phys. J.* **C 72** (2012) 2225 [arXiv:1206.0041] [INSPIRE].

[53] ATLAS collaboration, *The ATLAS simulation infrastructure*, *Eur. Phys. J.* **C 70** (2010) 823 [arXiv:1005.4568] [INSPIRE].

[54] GEANT4 collaboration, S. Agostinelli et al., *GEANT4: a simulation toolkit*, *Nucl. Instrum. Meth.* **A 506** (2003) 250 [INSPIRE].

[55] ATLAS collaboration, *The simulation principle and performance of the ATLAS fast calorimeter simulation FastCaloSim*, ATL-PHYS-PUB-2010-013 (2010).

[56] W. Lampl et al., *Calorimeter clustering algorithms: description and performance*, ATL-LARG-PUB-2008-002 (2008).

[57] ATLAS collaboration, *Jet energy measurement with the ATLAS detector in proton-proton collisions at* $\sqrt{s} = 7$ *TeV*, *Eur. Phys. J.* **C 73** (2013) 2304 [arXiv:1112.6426] [INSPIRE].

[58] M. Cacciari, G.P. Salam and G. Soyez, *The anti-*k_t *jet clustering algorithm*, *JHEP* **04** (2008) 063 [arXiv:0802.1189] [INSPIRE].

[59] M. Cacciari and G.P. Salam, *Dispelling the* N^3 *myth for the* k_t *jet-finder*, *Phys. Lett.* **B 641** (2006) 57 [hep-ph/0512210] [INSPIRE].

[60] M. Cacciari, G.P. Salam and G. Soyez, *FastJet user manual*, *Eur. Phys. J.* **C 72** (2012) 1896 [arXiv:1111.6097] [INSPIRE].

[61] M. Cacciari and G.P. Salam, *Pileup subtraction using jet areas*, *Phys. Lett.* **B 659** (2008) 119 [arXiv:0707.1378] [INSPIRE].

[62] ATLAS collaboration, *Calibration of b-tagging using dileptonic top pair events in a combinatorial likelihood approach with the ATLAS experiment*, ATLAS-CONF-2014-004 (2014).

[63] ATLAS collaboration, *Calibration of the b-tagging efficiency for c jets with the ATLAS detector using events with a W boson produced in association with a single c quark*, ATLAS-CONF-2013-109 (2013).

[64] ATLAS collaboration, *Measurement of the mistag rate with* $5\,fb^{-1}$ *of data collected by the ATLAS detector*, ATLAS-CONF-2012-040 (2012).

[65] ATLAS collaboration, *Electron performance measurements with the ATLAS detector using the 2010 LHC proton-proton collision data*, *Eur. Phys. J.* **C 72** (2012) 1909 [arXiv:1110.3174] [INSPIRE].

[66] ATLAS collaboration, *Measurement of the* $W \to \ell\nu$ *and* $Z/\gamma^* \to \ell\ell$ *production cross sections in proton-proton collisions at* $\sqrt{s} = 7$ *TeV with the ATLAS detector*, *JHEP* **12** (2010) 060 [arXiv:1010.2130] [INSPIRE].

[67] ATLAS collaboration, *Performance of missing transverse momentum reconstruction in proton-proton collisions at 7 TeV with ATLAS*, *Eur. Phys. J.* **C 72** (2012) 1844 [arXiv:1108.5602] [INSPIRE].

JHEP06(2014)035

[68] ATLAS collaboration, *Single hadron response measurement and calorimeter jet energy scale uncertainty with the ATLAS detector at the LHC*, *Eur. Phys. J.* **C 73** (2013) 2305 [arXiv:1203.1302] [INSPIRE].

[69] ATLAS collaboration, *Measurement of the b-tag efficiency in a sample of jets containing muons with 5 fb^{-1} of data from the ATLAS detector*, ATLAS-CONF-2012-043 (2012).

[70] ATLAS collaboration, *Jet energy resolution in proton-proton collisions at $\sqrt{s} = 7$ TeV recorded in 2010 with the ATLAS detector*, *Eur. Phys. J.* **C 73** (2013) 2306 [arXiv:1210.6210] [INSPIRE].

[71] ATLAS collaboration, *Preliminary results on the muon reconstruction efficiency, momentum resolution and momentum scale in ATLAS 2012 pp collision data*, ATLAS-CONF-2013-088 (2013).

[72] A.L. Read, *Presentation of search results: the CL_s technique*, *J. Phys.* **G 28** (2002) 2693 [INSPIRE].

[73] G. Cowan, K. Cranmer, E. Gross and O. Vitells, *Asymptotic formulae for likelihood-based tests of new physics*, *Eur. Phys. J.* **C 71** (2011) 1554 [arXiv:1007.1727] [INSPIRE].

[74] *The Durham HepData project*, http://hepdata.cedar.ac.uk/reaction.

[75] ATLAS collaboration, *Further search for supersymmetry at $\sqrt{s} = 7$ TeV in final states with jets, missing transverse momentum and isolated leptons with the ATLAS detector*, *Phys. Rev.* **D 86** (2012) 092002 [arXiv:1208.4688] [INSPIRE].

[76] ATLAS collaboration, *Search for squarks and gluinos with the ATLAS detector in final states with jets and missing transverse momentum using 4.7 fb^{-1} of $\sqrt{s} = 7$ TeV proton-proton collision data*, *Phys. Rev.* **D 87** (2013) 012008 [arXiv:1208.0949] [INSPIRE].

[77] ATLAS collaboration, *Search for supersymmetry in events with large missing transverse momentum, jets and at least one τ lepton in 7 TeV proton-proton collision data with the ATLAS detector*, *Eur. Phys. J.* **C 72** (2012) 2215 [arXiv:1210.1314] [INSPIRE].

[78] ATLAS collaboration, *Search for top and bottom squarks from gluino pair production in final states with missing transverse energy and at least three b-jets with the ATLAS detector*, *Eur. Phys. J.* **C 72** (2012) 2174 [arXiv:1207.4686] [INSPIRE].

[79] ATLAS collaboration, *Search for new phenomena in final states with large jet multiplicities and missing transverse momentum at $\sqrt{s} = 8$ TeV proton-proton collisions using the ATLAS experiment*, *JHEP* **10** (2013) 130 [arXiv:1308.1841] [INSPIRE].

[80] B.C. Allanach and B. Gripaios, *Hide and seek with natural supersymmetry at the LHC*, *JHEP* **05** (2012) 062 [arXiv:1202.6616] [INSPIRE].

[81] ATLAS collaboration, *Search for direct third-generation squark pair production in final states with missing transverse momentum and two b-jets in $\sqrt{s} = 8$ TeV pp collisions with the ATLAS detector*, *JHEP* **10** (2013) 189 [arXiv:1308.2631] [INSPIRE].

[82] A.H. Chamseddine, R.L. Arnowitt and P. Nath, *Locally supersymmetric grand unification*, *Phys. Rev. Lett.* **49** (1982) 970 [INSPIRE].

[83] R. Barbieri, S. Ferrara and C.A. Savoy, *Gauge models with spontaneously broken local supersymmetry*, *Phys. Lett.* **B 119** (1982) 343 [INSPIRE].

[84] L.E. Ibáñez, *Locally supersymmetric* SU(5) *grand unification*, *Phys. Lett.* **B 118** (1982) 73 [INSPIRE].

[85] L.J. Hall, J.D. Lykken and S. Weinberg, *Supergravity as the Messenger of supersymmetry breaking*, *Phys. Rev.* **D 27** (1983) 2359 [INSPIRE].

JHEP06(2014)035

[86] N. Ohta, *Grand unified theories based on local supersymmetry*, *Prog. Theor. Phys.* **70** (1983) 542 [INSPIRE].

[87] G.L. Kane, C.F. Kolda, L. Roszkowski and J.D. Wells, *Study of constrained minimal supersymmetry*, *Phys. Rev.* **D 49** (1994) 6173 [hep-ph/9312272] [INSPIRE].

[88] S. Roy and B. Mukhopadhyaya, *Some implications of a supersymmetric model with R-parity breaking bilinear interactions*, *Phys. Rev.* **D 55** (1997) 7020 [hep-ph/9612447] [INSPIRE].

[89] M. Dine and W. Fischler, *A phenomenological model of particle physics based on supersymmetry*, *Phys. Lett.* **B 110** (1982) 227 [INSPIRE].

[90] L. Álvarez-Gaumé, M. Claudson and M.B. Wise, *Low-energy supersymmetry*, *Nucl. Phys.* **B 207** (1982) 96 [INSPIRE].

[91] C.R. Nappi and B.A. Ovrut, *Supersymmetric extension of the* $SU(3) \times SU(2) \times U(1)$ *model*, *Phys. Lett.* **B 113** (1982) 175 [INSPIRE].

[92] M. Dine and A.E. Nelson, *Dynamical supersymmetry breaking at low-energies*, *Phys. Rev.* **D 48** (1993) 1277 [hep-ph/9303230] [INSPIRE].

[93] M. Dine, A.E. Nelson and Y. Shirman, *Low-energy dynamical supersymmetry breaking simplified*, *Phys. Rev.* **D 51** (1995) 1362 [hep-ph/9408384] [INSPIRE].

[94] M. Dine, A.E. Nelson, Y. Nir and Y. Shirman, *New tools for low-energy dynamical supersymmetry breaking*, *Phys. Rev.* **D 53** (1996) 2658 [hep-ph/9507378] [INSPIRE].

[95] Y. Grossman and S. Rakshit, *Neutrino masses in R-parity violating supersymmetric models*, *Phys. Rev.* **D 69** (2004) 093002 [hep-ph/0311310] [INSPIRE].

[96] D.F. Carvalho, M.E. Gomez and J.C. Romao, *Charged lepton flavor violation in supersymmetry with bilinear R-parity violation*, *Phys. Rev.* **D 65** (2002) 093013 [hep-ph/0202054] [INSPIRE].

[97] W. Porod, M. Hirsch, J. Romao and J.W.F. Valle, *Testing neutrino mixing at future collider experiments*, *Phys. Rev.* **D 63** (2001) 115004 [hep-ph/0011248] [INSPIRE].

[98] ATLAS collaboration, *Search for supersymmetry with jets, missing transverse momentum and at least one hadronically decaying* τ *lepton in proton-proton collisions at* $\sqrt{s} = 7$ *TeV with the ATLAS detector*, *Phys. Lett.* **B 714** (2012) 197 [arXiv:1204.3852] [INSPIRE].

[99] ATLAS collaboration, *Search for events with large missing transverse momentum, jets and at least two tau leptons in 7 TeV proton-proton collision data with the ATLAS detector*, *Phys. Lett.* **B 714** (2012) 180 [arXiv:1203.6580] [INSPIRE].

JHEP06(2014)035

The ATLAS collaboration

G. Aad[84], B. Abbott[112], J. Abdallah[152], S. Abdel Khalek[116], O. Abdinov[11], R. Aben[106], B. Abi[113], M. Abolins[89], O.S. AbouZeid[159], H. Abramowicz[154], H. Abreu[137], R. Abreu[30], Y. Abulaiti[147a,147b], B.S. Acharya[165a,165b,a], L. Adamczyk[38a], D.L. Adams[25], J. Adelman[177], S. Adomeit[99], T. Adye[130], T. Agatonovic-Jovin[13b], J.A. Aguilar-Saavedra[125f,125a], M. Agustoni[17], S.P. Ahlen[22], A. Ahmad[149], F. Ahmadov[64,b], G. Aielli[134a,134b], T.P.A. Åkesson[80], G. Akimoto[156], A.V. Akimov[95], G.L. Alberghi[20a,20b], J. Albert[170], S. Albrand[55], M.J. Alconada Verzini[70], M. Aleksa[30], I.N. Aleksandrov[64], C. Alexa[26a], G. Alexander[154], G. Alexandre[49], T. Alexopoulos[10], M. Alhroob[165a,165c], G. Alimonti[90a], L. Alio[84], J. Alison[31], B.M.M. Allbrooke[18], L.J. Allison[71], P.P. Allport[73], S.E. Allwood-Spiers[53], J. Almond[83], A. Aloisio[103a,103b], A. Alonso[36], F. Alonso[70], C. Alpigiani[75], A. Altheimer[35], B. Alvarez Gonzalez[89], M.G. Alviggi[103a,103b], K. Amako[65], Y. Amaral Coutinho[24a], C. Amelung[23], D. Amidei[88], S.P. Amor Dos Santos[125a,125c], A. Amorim[125a,125b], S. Amoroso[48], N. Amram[154], G. Amundsen[23], C. Anastopoulos[140], L.S. Ancu[49], N. Andari[30], T. Andeen[35], C.F. Anders[58b], G. Anders[30], K.J. Anderson[31], A. Andreazza[90a,90b], V. Andrei[58a], X.S. Anduaga[70], S. Angelidakis[9], I. Angelozzi[106], P. Anger[44], A. Angerami[35], F. Anghinolfi[30], A.V. Anisenkov[108], N. Anjos[125a], A. Annovi[47], A. Antonaki[9], M. Antonelli[47], A. Antonov[97], J. Antos[145b], F. Anulli[133a], M. Aoki[65], L. Aperio Bella[18], R. Apolle[119,c], G. Arabidze[89], I. Aracena[144], Y. Arai[65], J.P. Araque[125a], A.T.H. Arce[45], J-F. Arguin[94], S. Argyropoulos[42], M. Arik[19a], A.J. Armbruster[30], O. Arnaez[82], V. Arnal[81], H. Arnold[48], O. Arslan[21], A. Artamonov[96], G. Artoni[23], S. Asai[156], N. Asbah[94], A. Ashkenazi[154], S. Ask[28], B. Åsman[147a,147b], L. Asquith[6], K. Assamagan[25], R. Astalos[145a], M. Atkinson[166], N.B. Atlay[142], B. Auerbach[6], K. Augsten[127], M. Aurousseau[146b], G. Avolio[30], G. Azuelos[94,d], Y. Azuma[156], M.A. Baak[30], C. Bacci[135a,135b], H. Bachacou[137], K. Bachas[155], M. Backes[30], M. Backhaus[30], J. Backus Mayes[144], E. Badescu[26a], P. Bagiacchi[133a,133b], P. Bagnaia[133a,133b], Y. Bai[33a], T. Bain[35], J.T. Baines[130], O.K. Baker[177], S. Baker[77], P. Balek[128], F. Balli[137], E. Banas[39], Sw. Banerjee[174], D. Banfi[30], A. Bangert[151], A.A.E. Bannoura[176], V. Bansal[170], H.S. Bansil[18], L. Barak[173], S.P. Baranov[95], E.L. Barberio[87], D. Barberis[50a,50b], M. Barbero[84], T. Barillari[100], M. Barisonzi[176], T. Barklow[144], N. Barlow[28], B.M. Barnett[130], R.M. Barnett[15], Z. Barnovska[5], A. Baroncelli[135a], G. Barone[49], A.J. Barr[119], F. Barreiro[81], J. Barreiro Guimarães da Costa[57], R. Bartoldus[144], A.E. Barton[71], P. Bartos[145a], V. Bartsch[150], A. Bassalat[116], A. Basye[166], R.L. Bates[53], L. Batkova[145a], J.R. Batley[28], M. Battistin[30], F. Bauer[137], H.S. Bawa[144,e], T. Beau[79], P.H. Beauchemin[162], R. Beccherle[123a,123b], P. Bechtle[21], H.P. Beck[17], K. Becker[176], S. Becker[99], M. Beckingham[139], C. Becot[116], A.J. Beddall[19c], A. Beddall[19c], S. Bedikian[177], V.A. Bednyakov[64], C.P. Bee[149], L.J. Beemster[106], T.A. Beermann[176], M. Begel[25], K. Behr[119], C. Belanger-Champagne[86], P.J. Bell[49], W.H. Bell[49], G. Bella[154], L. Bellagamba[20a], A. Bellerive[29], M. Bellomo[85], A. Belloni[57], O.L. Beloborodova[108,f], K. Belotskiy[97], O. Beltramello[30], O. Benary[154], D. Benchekroun[136a], K. Bendtz[147a,147b], N. Benekos[166], Y. Benhammou[154], E. Benhar Noccioli[49], J.A. Benitez Garcia[160b], D.P. Benjamin[45], J.R. Bensinger[23], K. Benslama[131], S. Bentvelsen[106], D. Berge[106], E. Bergeaas Kuutmann[16], N. Berger[5], F. Berghaus[170], E. Berglund[106], J. Beringer[15], C. Bernard[22], P. Bernat[77], C. Bernius[78], F.U. Bernlochner[170], T. Berry[76], P. Berta[128], C. Bertella[84], F. Bertolucci[123a,123b], M.I. Besana[90a], G.J. Besjes[105], O. Bessidskaia[147a,147b], N. Besson[137], C. Betancourt[48], S. Bethke[100], W. Bhimji[46], R.M. Bianchi[124], L. Bianchini[23], M. Bianco[30], O. Biebel[99], S.P. Bieniek[77], K. Bierwagen[54], J. Biesiada[15], M. Biglietti[135a], J. Bilbao De Mendizabal[49], H. Bilokon[47], M. Bindi[54], S. Binet[116], A. Bingul[19c], C. Bini[133a,133b], C.W. Black[151], J.E. Black[144], K.M. Black[22], D. Blackburn[139], R.E. Blair[6], J.-B. Blanchard[137], T. Blazek[145a], I. Bloch[42], C. Blocker[23], W. Blum[82,*], U. Blumenschein[54], G.J. Bobbink[106], V.S. Bobrovnikov[108], S.S. Bocchetta[80], A. Bocci[45], C.R. Boddy[119], M. Boehler[48], J. Boek[176], T.T. Boek[176], J.A. Bogaerts[30], A.G. Bogdanchikov[108], A. Bogouch[91,*], C. Bohm[147a], J. Bohm[126], V. Boisvert[76], T. Bold[38a], V. Boldea[26a], A.S. Boldyrev[98], M. Bomben[79], M. Bona[75], M. Boonekamp[137], A. Borisov[129], G. Borissov[71], M. Borri[83], S. Borroni[42], J. Bortfeldt[99], V. Bortolotto[135a,135b], K. Bos[106], D. Boscherini[20a], M. Bosman[12], H. Boterenbrood[106],

JHEP06(2014)035

J. Boudreau[124], J. Bouffard[2], E.V. Bouhova-Thacker[71], D. Boumediene[34], C. Bourdarios[116], N. Bousson[113], S. Boutouil[136d], A. Boveia[31], J. Boyd[30], I.R. Boyko[64], I. Bozovic-Jelisavcic[13b], J. Bracinik[18], P. Branchini[135a], A. Brandt[8], G. Brandt[15], O. Brandt[58a], U. Bratzler[157], B. Brau[85], J.E. Brau[115], H.M. Braun[176,*], S.F. Brazzale[165a,165c], B. Brelier[159], K. Brendlinger[121], A.J. Brennan[87], R. Brenner[167], S. Bressler[173], K. Bristow[146c], T.M. Bristow[46], D. Britton[53], F.M. Brochu[28], I. Brock[21], R. Brock[89], C. Bromberg[89], J. Bronner[100], G. Brooijmans[35], T. Brooks[76], W.K. Brooks[32b], J. Brosamer[15], E. Brost[115], G. Brown[83], J. Brown[55], P.A. Bruckman de Renstrom[39], D. Bruncko[145b], R. Bruneliere[48], S. Brunet[60], A. Bruni[20a], G. Bruni[20a], M. Bruschi[20a], L. Bryngemark[80], T. Buanes[14], Q. Buat[143], F. Bucci[49], P. Buchholz[142], R.M. Buckingham[119], A.G. Buckley[53], S.I. Buda[26a], I.A. Budagov[64], F. Buehrer[48], L. Bugge[118], M.K. Bugge[118], O. Bulekov[97], A.C. Bundock[73], H. Burckhart[30], S. Burdin[73], B. Burghgrave[107], S. Burke[130], I. Burmeister[43], E. Busato[34], D. Büscher[48], V. Büscher[82], P. Bussey[53], C.P. Buszello[167], B. Butler[57], J.M. Butler[22], A.I. Butt[3], C.M. Buttar[53], J.M. Butterworth[77], P. Butti[106], W. Buttinger[28], A. Buzatu[53], M. Byszewski[10], S. Cabrera Urbán[168], D. Caforio[20a,20b], O. Cakir[4a], P. Calafiura[15], A. Calandri[137], G. Calderini[79], P. Calfayan[99], R. Calkins[107], L.P. Caloba[24a], D. Calvet[34], S. Calvet[34], R. Camacho Toro[49], S. Camarda[42], D. Cameron[118], L.M. Caminada[15], R. Caminal Armadans[12], S. Campana[30], M. Campanelli[77], A. Campoverde[149], V. Canale[103a,103b], A. Canepa[160a], J. Cantero[81], R. Cantrill[76], T. Cao[40], M.D.M. Capeans Garrido[30], I. Caprini[26a], M. Caprini[26a], M. Capua[37a,37b], R. Caputo[82], R. Cardarelli[134a], T. Carli[30], G. Carlino[103a], L. Carminati[90a,90b], S. Caron[105], E. Carquin[32a], G.D. Carrillo-Montoya[146c], A.A. Carter[75], J.R. Carter[28], J. Carvalho[125a,125c], D. Casadei[77], M.P. Casado[12], E. Castaneda-Miranda[146b], A. Castelli[106], V. Castillo Gimenez[168], N.F. Castro[125a], P. Catastini[57], A. Catinaccio[30], J.R. Catmore[118], A. Cattai[30], G. Cattani[134a,134b], S. Caughron[89], V. Cavaliere[166], D. Cavalli[90a], M. Cavalli-Sforza[12], V. Cavasinni[123a,123b], F. Ceradini[135a,135b], B. Cerio[45], K. Cerny[128], A.S. Cerqueira[24b], A. Cerri[150], L. Cerrito[75], F. Cerutti[15], M. Cerv[30], A. Cervelli[17], S.A. Cetin[19b], A. Chafaq[136a], D. Chakraborty[107], I. Chalupkova[128], K. Chan[3], P. Chang[166], B. Chapleau[86], J.D. Chapman[28], D. Charfeddine[116], D.G. Charlton[18], C.C. Chau[159], C.A. Chavez Barajas[150], S. Cheatham[86], A. Chegwidden[89], S. Chekanov[6], S.V. Chekulaev[160a], G.A. Chelkov[64], M.A. Chelstowska[88], C. Chen[63], H. Chen[25], K. Chen[149], L. Chen[33d,g], S. Chen[33c], X. Chen[146c], Y. Chen[35], H.C. Cheng[88], Y. Cheng[31], A. Cheplakov[64], R. Cherkaoui El Moursli[136e], V. Chernyatin[25,*], E. Cheu[7], L. Chevalier[137], V. Chiarella[47], G. Chiefari[103a,103b], J.T. Childers[6], A. Chilingarov[71], G. Chiodini[72a], A.S. Chisholm[18], R.T. Chislett[77], A. Chitan[26a], M.V. Chizhov[64], S. Chouridou[9], B.K.B. Chow[99], I.A. Christidi[77], D. Chromek-Burckhart[30], M.L. Chu[152], J. Chudoba[126], J.J. Chwastowski[39], L. Chytka[114], G. Ciapetti[133a,133b], A.K. Ciftci[4a], R. Ciftci[4a], D. Cinca[62], V. Cindro[74], A. Ciocio[15], P. Cirkovic[13b], Z.H. Citron[173], M. Citterio[90a], M. Ciubancan[26a], A. Clark[49], P.J. Clark[46], R.N. Clarke[15], W. Cleland[124], J.C. Clemens[84], C. Clement[147a,147b], Y. Coadou[84], M. Cobal[165a,165c], A. Coccaro[139], J. Cochran[63], L. Coffey[23], J.G. Cogan[144], J. Coggeshall[166], B. Cole[35], S. Cole[107], A.P. Colijn[106], C. Collins-Tooth[53], J. Collot[55], T. Colombo[58c], G. Colon[85], G. Compostella[100], P. Conde Muiño[125a,125b], E. Coniavitis[167], M.C. Conidi[12], S.H. Connell[146b], I.A. Connelly[76], S.M. Consonni[90a,90b], V. Consorti[48], S. Constantinescu[26a], C. Conta[120a,120b], G. Conti[57], F. Conventi[103a,h], M. Cooke[15], B.D. Cooper[77], A.M. Cooper-Sarkar[119], N.J. Cooper-Smith[76], K. Copic[15], T. Cornelissen[176], M. Corradi[20a], F. Corriveau[86,i], A. Corso-Radu[164], A. Cortes-Gonzalez[12], G. Cortiana[100], G. Costa[90a], M.J. Costa[168], D. Costanzo[140], D. Côté[8], G. Cottin[28], G. Cowan[76], B.E. Cox[83], K. Cranmer[109], G. Cree[29], S. Crépé-Renaudin[55], F. Crescioli[79], M. Crispin Ortuzar[119], M. Cristinziani[21], V. Croft[105], G. Crosetti[37a,37b], C.-M. Cuciuc[26a], C. Cuenca Almenar[177], T. Cuhadar Donszelmann[140], J. Cummings[177], M. Curatolo[47], C. Cuthbert[151], H. Czirr[142], P. Czodrowski[3], Z. Czyczula[177], S. D'Auria[53], M. D'Onofrio[73], M.J. Da Cunha Sargedas De Sousa[125a,125b], C. Da Via[83], W. Dabrowski[38a], A. Dafinca[119], T. Dai[88], O. Dale[14], F. Dallaire[94], C. Dallapiccola[85], M. Dam[36], A.C. Daniells[18], M. Dano Hoffmann[137], V. Dao[105], G. Darbo[50a], G.L. Darlea[26c], S. Darmora[8], J.A. Dassoulas[42],

JHEP06(2014)035

A. Dattagupta[60], W. Davey[21], C. David[170], T. Davidek[128], E. Davies[119,c], M. Davies[154], O. Davignon[79], A.R. Davison[77], P. Davison[77], Y. Davygora[58a], E. Dawe[143], I. Dawson[140], R.K. Daya-Ishmukhametova[23], K. De[8], R. de Asmundis[103a], S. De Castro[20a,20b], S. De Cecco[79], J. de Graat[99], N. De Groot[105], P. de Jong[106], H. De la Torre[81], F. De Lorenzi[63], L. De Nooij[106], D. De Pedis[133a], A. De Salvo[133a], U. De Sanctis[165a,165b], A. De Santo[150], J.B. De Vivie De Regie[116], G. De Zorzi[133a,133b], W.J. Dearnaley[71], R. Debbe[25], C. Debenedetti[46], B. Dechenaux[55], D.V. Dedovich[64], J. Degenhardt[121], I. Deigaard[106], J. Del Peso[81], T. Del Prete[123a,123b], F. Deliot[137], C.M. Delitzsch[49], M. Deliyergiyev[74], A. Dell'Acqua[30], L. Dell'Asta[22], M. Dell'Orso[123a,123b], M. Della Pietra[103a,h], D. della Volpe[49], M. Delmastro[5], P.A. Delsart[55], C. Deluca[106], S. Demers[177], M. Demichev[64], A. Demilly[79], S.P. Denisov[129], D. Derendarz[39], J.E. Derkaoui[136d], F. Derue[79], P. Dervan[73], K. Desch[21], C. Deterre[42], P.O. Deviveiros[106], A. Dewhurst[130], S. Dhaliwal[106], A. Di Ciaccio[134a,134b], L. Di Ciaccio[5], A. Di Domenico[133a,133b], C. Di Donato[103a,103b], A. Di Girolamo[30], B. Di Girolamo[30], A. Di Mattia[153], B. Di Micco[135a,135b], R. Di Nardo[47], A. Di Simone[48], R. Di Sipio[20a,20b], D. Di Valentino[29], M.A. Diaz[32a], E.B. Diehl[88], J. Dietrich[42], T.A. Dietzsch[58a], S. Diglio[84], A. Dimitrievska[13a], J. Dingfelder[21], C. Dionisi[133a,133b], P. Dita[26a], S. Dita[26a], F. Dittus[30], F. Djama[84], T. Djobava[51b], M.A.B. do Vale[24c], A. Do Valle Wemans[125a,125g], T.K.O. Doan[5], D. Dobos[30], E. Dobson[77], C. Doglioni[49], T. Doherty[53], T. Dohmae[156], J. Dolejsi[128], Z. Dolezal[128], B.A. Dolgoshein[97,*], M. Donadelli[24d], S. Donati[123a,123b], P. Dondero[120a,120b], J. Donini[34], J. Dopke[30], A. Doria[103a], A. Dos Anjos[174], M.T. Dova[70], A.T. Doyle[53], M. Dris[10], J. Dubbert[88], S. Dube[15], E. Dubreuil[34], E. Duchovni[173], G. Duckeck[99], O.A. Ducu[26a], D. Duda[176], A. Dudarev[30], F. Dudziak[63], L. Duflot[116], L. Duguid[76], M. Dührssen[30], M. Dunford[58a], H. Duran Yildiz[4a], M. Düren[52], A. Durglishvili[51b], M. Dwuznik[38a], M. Dyndal[38a], J. Ebke[99], W. Edson[2], N.C. Edwards[46], W. Ehrenfeld[21], T. Eifert[144], G. Eigen[14], K. Einsweiler[15], T. Ekelof[167], M. El Kacimi[136c], M. Ellert[167], S. Elles[5], F. Ellinghaus[82], N. Ellis[30], J. Elmsheuser[99], M. Elsing[30], D. Emeliyanov[130], Y. Enari[156], O.C. Endner[82], M. Endo[117], R. Engelmann[149], J. Erdmann[177], A. Ereditato[17], D. Eriksson[147a], G. Ernis[176], J. Ernst[2], M. Ernst[25], J. Ernwein[137], D. Errede[166], S. Errede[166], E. Ertel[82], M. Escalier[116], H. Esch[43], C. Escobar[124], B. Esposito[47], A.I. Etienvre[137], E. Etzion[154], H. Evans[60], L. Fabbri[20a,20b], G. Facini[30], R.M. Fakhrutdinov[129], S. Falciano[133a], Y. Fang[33a], M. Fanti[90a,90b], A. Farbin[8], A. Farilla[135a], T. Farooque[12], S. Farrell[164], S.M. Farrington[171], P. Farthouat[30], F. Fassi[168], P. Fassnacht[30], D. Fassouliotis[9], A. Favareto[50a,50b], L. Fayard[116], P. Federic[145a], O.L. Fedin[122,j], W. Fedorko[169], M. Fehling-Kaschek[48], S. Feigl[30], L. Feligioni[84], C. Feng[33d], E.J. Feng[6], H. Feng[88], A.B. Fenyuk[129], S. Fernandez Perez[30], S. Ferrag[53], J. Ferrando[53], A. Ferrari[167], P. Ferrari[106], R. Ferrari[120a], D.E. Ferreira de Lima[53], A. Ferrer[168], D. Ferrere[49], C. Ferretti[88], A. Ferretto Parodi[50a,50b], M. Fiascaris[31], F. Fiedler[82], A. Filipčič[74], M. Filipuzzi[42], F. Filthaut[105], M. Fincke-Keeler[170], K.D. Finelli[151], M.C.N. Fiolhais[125a,125c], L. Fiorini[168], A. Firan[40], J. Fischer[176], W.C. Fisher[89], E.A. Fitzgerald[23], M. Flechl[48], I. Fleck[142], P. Fleischmann[175], S. Fleischmann[176], G.T. Fletcher[140], G. Fletcher[75], T. Flick[176], A. Floderus[80], L.R. Flores Castillo[174], A.C. Florez Bustos[160b], M.J. Flowerdew[100], A. Formica[137], A. Forti[83], D. Fortin[160a], D. Fournier[116], H. Fox[71], S. Fracchia[12], P. Francavilla[79], M. Franchini[20a,20b], S. Franchino[30], D. Francis[30], M. Franklin[57], S. Franz[61], M. Fraternali[120a,120b], S.T. French[28], C. Friedrich[42], F. Friedrich[44], D. Froidevaux[30], J.A. Frost[28], C. Fukunaga[157], E. Fullana Torregrosa[82], B.G. Fulsom[144], J. Fuster[168], C. Gabaldon[55], O. Gabizon[173], A. Gabrielli[20a,20b], A. Gabrielli[133a,133b], S. Gadatsch[106], S. Gadomski[49], G. Gagliardi[50a,50b], P. Gagnon[60], C. Galea[105], B. Galhardo[125a,125c], E.J. Gallas[119], V. Gallo[17], B.J. Gallop[130], P. Gallus[127], G. Galster[36], K.K. Gan[110], R.P. Gandrajula[62], J. Gao[33b,g], Y.S. Gao[144,e], F.M. Garay Walls[46], F. Garberson[177], C. García[168], J.E. García Navarro[168], M. Garcia-Sciveres[15], R.W. Gardner[31], N. Garelli[144], V. Garonne[30], C. Gatti[47], G. Gaudio[120a], B. Gaur[142], L. Gauthier[94], P. Gauzzi[133a,133b], I.L. Gavrilenko[95], C. Gay[169], G. Gaycken[21], E.N. Gazis[10], P. Ge[33d], Z. Gecse[169], C.N.P. Gee[130], D.A.A. Geerts[106], Ch. Geich-Gimbel[21], K. Gellerstedt[147a,147b], C. Gemme[50a], A. Gemmell[53], M.H. Genest[55], S. Gentile[133a,133b],

JHEP06(2014)035

M. George[54], S. George[76], D. Gerbaudo[164], A. Gershon[154], H. Ghazlane[136b], N. Ghodbane[34], B. Giacobbe[20a], S. Giagu[133a,133b], V. Giangiobbe[12], P. Giannetti[123a,123b], F. Gianotti[30], B. Gibbard[25], S.M. Gibson[76], M. Gilchriese[15], T.P.S. Gillam[28], D. Gillberg[30], G. Gilles[34], D.M. Gingrich[3,d], N. Giokaris[9], M.P. Giordani[165a,165c], R. Giordano[103a,103b], F.M. Giorgi[16], P.F. Giraud[137], D. Giugni[90a], C. Giuliani[48], M. Giulini[58b], B.K. Gjelsten[118], I. Gkialas[155,k], L.K. Gladilin[98], C. Glasman[81], J. Glatzer[30], P.C.F. Glaysher[46], A. Glazov[42], G.L. Glonti[64], M. Goblirsch-Kolb[100], J.R. Goddard[75], J. Godfrey[143], J. Godlewski[30], C. Goeringer[82], S. Goldfarb[88], T. Golling[177], D. Golubkov[129], A. Gomes[125a,125b,125d], L.S. Gomez Fajardo[42], R. Gonçalo[125a], J. Goncalves Pinto Firmino Da Costa[42], L. Gonella[21], S. González de la Hoz[168], G. Gonzalez Parra[12], M.L. Gonzalez Silva[27], S. Gonzalez-Sevilla[49], L. Goossens[30], P.A. Gorbounov[96], H.A. Gordon[25], I. Gorelov[104], G. Gorfine[176], B. Gorini[30], E. Gorini[72a,72b], A. Gorišek[74], E. Gornicki[39], A.T. Goshaw[6], C. Gössling[43], M.I. Gostkin[64], M. Gouighri[136a], D. Goujdami[136c], M.P. Goulette[49], A.G. Goussiou[139], C. Goy[5], S. Gozpinar[23], H.M.X. Grabas[137], L. Graber[54], I. Grabowska-Bold[38a], P. Grafström[20a,20b], K-J. Grahn[42], J. Gramling[49], E. Gramstad[118], S. Grancagnolo[16], V. Grassi[149], V. Gratchev[122], H.M. Gray[30], E. Graziani[135a], O.G. Grebenyuk[122], Z.D. Greenwood[78,l], K. Gregersen[77], I.M. Gregor[42], P. Grenier[144], J. Griffiths[8], N. Grigalashvili[64], A.A. Grillo[138], K. Grimm[71], S. Grinstein[12,m], Ph. Gris[34], Y.V. Grishkevich[98], J.-F. Grivaz[116], J.P. Grohs[44], A. Grohsjean[42], E. Gross[173], J. Grosse-Knetter[54], G.C. Grossi[134a,134b], J. Groth-Jensen[173], Z.J. Grout[150], K. Grybel[142], L. Guan[33b], F. Guescini[49], D. Guest[177], O. Gueta[154], C. Guicheney[34], E. Guido[50a,50b], T. Guillemin[116], S. Guindon[2], U. Gul[53], C. Gumpert[44], J. Gunther[127], J. Guo[35], S. Gupta[119], P. Gutierrez[112], N.G. Gutierrez Ortiz[53], C. Gutschow[77], N. Guttman[154], C. Guyot[137], C. Gwenlan[119], C.B. Gwilliam[73], A. Haas[109], C. Haber[15], H.K. Hadavand[8], N. Haddad[136e], P. Haefner[21], S. Hageboeck[21], Z. Hajduk[39], H. Hakobyan[178], M. Haleem[42], D. Hall[119], G. Halladjian[89], K. Hamacher[176], P. Hamal[114], K. Hamano[87], M. Hamer[54], A. Hamilton[146a], S. Hamilton[162], P.G. Hamnett[42], L. Han[33b], K. Hanagaki[117], K. Hanawa[156], M. Hance[15], P. Hanke[58a], J.R. Hansen[36], J.B. Hansen[36], J.D. Hansen[36], P.H. Hansen[36], K. Hara[161], A.S. Hard[174], T. Harenberg[176], S. Harkusha[91], D. Harper[88], R.D. Harrington[46], O.M. Harris[139], P.F. Harrison[171], F. Hartjes[106], S. Hasegawa[102], Y. Hasegawa[141], A. Hasib[112], S. Hassani[137], S. Haug[17], M. Hauschild[30], R. Hauser[89], M. Havranek[126], C.M. Hawkes[18], R.J. Hawkings[30], A.D. Hawkins[80], T. Hayashi[161], D. Hayden[89], C.P. Hays[119], H.S. Hayward[73], S.J. Haywood[130], S.J. Head[18], T. Heck[82], V. Hedberg[80], L. Heelan[8], S. Heim[121], T. Heim[176], B. Heinemann[15], L. Heinrich[109], S. Heisterkamp[36], J. Hejbal[126], L. Helary[22], C. Heller[99], M. Heller[30], S. Hellman[147a,147b], D. Hellmich[21], C. Helsens[30], J. Henderson[119], R.C.W. Henderson[71], C. Hengler[42], A. Henrichs[177], A.M. Henriques Correia[30], S. Henrot-Versille[116], C. Hensel[54], G.H. Herbert[16], Y. Hernández Jiménez[168], R. Herrberg-Schubert[16], G. Herten[48], R. Hertenberger[99], L. Hervas[30], G.G. Hesketh[77], N.P. Hessey[106], R. Hickling[75], E. Higón-Rodriguez[168], E. Hill[170], J.C. Hill[28], K.H. Hiller[42], S. Hillert[21], S.J. Hillier[18], I. Hinchliffe[15], E. Hines[121], M. Hirose[117], D. Hirschbuehl[176], J. Hobbs[149], N. Hod[106], M.C. Hodgkinson[140], P. Hodgson[140], A. Hoecker[30], M.R. Hoeferkamp[104], J. Hoffman[40], D. Hoffmann[84], J.I. Hofmann[58a], M. Hohlfeld[82], T.R. Holmes[15], T.M. Hong[121], L. Hooft van Huysduynen[109], J-Y. Hostachy[55], S. Hou[152], A. Hoummada[136a], J. Howard[119], J. Howarth[42], M. Hrabovsky[114], I. Hristova[16], J. Hrivnac[116], T. Hryn'ova[5], P.J. Hsu[82], S.-C. Hsu[139], D. Hu[35], X. Hu[25], Y. Huang[42], Z. Hubacek[30], F. Hubaut[84], F. Huegging[21], T.B. Huffman[119], E.W. Hughes[35], G. Hughes[71], M. Huhtinen[30], T.A. Hülsing[82], M. Hurwitz[15], N. Huseynov[64,b], J. Huston[89], J. Huth[57], G. Iacobucci[49], G. Iakovidis[10], I. Ibragimov[142], L. Iconomidou-Fayard[116], J. Idarraga[116], E. Ideal[177], P. Iengo[103a], O. Igonkina[106], T. Iizawa[172], Y. Ikegami[65], K. Ikematsu[142], M. Ikeno[65], D. Iliadis[155], N. Ilic[159], Y. Inamaru[66], T. Ince[100], P. Ioannou[9], M. Iodice[135a], K. Iordanidou[9], V. Ippolito[57], A. Irles Quiles[168], C. Isaksson[167], M. Ishino[67], M. Ishitsuka[158], R. Ishmukhametov[110], C. Issever[119], S. Istin[19a], J.M. Iturbe Ponce[83], J. Ivarsson[80], A.V. Ivashin[129], W. Iwanski[39], H. Iwasaki[65], J.M. Izen[41], V. Izzo[103a], B. Jackson[121], J.N. Jackson[73], M. Jackson[73], P. Jackson[1], M.R. Jaekel[30], V. Jain[2], K. Jakobs[48], S. Jakobsen[30],

JHEP06(2014)035

T. Jakoubek[126], J. Jakubek[127], D.O. Jamin[152], D.K. Jana[78], E. Jansen[77], H. Jansen[30], J. Janssen[21], M. Janus[171], G. Jarlskog[80], N. Javadov[64,b], T. Javůrek[48], L. Jeanty[15], G.-Y. Jeng[151], D. Jennens[87], P. Jenni[48,n], J. Jentzsch[43], C. Jeske[171], S. Jézéquel[5], H. Ji[174], W. Ji[82], J. Jia[149], Y. Jiang[33b], M. Jimenez Belenguer[42], S. Jin[33a], A. Jinaru[26a], O. Jinnouchi[158], M.D. Joergensen[36], K.E. Johansson[147a], P. Johansson[140], K.A. Johns[7], K. Jon-And[147a,147b], G. Jones[171], R.W.L. Jones[71], T.J. Jones[73], J. Jongmanns[58a], P.M. Jorge[125a,125b], K.D. Joshi[83], J. Jovicevic[148], X. Ju[174], C.A. Jung[43], R.M. Jungst[30], P. Jussel[61], A. Juste Rozas[12,m], M. Kaci[168], A. Kaczmarska[39], M. Kado[116], H. Kagan[110], M. Kagan[144], E. Kajomovitz[45], S. Kama[40], N. Kanaya[156], M. Kaneda[30], S. Kaneti[28], T. Kanno[158], V.A. Kantserov[97], J. Kanzaki[65], B. Kaplan[109], A. Kapliy[31], D. Kar[53], K. Karakostas[10], N. Karastathis[10], M. Karnevskiy[82], S.N. Karpov[64], K. Karthik[109], V. Kartvelishvili[71], A.N. Karyukhin[129], L. Kashif[174], G. Kasieczka[58b], R.D. Kass[110], A. Kastanas[14], Y. Kataoka[156], A. Katre[49], J. Katzy[42], V. Kaushik[7], K. Kawagoe[69], T. Kawamoto[156], G. Kawamura[54], S. Kazama[156], V.F. Kazanin[108], M.Y. Kazarinov[64], R. Keeler[170], P.T. Keener[121], R. Kehoe[40], M. Keil[54], J.S. Keller[42], H. Keoshkerian[5], O. Kepka[126], B.P. Kerševan[74], S. Kersten[176], K. Kessoku[156], J. Keung[159], F. Khalil-zada[11], H. Khandanyan[147a,147b], A. Khanov[113], A. Khodinov[97], A. Khomich[58a], T.J. Khoo[28], G. Khoriauli[21], A. Khoroshilov[176], V. Khovanskiy[96], E. Khramov[64], J. Khubua[51b], H.Y. Kim[8], H. Kim[147a,147b], S.H. Kim[161], N. Kimura[172], O. Kind[16], B.T. King[73], M. King[168], R.S.B. King[119], S.B. King[169], J. Kirk[130], A.E. Kiryunin[100], T. Kishimoto[66], D. Kisielewska[38a], F. Kiss[48], T. Kitamura[66], T. Kittelmann[124], K. Kiuchi[161], E. Kladiva[145b], M. Klein[73], U. Klein[73], K. Kleinknecht[82], P. Klimek[147a,147b], A. Klimentov[25], R. Klingenberg[43], J.A. Klinger[83], T. Klioutchnikova[30], P.F. Klok[105], E.-E. Kluge[58a], P. Kluit[106], S. Kluth[100], E. Kneringer[61], E.B.F.G. Knoops[84], A. Knue[53], T. Kobayashi[156], M. Kobel[44], M. Kocian[144], P. Kodys[128], P. Koevesarki[21], T. Koffas[29], E. Koffeman[106], L.A. Kogan[119], S. Kohlmann[176], Z. Kohout[127], T. Kohriki[65], T. Koi[144], H. Kolanoski[16], I. Koletsou[5], J. Koll[89], A.A. Komar[95,*], Y. Komori[156], T. Kondo[65], N. Kondrashova[42], K. Köneke[48], A.C. König[105], S. König[82], T. Kono[65,o], R. Konoplich[109,p], N. Konstantinidis[77], R. Kopeliansky[153], S. Koperny[38a], L. Köpke[82], A.K. Kopp[48], K. Korcyl[39], K. Kordas[155], A. Korn[77], A.A. Korol[108], I. Korolkov[12], E.V. Korolkova[140], V.A. Korotkov[129], O. Kortner[100], S. Kortner[100], V.V. Kostyukhin[21], S. Kotov[100], V.M. Kotov[64], A. Kotwal[45], C. Kourkoumelis[9], V. Kouskoura[155], A. Koutsman[160a], R. Kowalewski[170], T.Z. Kowalski[38a], W. Kozanecki[137], A.S. Kozhin[129], V. Kral[127], V.A. Kramarenko[98], G. Kramberger[74], D. Krasnopevtsev[97], M.W. Krasny[79], A. Krasznahorkay[30], J.K. Kraus[21], A. Kravchenko[25], S. Kreiss[109], M. Kretz[58c], J. Kretzschmar[73], K. Kreutzfeldt[52], P. Krieger[159], K. Kroeninger[54], H. Kroha[100], J. Kroll[121], J. Kroseberg[21], J. Krstic[13a], U. Kruchonak[64], H. Krüger[21], T. Kruker[17], N. Krumnack[63], Z.V. Krumshteyn[64], A. Kruse[174], M.C. Kruse[45], M. Kruskal[22], T. Kubota[87], S. Kuday[4a], S. Kuehn[48], A. Kugel[58c], A. Kuhl[138], T. Kuhl[42], V. Kukhtin[64], Y. Kulchitsky[91], S. Kuleshov[32b], M. Kuna[133a,133b], J. Kunkle[121], A. Kupco[126], H. Kurashige[66], Y.A. Kurochkin[91], R. Kurumida[66], V. Kus[126], E.S. Kuwertz[148], M. Kuze[158], J. Kvita[114], A. La Rosa[49], L. La Rotonda[37a,37b], C. Lacasta[168], F. Lacava[133a,133b], J. Lacey[29], H. Lacker[16], D. Lacour[79], V.R. Lacuesta[168], E. Ladygin[64], R. Lafaye[5], B. Laforge[79], T. Lagouri[177], S. Lai[48], H. Laier[58a], L. Lambourne[77], S. Lammers[60], C.L. Lampen[7], W. Lampl[7], E. Lançon[137], U. Landgraf[48], M.P.J. Landon[75], V.S. Lang[58a], C. Lange[42], A.J. Lankford[164], F. Lanni[25], K. Lantzsch[30], S. Laplace[79], C. Lapoire[21], J.F. Laporte[137], T. Lari[90a], M. Lassnig[30], P. Laurelli[47], W. Lavrijsen[15], A.T. Law[138], P. Laycock[73], B.T. Le[55], O. Le Dortz[79], E. Le Guirriec[84], E. Le Menedeu[12], T. LeCompte[6], F. Ledroit-Guillon[55], C.A. Lee[152], H. Lee[106], J.S.H. Lee[117], S.C. Lee[152], L. Lee[177], G. Lefebvre[79], M. Lefebvre[170], F. Legger[99], C. Leggett[15], A. Lehan[73], M. Lehmacher[21], G. Lehmann Miotto[30], X. Lei[7], A.G. Leister[177], M.A.L. Leite[24d], R. Leitner[128], D. Lellouch[173], B. Lemmer[54], K.J.C. Leney[77], T. Lenz[106], G. Lenzen[176], B. Lenzi[30], R. Leone[7], K. Leonhardt[44], S. Leontsinis[10], C. Leroy[94], C.G. Lester[28], C.M. Lester[121], M. Levchenko[122], J. Levêque[5], D. Levin[88], L.J. Levinson[173], M. Levy[18], A. Lewis[119], G.H. Lewis[109], A.M. Leyko[21], M. Leyton[41], B. Li[33b,q], B. Li[84], H. Li[149], H.L. Li[31], L. Li[33e], S. Li[45], Y. Li[33c,r], Z. Liang[119,s], H. Liao[34], B. Liberti[134a], P. Lichard[30], K. Lie[166], J. Liebal[21],

JHEP06(2014)035

W. Liebig[14], C. Limbach[21], A. Limosani[87], M. Limper[62], S.C. Lin[152,t], F. Linde[106], B.E. Lindquist[149], J.T. Linnemann[89], E. Lipeles[121], A. Lipniacka[14], M. Lisovyi[42], T.M. Liss[166], D. Lissauer[25], A. Lister[169], A.M. Litke[138], B. Liu[152], D. Liu[152], J.B. Liu[33b], K. Liu[33b,u], L. Liu[88], M. Liu[45], M. Liu[33b], Y. Liu[33b], M. Livan[120a,120b], S.S.A. Livermore[119], A. Lleres[55], J. Llorente Merino[81], S.L. Lloyd[75], F. Lo Sterzo[152], E. Lobodzinska[42], P. Loch[7], W.S. Lockman[138], T. Loddenkoetter[21], F.K. Loebinger[83], A.E. Loevschall-Jensen[36], A. Loginov[177], C.W. Loh[169], T. Lohse[16], K. Lohwasser[48], M. Lokajicek[126], V.P. Lombardo[5], B.A. Long[22], J.D. Long[88], R.E. Long[71], L. Lopes[125a], D. Lopez Mateos[57], B. Lopez Paredes[140], J. Lorenz[99], N. Lorenzo Martinez[60], M. Losada[163], P. Loscutoff[15], X. Lou[41], A. Lounis[116], J. Love[6], P.A. Love[71], A.J. Lowe[144,e], F. Lu[33a], H.J. Lubatti[139], C. Luci[133a,133b], A. Lucotte[55], F. Luehring[60], W. Lukas[61], L. Luminari[133a], O. Lundberg[147a,147b], B. Lund-Jensen[148], M. Lungwitz[82], D. Lynn[25], R. Lysak[126], E. Lytken[80], H. Ma[25], L.L. Ma[33d], G. Maccarrone[47], A. Macchiolo[100], J. Machado Miguens[125a,125b], D. Macina[30], D. Madaffari[84], R. Madar[48], H.J. Maddocks[71], W.F. Mader[44], A. Madsen[167], M. Maeno[8], T. Maeno[25], E. Magradze[54], K. Mahboubi[48], J. Mahlstedt[106], S. Mahmoud[73], C. Maiani[137], C. Maidantchik[24a], A. Maio[125a,125b,125d], S. Majewski[115], Y. Makida[65], N. Makovec[116], P. Mal[137,v], B. Malaescu[79], Pa. Malecki[39], V.P. Maleev[122], F. Malek[55], U. Mallik[62], D. Malon[6], C. Malone[144], S. Maltezos[10], V.M. Malyshev[108], S. Malyukov[30], J. Mamuzic[13b], B. Mandelli[30], L. Mandelli[90a], I. Mandić[74], R. Mandrysch[62], J. Maneira[125a,125b], A. Manfredini[100], L. Manhaes de Andrade Filho[24b], J.A. Manjarres Ramos[160b], A. Mann[99], P.M. Manning[138], A. Manousakis-Katsikakis[9], B. Mansoulie[137], R. Mantifel[86], L. Mapelli[30], L. March[168], J.F. Marchand[29], G. Marchiori[79], M. Marcisovsky[126], C.P. Marino[170], C.N. Marques[125a], F. Marroquim[24a], S.P. Marsden[83], Z. Marshall[15], L.F. Marti[17], S. Marti-Garcia[168], B. Martin[30], B. Martin[89], J.P. Martin[94], T.A. Martin[171], V.J. Martin[46], B. Martin dit Latour[14], H. Martinez[137], M. Martinez[12,m], S. Martin-Haugh[130], A.C. Martyniuk[77], M. Marx[139], F. Marzano[133a], A. Marzin[30], L. Masetti[82], T. Mashimo[156], R. Mashinistov[95], J. Masik[83], A.L. Maslennikov[108], I. Massa[20a,20b], N. Massol[5], P. Mastrandrea[149], A. Mastroberardino[37a,37b], T. Masubuchi[156], P. Matricon[116], H. Matsunaga[156], T. Matsushita[66], P. Mättig[176], S. Mättig[42], J. Mattmann[82], J. Maurer[26a], S.J. Maxfield[73], D.A. Maximov[108,f], R. Mazini[152], L. Mazzaferro[134a,134b], G. Mc Goldrick[159], S.P. Mc Kee[88], A. McCarn[88], R.L. McCarthy[149], T.G. McCarthy[29], N.A. McCubbin[130], K.W. McFarlane[56,*], J.A. Mcfayden[77], G. Mchedlidze[54], T. Mclaughlan[18], S.J. McMahon[130], R.A. McPherson[170,i], A. Meade[85], J. Mechnich[106], M. Medinnis[42], S. Meehan[31], S. Mehlhase[36], A. Mehta[73], K. Meier[58a], C. Meineck[99], B. Meirose[80], C. Melachrinos[31], B.R. Mellado Garcia[146c], F. Meloni[90a,90b], A. Mengarelli[20a,20b], S. Menke[100], E. Meoni[162], K.M. Mercurio[57], S. Mergelmeyer[21], N. Meric[137], P. Mermod[49], L. Merola[103a,103b], C. Meroni[90a], F.S. Merritt[31], H. Merritt[110], A. Messina[30,w], J. Metcalfe[25], A.S. Mete[164], C. Meyer[82], C. Meyer[31], J-P. Meyer[137], J. Meyer[30], R.P. Middleton[130], S. Migas[73], L. Mijović[137], G. Mikenberg[173], M. Mikestikova[126], M. Mikuž[74], D.W. Miller[31], C. Mills[46], A. Milov[173], D.A. Milstead[147a,147b], D. Milstein[173], A.A. Minaenko[129], M. Miñano Moya[168], I.A. Minashvili[64], A.I. Mincer[109], B. Mindur[38a], M. Mineev[64], Y. Ming[174], L.M. Mir[12], G. Mirabelli[133a], T. Mitani[172], J. Mitrevski[99], V.A. Mitsou[168], S. Mitsui[65], A. Miucci[49], P.S. Miyagawa[140], J.U. Mjörnmark[80], T. Moa[147a,147b], K. Mochizuki[84], V. Moeller[28], S. Mohapatra[35], W. Mohr[48], S. Molander[147a,147b], R. Moles-Valls[168], K. Mönig[42], C. Monini[55], J. Monk[36], E. Monnier[84], J. Montejo Berlingen[12], F. Monticelli[70], S. Monzani[133a,133b], R.W. Moore[3], A. Moraes[53], N. Morange[62], J. Morel[54], D. Moreno[82], M. Moreno Llácer[54], P. Morettini[50a], M. Morgenstern[44], M. Morii[57], S. Moritz[82], A.K. Morley[148], G. Mornacchi[30], J.D. Morris[75], L. Morvaj[102], H.G. Moser[100], M. Mosidze[51b], J. Moss[110], R. Mount[144], E. Mountricha[25], S.V. Mouraviev[95,*], E.J.W. Moyse[85], S. Muanza[84], R.D. Mudd[18], F. Mueller[58a], J. Mueller[124], K. Mueller[21], T. Mueller[28], T. Mueller[82], D. Muenstermann[49], Y. Munwes[154], J.A. Murillo Quijada[18], W.J. Murray[171,130], H. Musheghyan[54], E. Musto[153], A.G. Myagkov[129,x], M. Myska[127], O. Nackenhorst[54], J. Nadal[54], K. Nagai[61], R. Nagai[158], Y. Nagai[84], K. Nagano[65], A. Nagarkar[110], Y. Nagasaka[59], M. Nagel[100], A.M. Nairz[30], Y. Nakahama[30], K. Nakamura[65], T. Nakamura[156], I. Nakano[111],

JHEP06(2014)035

H. Namasivayam[41], G. Nanava[21], R. Narayan[58b], T. Nattermann[21], T. Naumann[42], G. Navarro[163], R. Nayyar[7], H.A. Neal[88], P.Yu. Nechaeva[95], T.J. Neep[83], A. Negri[120a,120b], G. Negri[30], M. Negrini[20a], S. Nektarijevic[49], A. Nelson[164], T.K. Nelson[144], S. Nemecek[126], P. Nemethy[109], A.A. Nepomuceno[24a], M. Nessi[30,y], M.S. Neubauer[166], M. Neumann[176], R.M. Neves[109], P. Nevski[25], F.M. Newcomer[121], P.R. Newman[18], D.H. Nguyen[6], R.B. Nickerson[119], R. Nicolaidou[137], B. Nicquevert[30], J. Nielsen[138], N. Nikiforou[35], A. Nikiforov[16], V. Nikolaenko[129,x], I. Nikolic-Audit[79], K. Nikolics[49], K. Nikolopoulos[18], P. Nilsson[8], Y. Ninomiya[156], A. Nisati[133a], R. Nisius[100], T. Nobe[158], L. Nodulman[6], M. Nomachi[117], I. Nomidis[155], S. Norberg[112], M. Nordberg[30], J. Novakova[128], S. Nowak[100], M. Nozaki[65], L. Nozka[114], K. Ntekas[10], G. Nunes Hanninger[87], T. Nunnemann[99], E. Nurse[77], F. Nuti[87], B.J. O'Brien[46], F. O'grady[7], D.C. O'Neil[143], V. O'Shea[53], F.G. Oakham[29,d], H. Oberlack[100], T. Obermann[21], J. Ocariz[79], A. Ochi[66], M.I. Ochoa[77], S. Oda[69], S. Odaka[65], H. Ogren[60], A. Oh[83], S.H. Oh[45], C.C. Ohm[30], H. Ohman[167], T. Ohshima[102], W. Okamura[117], H. Okawa[25], Y. Okumura[31], T. Okuyama[156], A. Olariu[26a], A.G. Olchevski[64], S.A. Olivares Pino[46], D. Oliveira Damazio[25], E. Oliver Garcia[168], A. Olszewski[39], J. Olszowska[39], A. Onofre[125a,125e], P.U.E. Onyisi[31,z], C.J. Oram[160a], M.J. Oreglia[31], Y. Oren[154], D. Orestano[135a,135b], N. Orlando[72a,72b], C. Oropeza Barrera[53], R.S. Orr[159], B. Osculati[50a,50b], R. Ospanov[121], G. Otero y Garzon[27], H. Otono[69], M. Ouchrif[136d], E.A. Ouellette[170], F. Ould-Saada[118], A. Ouraou[137], K.P. Oussoren[106], Q. Ouyang[33a], A. Ovcharova[15], M. Owen[83], V.E. Ozcan[19a], N. Ozturk[8], K. Pachal[119], A. Pacheco Pages[12], C. Padilla Aranda[12], M. Pagáčová[48], S. Pagan Griso[15], E. Paganis[140], C. Pahl[100], F. Paige[25], P. Pais[85], K. Pajchel[118], G. Palacino[160b], S. Palestini[30], D. Pallin[34], A. Palma[125a,125b], J.D. Palmer[18], Y.B. Pan[174], E. Panagiotopoulou[10], J.G. Panduro Vazquez[76], P. Pani[106], N. Panikashvili[88], S. Panitkin[25], D. Pantea[26a], L. Paolozzi[134a,134b], Th.D. Papadopoulou[10], K. Papageorgiou[155,k], A. Paramonov[6], D. Paredes Hernandez[34], M.A. Parker[28], F. Parodi[50a,50b], J.A. Parsons[35], U. Parzefall[48], E. Pasqualucci[133a], S. Passaggio[50a], A. Passeri[135a], F. Pastore[135a,135b,*], Fr. Pastore[76], G. Pásztor[49,aa], S. Pataraia[176], N.D. Patel[151], J.R. Pater[83], S. Patricelli[103a,103b], T. Pauly[30], J. Pearce[170], M. Pedersen[118], S. Pedraza Lopez[168], R. Pedro[125a,125b], S.V. Peleganchuk[108], D. Pelikan[167], H. Peng[33b], B. Penning[31], J. Penwell[60], D.V. Perepelitsa[25], E. Perez Codina[160a], M.T. Pérez García-Estañ[168], V. Perez Reale[35], L. Perini[90a,90b], H. Pernegger[30], R. Perrino[72a], R. Peschke[42], V.D. Peshekhonov[64], K. Peters[30], R.F.Y. Peters[83], B.A. Petersen[87], J. Petersen[30], T.C. Petersen[36], E. Petit[42], A. Petridis[147a,147b], C. Petridou[155], E. Petrolo[133a], F. Petrucci[135a,135b], M. Petteni[143], N.E. Pettersson[158], R. Pezoa[32b], P.W. Phillips[130], G. Piacquadio[144], E. Pianori[171], A. Picazio[49], E. Piccaro[75], M. Piccinini[20a,20b], R. Piegaia[27], D.T. Pignotti[110], J.E. Pilcher[31], A.D. Pilkington[77], J. Pina[125a,125b,125d], M. Pinamonti[165a,165c,ab], A. Pinder[119], J.L. Pinfold[3], A. Pingel[36], B. Pinto[125a], S. Pires[79], M. Pitt[173], C. Pizio[90a,90b], M.-A. Pleier[25], V. Pleskot[128], E. Plotnikova[64], P. Plucinski[147a,147b], S. Poddar[58a], F. Podlyski[34], R. Poettgen[82], L. Poggioli[116], D. Pohl[21], M. Pohl[49], G. Polesello[120a], A. Policicchio[37a,37b], R. Polifka[159], A. Polini[20a], C.S. Pollard[45], V. Polychronakos[25], K. Pommès[30], L. Pontecorvo[133a], B.G. Pope[89], G.A. Popeneciu[26b], D.S. Popovic[13a], A. Poppleton[30], X. Portell Bueso[12], G.E. Pospelov[100], S. Pospisil[127], K. Potamianos[15], I.N. Potrap[64], C.J. Potter[150], C.T. Potter[115], G. Poulard[30], J. Poveda[60], V. Pozdnyakov[64], P. Pralavorio[84], A. Pranko[15], S. Prasad[30], R. Pravahan[8], S. Prell[63], D. Price[83], J. Price[73], L.E. Price[6], D. Prieur[124], M. Primavera[72a], M. Proissl[46], K. Prokofiev[47], F. Prokoshin[32b], E. Protopapadaki[137], S. Protopopescu[25], J. Proudfoot[6], M. Przybycien[38a], H. Przysiezniak[5], E. Ptacek[115], E. Pueschel[85], D. Puldon[149], M. Purohit[25,ac], P. Puzo[116], J. Qian[88], G. Qin[53], Y. Qin[83], A. Quadt[54], D.R. Quarrie[15], W.B. Quayle[165a,165b], D. Quilty[53], A. Qureshi[160b], V. Radeka[25], V. Radescu[42], S.K. Radhakrishnan[149], P. Radloff[115], P. Rados[87], F. Ragusa[90a,90b], G. Rahal[179], S. Rajagopalan[25], M. Rammensee[30], A.S. Randle-Conde[40], C. Rangel-Smith[167], K. Rao[164], F. Rauscher[99], T.C. Rave[48], T. Ravenscroft[53], M. Raymond[30], A.L. Read[118], D.M. Rebuzzi[120a,120b], A. Redelbach[175], G. Redlinger[25], R. Reece[138], K. Reeves[41], L. Rehnisch[16], A. Reinsch[115], H. Reisin[27], M. Relich[164], C. Rembser[30], Z.L. Ren[152], A. Renaud[116],

JHEP06(2014)035

M. Rescigno[133a], S. Resconi[90a], B. Resende[137], P. Reznicek[128], R. Rezvani[94], R. Richter[100], M. Ridel[79], P. Rieck[16], M. Rijssenbeek[149], A. Rimoldi[120a,120b], L. Rinaldi[20a], E. Ritsch[61], I. Riu[12], F. Rizatdinova[113], E. Rizvi[75], S.H. Robertson[86,i], A. Robichaud-Veronneau[119], D. Robinson[28], J.E.M. Robinson[83], A. Robson[53], C. Roda[123a,123b], L. Rodrigues[30], S. Roe[30], O. Røhne[118], S. Rolli[162], A. Romaniouk[97], M. Romano[20a,20b], G. Romeo[27], E. Romero Adam[168], N. Rompotis[139], L. Roos[79], E. Ros[168], S. Rosati[133a], K. Rosbach[49], M. Rose[76], P.L. Rosendahl[14], O. Rosenthal[142], V. Rossetti[147a,147b], E. Rossi[103a,103b], L.P. Rossi[50a], R. Rosten[139], M. Rotaru[26a], I. Roth[173], J. Rothberg[139], D. Rousseau[116], C.R. Royon[137], A. Rozanov[84], Y. Rozen[153], X. Ruan[146c], F. Rubbo[12], I. Rubinskiy[42], V.I. Rud[98], C. Rudolph[44], M.S. Rudolph[159], F. Rühr[48], A. Ruiz-Martinez[30], Z. Rurikova[48], N.A. Rusakovich[64], A. Ruschke[99], J.P. Rutherfoord[7], N. Ruthmann[48], Y.F. Ryabov[122], M. Rybar[128], G. Rybkin[116], N.C. Ryder[119], A.F. Saavedra[151], S. Sacerdoti[27], A. Saddique[3], I. Sadeh[154], H.F-W. Sadrozinski[138], R. Sadykov[64], F. Safai Tehrani[133a], H. Sakamoto[156], Y. Sakurai[172], G. Salamanna[75], A. Salamon[134a], M. Saleem[112], D. Salek[106], P.H. Sales De Bruin[139], D. Salihagic[100], A. Salnikov[144], J. Salt[168], B.M. Salvachua Ferrando[6], D. Salvatore[37a,37b], F. Salvatore[150], A. Salvucci[105], A. Salzburger[30], D. Sampsonidis[155], A. Sanchez[103a,103b], J. Sánchez[168], V. Sanchez Martinez[168], H. Sandaker[14], R.L. Sandbach[75], H.G. Sander[82], M.P. Sanders[99], M. Sandhoff[176], T. Sandoval[28], C. Sandoval[163], R. Sandstroem[100], D.P.C. Sankey[130], A. Sansoni[47], C. Santoni[34], R. Santonico[134a,134b], H. Santos[125a], I. Santoyo Castillo[150], K. Sapp[124], A. Sapronov[64], J.G. Saraiva[125a,125d], B. Sarrazin[21], G. Sartisohn[176], O. Sasaki[65], Y. Sasaki[156], I. Satsounkevitch[91], G. Sauvage[5,*], E. Sauvan[5], P. Savard[159,d], D.O. Savu[30], C. Sawyer[119], L. Sawyer[78,l], D.H. Saxon[53], J. Saxon[121], C. Sbarra[20a], A. Sbrizzi[3], T. Scanlon[30], D.A. Scannicchio[164], M. Scarcella[151], J. Schaarschmidt[173], P. Schacht[100], D. Schaefer[121], R. Schaefer[42], S. Schaepe[21], S. Schaetzel[58b], U. Schäfer[82], A.C. Schaffer[116], D. Schaile[99], R.D. Schamberger[149], V. Scharf[58a], V.A. Schegelsky[122], D. Scheirich[128], M. Schernau[164], M.I. Scherzer[35], C. Schiavi[50a,50b], J. Schieck[99], C. Schillo[48], M. Schioppa[37a,37b], S. Schlenker[30], E. Schmidt[48], K. Schmieden[30], C. Schmitt[82], C. Schmitt[99], S. Schmitt[58b], B. Schneider[17], Y.J. Schnellbach[73], U. Schnoor[44], L. Schoeffel[137], A. Schoening[58b], B.D. Schoenrock[89], A.L.S. Schorlemmer[54], M. Schott[82], D. Schouten[160a], J. Schovancova[25], M. Schram[86], S. Schramm[159], M. Schreyer[175], C. Schroeder[82], N. Schuh[82], M.J. Schultens[21], H.-C. Schultz-Coulon[58a], H. Schulz[16], M. Schumacher[48], B.A. Schumm[138], Ph. Schune[137], A. Schwartzman[144], Ph. Schwegler[100], Ph. Schwemling[137], R. Schwienhorst[89], J. Schwindling[137], T. Schwindt[21], M. Schwoerer[5], F.G. Sciacca[17], E. Scifo[116], G. Sciolla[23], W.G. Scott[130], F. Scuri[123a,123b], F. Scutti[21], J. Searcy[88], G. Sedov[42], E. Sedykh[122], S.C. Seidel[104], A. Seiden[138], F. Seifert[127], J.M. Seixas[24a], G. Sekhniaidze[103a], S.J. Sekula[40], K.E. Selbach[46], D.M. Seliverstov[122,*], G. Sellers[73], N. Semprini-Cesari[20a,20b], C. Serfon[30], L. Serin[116], L. Serkin[54], T. Serre[84], R. Seuster[160a], H. Severini[112], F. Sforza[100], A. Sfyrla[30], E. Shabalina[54], M. Shamim[115], L.Y. Shan[33a], J.T. Shank[22], Q.T. Shao[87], M. Shapiro[15], P.B. Shatalov[96], K. Shaw[165a,165b], P. Sherwood[77], S. Shimizu[66], C.O. Shimmin[164], M. Shimojima[101], T. Shin[56], M. Shiyakova[64], A. Shmeleva[95], M.J. Shochet[31], D. Short[119], S. Shrestha[63], E. Shulga[97], M.A. Shupe[7], S. Shushkevich[42], P. Sicho[126], D. Sidorov[113], A. Sidoti[133a], F. Siegert[44], Dj. Sijacki[13a], O. Silbert[173], J. Silva[125a,125d], Y. Silver[154], D. Silverstein[144], S.B. Silverstein[147a], V. Simak[127], O. Simard[5], Lj. Simic[13a], S. Simion[116], E. Simioni[82], B. Simmons[77], R. Simoniello[90a,90b], M. Simonyan[36], P. Sinervo[159], N.B. Sinev[115], V. Sipica[142], G. Siragusa[175], A. Sircar[78], A.N. Sisakyan[64,*], S.Yu. Sivoklokov[98], J. Sjölin[147a,147b], T.B. Sjursen[14], H.P. Skottowe[57], K.Yu. Skovpen[108], P. Skubic[112], M. Slater[18], T. Slavicek[127], K. Sliwa[162], V. Smakhtin[173], B.H. Smart[46], L. Smestad[14], S.Yu. Smirnov[97], Y. Smirnov[97], L.N. Smirnova[98,ad], O. Smirnova[80], K.M. Smith[53], M. Smizanska[71], K. Smolek[127], A.A. Snesarev[95], G. Snidero[75], J. Snow[112], S. Snyder[25], R. Sobie[170,i], F. Socher[44], J. Sodomka[127], A. Soffer[154], D.A. Soh[152,s], C.A. Solans[30], M. Solar[127], J. Solc[127], E.Yu. Soldatov[97], U. Soldevila[168], E. Solfaroli Camillocci[133a,133b], A.A. Solodkov[129], O.V. Solovyanov[129], V. Solovyev[122], P. Sommer[48], H.Y. Song[33b], N. Soni[1], A. Sood[15], A. Sopczak[127], V. Sopko[127], B. Sopko[127], V. Sorin[12], M. Sosebee[8], R. Soualah[165a,165c], P. Soueid[94], A.M. Soukharev[108], D. South[42], S. Spagnolo[72a,72b], F. Spanò[76], W.R. Spearman[57],

JHEP06(2014)035

R. Spighi[20a], G. Spigo[30], M. Spousta[128], T. Spreitzer[159], B. Spurlock[8], R.D. St. Denis[53], S. Staerz[44], J. Stahlman[121], R. Stamen[58a], E. Stanecka[39], R.W. Stanek[6], C. Stanescu[135a], M. Stanescu-Bellu[42], M.M. Stanitzki[42], S. Stapnes[118], E.A. Starchenko[129], J. Stark[55], P. Staroba[126], P. Starovoitov[42], R. Staszewski[39], P. Stavina[145a,*], G. Steele[53], P. Steinberg[25], I. Stekl[127], B. Stelzer[143], H.J. Stelzer[30], O. Stelzer-Chilton[160a], H. Stenzel[52], S. Stern[100], G.A. Stewart[53], J.A. Stillings[21], M.C. Stockton[86], M. Stoebe[86], G. Stoicea[26a], P. Stolte[54], S. Stonjek[100], A.R. Stradling[8], A. Straessner[44], M.E. Stramaglia[17], J. Strandberg[148], S. Strandberg[147a,147b], A. Strandlie[118], E. Strauss[144], M. Strauss[112], P. Strizenec[145b], R. Ströhmer[175], D.M. Strom[115], R. Stroynowski[40], S.A. Stucci[17], B. Stugu[14], N.A. Styles[42], D. Su[144], J. Su[124], HS. Subramania[3], R. Subramaniam[78], A. Succurro[12], Y. Sugaya[117], C. Suhr[107], M. Suk[127], V.V. Sulin[95], S. Sultansoy[4c], T. Sumida[67], X. Sun[33a], J.E. Sundermann[48], K. Suruliz[140], G. Susinno[37a,37b], M.R. Sutton[150], Y. Suzuki[65], M. Svatos[126], S. Swedish[169], M. Swiatlowski[144], I. Sykora[145a], T. Sykora[128], D. Ta[89], K. Tackmann[42], J. Taenzer[159], A. Taffard[164], R. Tafirout[160a], N. Taiblum[154], Y. Takahashi[102], H. Takai[25], R. Takashima[68], H. Takeda[66], T. Takeshita[141], Y. Takubo[65], M. Talby[84], A.A. Talyshev[108,f], J.Y.C. Tam[175], M.C. Tamsett[78,ae], K.G. Tan[87], J. Tanaka[156], R. Tanaka[116], S. Tanaka[132], S. Tanaka[65], A.J. Tanasijczuk[143], K. Tani[66], N. Tannoury[84], S. Tapprogge[82], S. Tarem[153], F. Tarrade[29], G.F. Tartarelli[90a], P. Tas[128], M. Tasevsky[126], T. Tashiro[67], E. Tassi[37a,37b], A. Tavares Delgado[125a,125b], Y. Tayalati[136d], F.E. Taylor[93], G.N. Taylor[87], W. Taylor[160b], F.A. Teischinger[30], M. Teixeira Dias Castanheira[75], P. Teixeira-Dias[76], K.K. Temming[48], H. Ten Kate[30], P.K. Teng[152], S. Terada[65], K. Terashi[156], J. Terron[81], S. Terzo[100], M. Testa[47], R.J. Teuscher[159,i], J. Therhaag[21], T. Theveneaux-Pelzer[34], S. Thoma[48], J.P. Thomas[18], J. Thomas-Wilsker[76], E.N. Thompson[35], P.D. Thompson[18], P.D. Thompson[159], A.S. Thompson[53], L.A. Thomsen[36], E. Thomson[121], M. Thomson[28], W.M. Thong[87], R.P. Thun[88,*], F. Tian[35], M.J. Tibbetts[15], V.O. Tikhomirov[95,af], Yu.A. Tikhonov[108,f], S. Timoshenko[97], E. Tiouchichine[84], P. Tipton[177], S. Tisserant[84], T. Todorov[5], S. Todorova-Nova[128], B. Toggerson[7], J. Tojo[69], S. Tokár[145a], K. Tokushuku[65], K. Tollefson[89], L. Tomlinson[83], M. Tomoto[102], L. Tompkins[31], K. Toms[104], N.D. Topilin[64], E. Torrence[115], H. Torres[143], E. Torró Pastor[168], J. Toth[84,aa], F. Touchard[84], D.R. Tovey[140], H.L. Tran[116], T. Trefzger[175], L. Tremblet[30], A. Tricoli[30], I.M. Trigger[160a], S. Trincaz-Duvoid[79], M.F. Tripiana[70], N. Triplett[25], W. Trischuk[159], B. Trocmé[55], C. Troncon[90a], M. Trottier-McDonald[143], M. Trovatelli[135a,135b], P. True[89], M. Trzebinski[39], A. Trzupek[39], C. Tsarouchas[30], J.C-L. Tseng[119], P.V. Tsiareshka[91], D. Tsionou[137], G. Tsipolitis[10], N. Tsirintanis[9], S. Tsiskaridze[12], V. Tsiskaridze[48], E.G. Tskhadadze[51a], I.I. Tsukerman[96], V. Tsulaia[15], S. Tsuno[65], D. Tsybychev[149], A. Tudorache[26a], V. Tudorache[26a], A.N. Tuna[121], S.A. Tupputi[20a,20b], S. Turchikhin[98,ad], D. Turecek[127], I. Turk Cakir[4d], R. Turra[90a,90b], P.M. Tuts[35], A. Tykhonov[74], M. Tylmad[147a,147b], M. Tyndel[130], K. Uchida[21], I. Ueda[156], R. Ueno[29], M. Ughetto[84], M. Ugland[14], M. Uhlenbrock[21], F. Ukegawa[161], G. Unal[30], A. Undrus[25], G. Unel[164], F.C. Ungaro[48], Y. Unno[65], D. Urbaniec[35], P. Urquijo[21], G. Usai[8], A. Usanova[61], L. Vacavant[84], V. Vacek[127], B. Vachon[86], N. Valencic[106], S. Valentinetti[20a,20b], A. Valero[168], L. Valery[34], S. Valkar[128], E. Valladolid Gallego[168], S. Vallecorsa[49], J.A. Valls Ferrer[168], R. Van Berg[121], P.C. Van Der Deijl[106], R. van der Geer[106], H. van der Graaf[106], R. Van Der Leeuw[106], D. van der Ster[30], N. van Eldik[30], P. van Gemmeren[6], J. Van Nieuwkoop[143], I. van Vulpen[106], M.C. van Woerden[30], M. Vanadia[133a,133b], W. Vandelli[30], R. Vanguri[121], A. Vaniachine[6], P. Vankov[42], F. Vannucci[79], G. Vardanyan[178], R. Vari[133a], E.W. Varnes[7], T. Varol[85], D. Varouchas[79], A. Vartapetian[8], K.E. Varvell[151], V.I. Vassilakopoulos[56], F. Vazeille[34], T. Vazquez Schroeder[54], J. Veatch[7], F. Veloso[125a,125c], S. Veneziano[133a], A. Ventura[72a,72b], D. Ventura[85], M. Venturi[48], N. Venturi[159], A. Venturini[23], V. Vercesi[120a], M. Verducci[139], W. Verkerke[106], J.C. Vermeulen[106], A. Vest[44], M.C. Vetterli[143,d], O. Viazlo[80], I. Vichou[166], T. Vickey[146c,ag], O.E. Vickey Boeriu[146c], G.H.A. Viehhauser[119], S. Viel[169], R. Vigne[30], M. Villa[20a,20b], M. Villaplana Perez[168], E. Vilucchi[47], M.G. Vincter[29], V.B. Vinogradov[64], J. Virzi[15], I. Vivarelli[150], F. Vives Vaque[3], S. Vlachos[10], D. Vladoiu[99], M. Vlasak[127], A. Vogel[21], P. Vokac[127], G. Volpi[123a,123b], M. Volpi[87], H. von der Schmitt[100],

JHEP06(2014)035

H. von Radziewski[48], E. von Toerne[21], V. Vorobel[128], K. Vorobev[97], M. Vos[168], R. Voss[30], J.H. Vossebeld[73], N. Vranjes[137], M. Vranjes Milosavljevic[106], V. Vrba[126], M. Vreeswijk[106], T. Vu Anh[48], R. Vuillermet[30], I. Vukotic[31], Z. Vykydal[127], W. Wagner[176], P. Wagner[21], S. Wahrmund[44], J. Wakabayashi[102], J. Walder[71], R. Walker[99], W. Walkowiak[142], R. Wall[177], P. Waller[73], B. Walsh[177], C. Wang[152,ah], C. Wang[45], F. Wang[174], H. Wang[15], H. Wang[40], J. Wang[42], J. Wang[33a], K. Wang[86], R. Wang[104], S.M. Wang[152], T. Wang[21], X. Wang[177], C. Wanotayaroj[115], A. Warburton[86], C.P. Ward[28], D.R. Wardrope[77], M. Warsinsky[48], A. Washbrook[46], C. Wasicki[42], I. Watanabe[66], P.M. Watkins[18], A.T. Watson[18], I.J. Watson[151], M.F. Watson[18], G. Watts[139], S. Watts[83], B.M. Waugh[77], S. Webb[83], M.S. Weber[17], S.W. Weber[175], J.S. Webster[31], A.R. Weidberg[119], P. Weigell[100], B. Weinert[60], J. Weingarten[54], C. Weiser[48], H. Weits[106], P.S. Wells[30], T. Wenaus[25], D. Wendland[16], Z. Weng[152,s], T. Wengler[30], S. Wenig[30], N. Wermes[21], M. Werner[48], P. Werner[30], M. Wessels[58a], J. Wetter[162], K. Whalen[29], A. White[8], M.J. White[1], R. White[32b], S. White[123a,123b], D. Whiteson[164], D. Wicke[176], F.J. Wickens[130], W. Wiedenmann[174], M. Wielers[130], P. Wienemann[21], C. Wiglesworth[36], L.A.M. Wiik-Fuchs[21], P.A. Wijeratne[77], A. Wildauer[100], M.A. Wildt[42,ai], H.G. Wilkens[30], J.Z. Will[99], H.H. Williams[121], S. Williams[28], C. Willis[89], S. Willocq[85], J.A. Wilson[18], A. Wilson[88], I. Wingerter-Seez[5], F. Winklmeier[115], M. Wittgen[144], T. Wittig[43], J. Wittkowski[99], S.J. Wollstadt[82], M.W. Wolter[39], H. Wolters[125a,125c], B.K. Wosiek[39], J. Wotschack[30], M.J. Woudstra[83], K.W. Wozniak[39], M. Wright[53], M. Wu[55], S.L. Wu[174], X. Wu[49], Y. Wu[88], E. Wulf[35], T.R. Wyatt[83], B.M. Wynne[46], S. Xella[36], M. Xiao[137], D. Xu[33a], L. Xu[33b,aj], B. Yabsley[151], S. Yacoob[146b,ak], M. Yamada[65], H. Yamaguchi[156], Y. Yamaguchi[156], A. Yamamoto[65], K. Yamamoto[63], S. Yamamoto[156], T. Yamamura[156], T. Yamanaka[156], K. Yamauchi[102], Y. Yamazaki[66], Z. Yan[22], H. Yang[33e], H. Yang[174], U.K. Yang[83], Y. Yang[110], S. Yanush[92], L. Yao[33a], W-M. Yao[15], Y. Yasu[65], E. Yatsenko[42], K.H. Yau Wong[21], J. Ye[40], S. Ye[25], A.L. Yen[57], E. Yildirim[42], M. Yilmaz[4b], R. Yoosoofmiya[124], K. Yorita[172], R. Yoshida[6], K. Yoshihara[156], C. Young[144], C.J.S. Young[30], S. Youssef[22], D.R. Yu[15], J. Yu[8], J.M. Yu[88], J. Yu[113], L. Yuan[66], A. Yurkewicz[107], B. Zabinski[39], R. Zaidan[62], A.M. Zaitsev[129,x], A. Zaman[149], S. Zambito[23], L. Zanello[133a,133b], D. Zanzi[100], A. Zaytsev[25], C. Zeitnitz[176], M. Zeman[127], A. Zemla[38a], K. Zengel[23], O. Zenin[129], T. Ženiš[145a], D. Zerwas[116], G. Zevi della Porta[57], D. Zhang[88], F. Zhang[174], H. Zhang[89], J. Zhang[6], L. Zhang[152], X. Zhang[33d], Z. Zhang[116], Z. Zhao[33b], A. Zhemchugov[64], J. Zhong[119], B. Zhou[88], C. Zhou[45], L. Zhou[35], N. Zhou[164], C.G. Zhu[33d], H. Zhu[33a], J. Zhu[88], Y. Zhu[33b], X. Zhuang[33a], A. Zibell[175], D. Zieminska[60], N.I. Zimine[64], C. Zimmermann[82], R. Zimmermann[21], S. Zimmermann[21], S. Zimmermann[48], Z. Zinonos[54], M. Ziolkowski[142], G. Zobernig[174], A. Zoccoli[20a,20b], M. zur Nedden[16], G. Zurzolo[103a,103b], V. Zutshi[107], L. Zwalinski[30]

[1] Department of Physics, University of Adelaide, Adelaide, Australia
[2] Physics Department, SUNY Albany, Albany NY, United States of America
[3] Department of Physics, University of Alberta, Edmonton AB, Canada
[4] [(a)] Department of Physics, Ankara University, Ankara; [(b)] Department of Physics, Gazi University, Ankara; [(c)] Division of Physics, TOBB University of Economics and Technology, Ankara; [(d)] Turkish Atomic Energy Authority, Ankara, Turkey
[5] LAPP, CNRS/IN2P3 and Université de Savoie, Annecy-le-Vieux, France
[6] High Energy Physics Division, Argonne National Laboratory, Argonne IL, United States of America
[7] Department of Physics, University of Arizona, Tucson AZ, United States of America
[8] Department of Physics, The University of Texas at Arlington, Arlington TX, United States of America
[9] Physics Department, University of Athens, Athens, Greece
[10] Physics Department, National Technical University of Athens, Zografou, Greece
[11] Institute of Physics, Azerbaijan Academy of Sciences, Baku, Azerbaijan
[12] Institut de Física d'Altes Energies and Departament de Física de la Universitat Autònoma de Barcelona, Barcelona, Spain

JHEP06(2014)035

[13] [(a)] Institute of Physics, University of Belgrade, Belgrade; [(b)] Vinca Institute of Nuclear Sciences, University of Belgrade, Belgrade, Serbia
[14] Department for Physics and Technology, University of Bergen, Bergen, Norway
[15] Physics Division, Lawrence Berkeley National Laboratory and University of California, Berkeley CA, United States of America
[16] Department of Physics, Humboldt University, Berlin, Germany
[17] Albert Einstein Center for Fundamental Physics and Laboratory for High Energy Physics, University of Bern, Bern, Switzerland
[18] School of Physics and Astronomy, University of Birmingham, Birmingham, United Kingdom
[19] [(a)] Department of Physics, Bogazici University, Istanbul; [(b)] Department of Physics, Dogus University, Istanbul; [(c)] Department of Physics Engineering, Gaziantep University, Gaziantep, Turkey
[20] [(a)] INFN Sezione di Bologna; [(b)] Dipartimento di Fisica e Astronomia, Università di Bologna, Bologna, Italy
[21] Physikalisches Institut, University of Bonn, Bonn, Germany
[22] Department of Physics, Boston University, Boston MA, United States of America
[23] Department of Physics, Brandeis University, Waltham MA, United States of America
[24] [(a)] Universidade Federal do Rio De Janeiro COPPE/EE/IF, Rio de Janeiro; [(b)] Federal University of Juiz de Fora (UFJF), Juiz de Fora; [(c)] Federal University of Sao Joao del Rei (UFSJ), Sao Joao del Rei; [(d)] Instituto de Fisica, Universidade de Sao Paulo, Sao Paulo, Brazil
[25] Physics Department, Brookhaven National Laboratory, Upton NY, United States of America
[26] [(a)] National Institute of Physics and Nuclear Engineering, Bucharest; [(b)] National Institute for Research and Development of Isotopic and Molecular Technologies, Physics Department, Cluj Napoca; [(c)] University Politehnica Bucharest, Bucharest; [(d)] West University in Timisoara, Timisoara, Romania
[27] Departamento de Física, Universidad de Buenos Aires, Buenos Aires, Argentina
[28] Cavendish Laboratory, University of Cambridge, Cambridge, United Kingdom
[29] Department of Physics, Carleton University, Ottawa ON, Canada
[30] CERN, Geneva, Switzerland
[31] Enrico Fermi Institute, University of Chicago, Chicago IL, United States of America
[32] [(a)] Departamento de Física, Pontificia Universidad Católica de Chile, Santiago; [(b)] Departamento de Física, Universidad Técnica Federico Santa María, Valparaíso, Chile
[33] [(a)] Institute of High Energy Physics, Chinese Academy of Sciences, Beijing; [(b)] Department of Modern Physics, University of Science and Technology of China, Anhui; [(c)] Department of Physics, Nanjing University, Jiangsu; [(d)] School of Physics, Shandong University, Shandong; [(e)] Physics Department, Shanghai Jiao Tong University, Shanghai, China
[34] Laboratoire de Physique Corpusculaire, Clermont Université and Université Blaise Pascal and CNRS/IN2P3, Clermont-Ferrand, France
[35] Nevis Laboratory, Columbia University, Irvington NY, United States of America
[36] Niels Bohr Institute, University of Copenhagen, Kobenhavn, Denmark
[37] [(a)] INFN Gruppo Collegato di Cosenza, Laboratori Nazionali di Frascati; [(b)] Dipartimento di Fisica, Università della Calabria, Rende, Italy
[38] [(a)] AGH University of Science and Technology, Faculty of Physics and Applied Computer Science, Krakow; [(b)] Marian Smoluchowski Institute of Physics, Jagiellonian University, Krakow, Poland
[39] The Henryk Niewodniczanski Institute of Nuclear Physics, Polish Academy of Sciences, Krakow, Poland
[40] Physics Department, Southern Methodist University, Dallas TX, United States of America
[41] Physics Department, University of Texas at Dallas, Richardson TX, United States of America
[42] DESY, Hamburg and Zeuthen, Germany
[43] Institut für Experimentelle Physik IV, Technische Universität Dortmund, Dortmund, Germany
[44] Institut für Kern- und Teilchenphysik, Technische Universität Dresden, Dresden, Germany
[45] Department of Physics, Duke University, Durham NC, United States of America

JHEP06(2014)035

[46] SUPA - School of Physics and Astronomy, University of Edinburgh, Edinburgh, United Kingdom
[47] INFN Laboratori Nazionali di Frascati, Frascati, Italy
[48] Fakultät für Mathematik und Physik, Albert-Ludwigs-Universität, Freiburg, Germany
[49] Section de Physique, Université de Genève, Geneva, Switzerland
[50] [(a)] INFN Sezione di Genova; [(b)] Dipartimento di Fisica, Università di Genova, Genova, Italy
[51] [(a)] E. Andronikashvili Institute of Physics, Iv. Javakhishvili Tbilisi State University, Tbilisi; [(b)] High Energy Physics Institute, Tbilisi State University, Tbilisi, Georgia
[52] II Physikalisches Institut, Justus-Liebig-Universität Giessen, Giessen, Germany
[53] SUPA - School of Physics and Astronomy, University of Glasgow, Glasgow, United Kingdom
[54] II Physikalisches Institut, Georg-August-Universität, Göttingen, Germany
[55] Laboratoire de Physique Subatomique et de Cosmologie, Université Grenoble-Alpes, CNRS/IN2P3, Grenoble, France
[56] Department of Physics, Hampton University, Hampton VA, United States of America
[57] Laboratory for Particle Physics and Cosmology, Harvard University, Cambridge MA, United States of America
[58] [(a)] Kirchhoff-Institut für Physik, Ruprecht-Karls-Universität Heidelberg, Heidelberg; [(b)] Physikalisches Institut, Ruprecht-Karls-Universität Heidelberg, Heidelberg; [(c)] ZITI Institut für technische Informatik, Ruprecht-Karls-Universität Heidelberg, Mannheim, Germany
[59] Faculty of Applied Information Science, Hiroshima Institute of Technology, Hiroshima, Japan
[60] Department of Physics, Indiana University, Bloomington IN, United States of America
[61] Institut für Astro- und Teilchenphysik, Leopold-Franzens-Universität, Innsbruck, Austria
[62] University of Iowa, Iowa City IA, United States of America
[63] Department of Physics and Astronomy, Iowa State University, Ames IA, United States of America
[64] Joint Institute for Nuclear Research, JINR Dubna, Dubna, Russia
[65] KEK, High Energy Accelerator Research Organization, Tsukuba, Japan
[66] Graduate School of Science, Kobe University, Kobe, Japan
[67] Faculty of Science, Kyoto University, Kyoto, Japan
[68] Kyoto University of Education, Kyoto, Japan
[69] Department of Physics, Kyushu University, Fukuoka, Japan
[70] Instituto de Física La Plata, Universidad Nacional de La Plata and CONICET, La Plata, Argentina
[71] Physics Department, Lancaster University, Lancaster, United Kingdom
[72] [(a)] INFN Sezione di Lecce; [(b)] Dipartimento di Matematica e Fisica, Università del Salento, Lecce, Italy
[73] Oliver Lodge Laboratory, University of Liverpool, Liverpool, United Kingdom
[74] Department of Physics, Jožef Stefan Institute and University of Ljubljana, Ljubljana, Slovenia
[75] School of Physics and Astronomy, Queen Mary University of London, London, United Kingdom
[76] Department of Physics, Royal Holloway University of London, Surrey, United Kingdom
[77] Department of Physics and Astronomy, University College London, London, United Kingdom
[78] Louisiana Tech University, Ruston LA, United States of America
[79] Laboratoire de Physique Nucléaire et de Hautes Energies, UPMC and Université Paris-Diderot and CNRS/IN2P3, Paris, France
[80] Fysiska institutionen, Lunds universitet, Lund, Sweden
[81] Departamento de Fisica Teorica C-15, Universidad Autonoma de Madrid, Madrid, Spain
[82] Institut für Physik, Universität Mainz, Mainz, Germany
[83] School of Physics and Astronomy, University of Manchester, Manchester, United Kingdom
[84] CPPM, Aix-Marseille Université and CNRS/IN2P3, Marseille, France
[85] Department of Physics, University of Massachusetts, Amherst MA, United States of America
[86] Department of Physics, McGill University, Montreal QC, Canada
[87] School of Physics, University of Melbourne, Victoria, Australia
[88] Department of Physics, The University of Michigan, Ann Arbor MI, United States of America
[89] Department of Physics and Astronomy, Michigan State University, East Lansing MI, United States of America

JHEP06(2014)035

[90] [a] INFN Sezione di Milano; [b] Dipartimento di Fisica, Università di Milano, Milano, Italy
[91] B.I. Stepanov Institute of Physics, National Academy of Sciences of Belarus, Minsk, Republic of Belarus
[92] National Scientific and Educational Centre for Particle and High Energy Physics, Minsk, Republic of Belarus
[93] Department of Physics, Massachusetts Institute of Technology, Cambridge MA, United States of America
[94] Group of Particle Physics, University of Montreal, Montreal QC, Canada
[95] P.N. Lebedev Institute of Physics, Academy of Sciences, Moscow, Russia
[96] Institute for Theoretical and Experimental Physics (ITEP), Moscow, Russia
[97] Moscow Engineering and Physics Institute (MEPhI), Moscow, Russia
[98] D.V.Skobeltsyn Institute of Nuclear Physics, M.V.Lomonosov Moscow State University, Moscow, Russia
[99] Fakultät für Physik, Ludwig-Maximilians-Universität München, München, Germany
[100] Max-Planck-Institut für Physik (Werner-Heisenberg-Institut), München, Germany
[101] Nagasaki Institute of Applied Science, Nagasaki, Japan
[102] Graduate School of Science and Kobayashi-Maskawa Institute, Nagoya University, Nagoya, Japan
[103] [a] INFN Sezione di Napoli; [b] Dipartimento di Fisica, Università di Napoli, Napoli, Italy
[104] Department of Physics and Astronomy, University of New Mexico, Albuquerque NM, United States of America
[105] Institute for Mathematics, Astrophysics and Particle Physics, Radboud University Nijmegen/Nikhef, Nijmegen, Netherlands
[106] Nikhef National Institute for Subatomic Physics and University of Amsterdam, Amsterdam, Netherlands
[107] Department of Physics, Northern Illinois University, DeKalb IL, United States of America
[108] Budker Institute of Nuclear Physics, SB RAS, Novosibirsk, Russia
[109] Department of Physics, New York University, New York NY, United States of America
[110] Ohio State University, Columbus OH, United States of America
[111] Faculty of Science, Okayama University, Okayama, Japan
[112] Homer L. Dodge Department of Physics and Astronomy, University of Oklahoma, Norman OK, United States of America
[113] Department of Physics, Oklahoma State University, Stillwater OK, United States of America
[114] Palacký University, RCPTM, Olomouc, Czech Republic
[115] Center for High Energy Physics, University of Oregon, Eugene OR, United States of America
[116] LAL, Université Paris-Sud and CNRS/IN2P3, Orsay, France
[117] Graduate School of Science, Osaka University, Osaka, Japan
[118] Department of Physics, University of Oslo, Oslo, Norway
[119] Department of Physics, Oxford University, Oxford, United Kingdom
[120] [a] INFN Sezione di Pavia; [b] Dipartimento di Fisica, Università di Pavia, Pavia, Italy
[121] Department of Physics, University of Pennsylvania, Philadelphia PA, United States of America
[122] Petersburg Nuclear Physics Institute, Gatchina, Russia
[123] [a] INFN Sezione di Pisa; [b] Dipartimento di Fisica E. Fermi, Università di Pisa, Pisa, Italy
[124] Department of Physics and Astronomy, University of Pittsburgh, Pittsburgh PA, United States of America
[125] [a] Laboratorio de Instrumentacao e Fisica Experimental de Particulas - LIP, Lisboa; [b] Faculdade de Ciências, Universidade de Lisboa, Lisboa; [c] Department of Physics, University of Coimbra, Coimbra; [d] Centro de Física Nuclear da Universidade de Lisboa, Lisboa; [e] Departamento de Fisica, Universidade do Minho, Braga; [f] Departamento de Fisica Teorica y del Cosmos and CAFPE, Universidad de Granada, Granada (Spain); [g] Dep Fisica and CEFITEC of Faculdade de Ciencias e Tecnologia, Universidade Nova de Lisboa, Caparica, Portugal
[126] Institute of Physics, Academy of Sciences of the Czech Republic, Praha, Czech Republic
[127] Czech Technical University in Prague, Praha, Czech Republic

JHEP06(2014)035

[128] Faculty of Mathematics and Physics, Charles University in Prague, Praha, Czech Republic
[129] State Research Center Institute for High Energy Physics, Protvino, Russia
[130] Particle Physics Department, Rutherford Appleton Laboratory, Didcot, United Kingdom
[131] Physics Department, University of Regina, Regina SK, Canada
[132] Ritsumeikan University, Kusatsu, Shiga, Japan
[133] [(a)] INFN Sezione di Roma; [(b)] Dipartimento di Fisica, Sapienza Università di Roma, Roma, Italy
[134] [(a)] INFN Sezione di Roma Tor Vergata; [(b)] Dipartimento di Fisica, Università di Roma Tor Vergata, Roma, Italy
[135] [(a)] INFN Sezione di Roma Tre; [(b)] Dipartimento di Matematica e Fisica, Università Roma Tre, Roma, Italy
[136] [(a)] Faculté des Sciences Ain Chock, Réseau Universitaire de Physique des Hautes Energies - Université Hassan II, Casablanca; [(b)] Centre National de l'Energie des Sciences Techniques Nucleaires, Rabat; [(c)] Faculté des Sciences Semlalia, Université Cadi Ayyad, LPHEA-Marrakech; [(d)] Faculté des Sciences, Université Mohamed Premier and LPTPM, Oujda; [(e)] Faculté des sciences, Université Mohammed V-Agdal, Rabat, Morocco
[137] DSM/IRFU (Institut de Recherches sur les Lois Fondamentales de l'Univers), CEA Saclay (Commissariat à l'Energie Atomique et aux Energies Alternatives), Gif-sur-Yvette, France
[138] Santa Cruz Institute for Particle Physics, University of California Santa Cruz, Santa Cruz CA, United States of America
[139] Department of Physics, University of Washington, Seattle WA, United States of America
[140] Department of Physics and Astronomy, University of Sheffield, Sheffield, United Kingdom
[141] Department of Physics, Shinshu University, Nagano, Japan
[142] Fachbereich Physik, Universität Siegen, Siegen, Germany
[143] Department of Physics, Simon Fraser University, Burnaby BC, Canada
[144] SLAC National Accelerator Laboratory, Stanford CA, United States of America
[145] [(a)] Faculty of Mathematics, Physics & Informatics, Comenius University, Bratislava; [(b)] Department of Subnuclear Physics, Institute of Experimental Physics of the Slovak Academy of Sciences, Kosice, Slovak Republic
[146] [(a)] Department of Physics, University of Cape Town, Cape Town; [(b)] Department of Physics, University of Johannesburg, Johannesburg; [(c)] School of Physics, University of the Witwatersrand, Johannesburg, South Africa
[147] [(a)] Department of Physics, Stockholm University; [(b)] The Oskar Klein Centre, Stockholm, Sweden
[148] Physics Department, Royal Institute of Technology, Stockholm, Sweden
[149] Departments of Physics & Astronomy and Chemistry, Stony Brook University, Stony Brook NY, United States of America
[150] Department of Physics and Astronomy, University of Sussex, Brighton, United Kingdom
[151] School of Physics, University of Sydney, Sydney, Australia
[152] Institute of Physics, Academia Sinica, Taipei, Taiwan
[153] Department of Physics, Technion: Israel Institute of Technology, Haifa, Israel
[154] Raymond and Beverly Sackler School of Physics and Astronomy, Tel Aviv University, Tel Aviv, Israel
[155] Department of Physics, Aristotle University of Thessaloniki, Thessaloniki, Greece
[156] International Center for Elementary Particle Physics and Department of Physics, The University of Tokyo, Tokyo, Japan
[157] Graduate School of Science and Technology, Tokyo Metropolitan University, Tokyo, Japan
[158] Department of Physics, Tokyo Institute of Technology, Tokyo, Japan
[159] Department of Physics, University of Toronto, Toronto ON, Canada
[160] [(a)] TRIUMF, Vancouver BC; [(b)] Department of Physics and Astronomy, York University, Toronto ON, Canada
[161] Faculty of Pure and Applied Sciences, University of Tsukuba, Tsukuba, Japan
[162] Department of Physics and Astronomy, Tufts University, Medford MA, United States of America
[163] Centro de Investigaciones, Universidad Antonio Narino, Bogota, Colombia

JHEP06(2014)035

[164] Department of Physics and Astronomy, University of California Irvine, Irvine CA, United States of America
[165] [(a)] INFN Gruppo Collegato di Udine, Sezione di Trieste, Udine; [(b)] ICTP, Trieste; [(c)] Dipartimento di Chimica, Fisica e Ambiente, Università di Udine, Udine, Italy
[166] Department of Physics, University of Illinois, Urbana IL, United States of America
[167] Department of Physics and Astronomy, University of Uppsala, Uppsala, Sweden
[168] Instituto de Física Corpuscular (IFIC) and Departamento de Física Atómica, Molecular y Nuclear and Departamento de Ingeniería Electrónica and Instituto de Microelectrónica de Barcelona (IMB-CNM), University of Valencia and CSIC, Valencia, Spain
[169] Department of Physics, University of British Columbia, Vancouver BC, Canada
[170] Department of Physics and Astronomy, University of Victoria, Victoria BC, Canada
[171] Department of Physics, University of Warwick, Coventry, United Kingdom
[172] Waseda University, Tokyo, Japan
[173] Department of Particle Physics, The Weizmann Institute of Science, Rehovot, Israel
[174] Department of Physics, University of Wisconsin, Madison WI, United States of America
[175] Fakultät für Physik und Astronomie, Julius-Maximilians-Universität, Würzburg, Germany
[176] Fachbereich C Physik, Bergische Universität Wuppertal, Wuppertal, Germany
[177] Department of Physics, Yale University, New Haven CT, United States of America
[178] Yerevan Physics Institute, Yerevan, Armenia
[179] Centre de Calcul de l'Institut National de Physique Nucléaire et de Physique des Particules (IN2P3), Villeurbanne, France

[a] Also at Department of Physics, King's College London, London, United Kingdom
[b] Also at Institute of Physics, Azerbaijan Academy of Sciences, Baku, Azerbaijan
[c] Also at Particle Physics Department, Rutherford Appleton Laboratory, Didcot, United Kingdom
[d] Also at TRIUMF, Vancouver BC, Canada
[e] Also at Department of Physics, California State University, Fresno CA, United States of America
[f] Also at Novosibirsk State University, Novosibirsk, Russia
[g] Also at CPPM, Aix-Marseille Université and CNRS/IN2P3, Marseille, France
[h] Also at Università di Napoli Parthenope, Napoli, Italy
[i] Also at Institute of Particle Physics (IPP), Canada
[j] Also at Department of Physics, St. Petersburg State Polytechnical University, St. Petersburg, Russia
[k] Also at Department of Financial and Management Engineering, University of the Aegean, Chios, Greece
[l] Also at Louisiana Tech University, Ruston LA, United States of America
[m] Also at Institucio Catalana de Recerca i Estudis Avancats, ICREA, Barcelona, Spain
[n] Also at CERN, Geneva, Switzerland
[o] Also at Ochadai Academic Production, Ochanomizu University, Tokyo, Japan
[p] Also at Manhattan College, New York NY, United States of America
[q] Also at Institute of Physics, Academia Sinica, Taipei, Taiwan
[r] Also at LAL, Université Paris-Sud and CNRS/IN2P3, Orsay, France
[s] Also at School of Physics and Engineering, Sun Yat-sen University, Guangzhou, China
[t] Also at Academia Sinica Grid Computing, Institute of Physics, Academia Sinica, Taipei, Taiwan
[u] Also at Laboratoire de Physique Nucléaire et de Hautes Energies, UPMC and Université Paris-Diderot and CNRS/IN2P3, Paris, France
[v] Also at School of Physical Sciences, National Institute of Science Education and Research, Bhubaneswar, India
[w] Also at Dipartimento di Fisica, Sapienza Università di Roma, Roma, Italy
[x] Also at Moscow Institute of Physics and Technology State University, Dolgoprudny, Russia
[y] Also at Section de Physique, Université de Genève, Geneva, Switzerland
[z] Also at Department of Physics, The University of Texas at Austin, Austin TX, United States of America

JHEP06(2014)035

[aa] Also at Institute for Particle and Nuclear Physics, Wigner Research Centre for Physics, Budapest, Hungary
[ab] Also at International School for Advanced Studies (SISSA), Trieste, Italy
[ac] Also at Department of Physics and Astronomy, University of South Carolina, Columbia SC, United States of America
[ad] Also at Faculty of Physics, M.V.Lomonosov Moscow State University, Moscow, Russia
[ae] Also at Physics Department, Brookhaven National Laboratory, Upton NY, United States of America
[af] Also at Moscow Engineering and Physics Institute (MEPhI), Moscow, Russia
[ag] Also at Department of Physics, Oxford University, Oxford, United Kingdom
[ah] Also at Department of Physics, Nanjing University, Jiangsu, China
[ai] Also at Institut für Experimentalphysik, Universität Hamburg, Hamburg, Germany
[aj] Also at Department of Physics, The University of Michigan, Ann Arbor MI, United States of America
[ak] Also at Discipline of Physics, University of KwaZulu-Natal, Durban, South Africa
[*] Deceased

JHEP06(2014)035